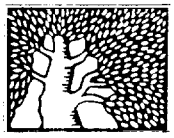

Weizmann Institute of Science
The Faculty of Physics

The 44th Annual Meeting of The Israel Physical Society

PROGRAM and ABSTRACTS

Bulletin of the Israel Physical Society
vol. 44, 1998

Acknowledgments

On behalf of the Israel Physical Society and the Organizing Committee, I would like to acknowledge the financial support extended to us in preparing the 44th Annual Meeting of the Israel Physical Society.

Special thanks are due to:

The Maurice and Gabriela Goldschleger Conference Foundation at the Weizmann Institute of Science
The Faculty of Physics - Weizmann Institute of Science
The Department of Condensed Matter - Weizmann Institute of Science
The Department of Particle Physics - Weizmann Institute of Science
The Department of Complex Systems - Weizmann Institute of Science
The Albert Einstein Minerva Center for Theoretical Physics

Prof. D. Zajfman
Chairman of the Local Organizing Committee

Council of the Israel Physical Society

Prof. Shlomo Havlin; Bar-Ilan University - President
Prof. Amnon Moalem; Ben-Gurion University - Vice-President
Prof. Haim (Vivian) Halpern; Bar-Ilan University - Secretary
Prof. Victor Fleurov; Tel-Aviv University - Treasurer
Prof. L. Gilles Benguigi; Technion
Dr. Arie Levine; Negev Nuclear Research Center, Dimona
Dr. Yossi Shiloh; Rafael
Prof. Arie Zigler; Hebrew University
Dr. Arie Raizman; Soreq Nuclear Research Center, Yavne
Prof. M. Kugler; Weizmann Institute of Science

Corporate Members

Bar-Ilan University
Ben-Gurion University
Hebrew University
Israel Atomic Energy Commission
Technion
Tel-Aviv University
Weizmann Institute of Science

Organizing Committee

D. Zajfman; Weizmann Institute of Science - Chairman
Y. Gefen; Weizmann Institute of Science
I. Maron; Weizmann Institute of Science
S. Akselrod; Tel-Aviv University
M. Kugler; Weizmann Institute of Science
Y. Silberberg; Weizmann Institute of Science
B. Eylon; Weizmann Institute of Science
I. Tserruya; Weizmann Institute of Science
M. Milgrom; Weizmann Institute of Science
D. Lellouch; Weizmann Institute of Science

44th Meeting of the Israel Physical Society

Weizmann Institute of Science

April 8, 1998

08:30-09:30	Wix aud. lobby	Registration and coffee
09:30-09:50	Wix aud.	Opening Remarks: Prof. Y. Groner, Vice President of WIS Prof. S. Havlin, President of IPS: Presentation of the IPS award for outstanding graduate research
09:50-10:40	Wix aud.	Plenary lecture: Prof. Paul Chaikin, Princeton **Hard Spheres in Space: Colloidal Crystals in Gravity and Microgravity**
10:40-11:00	Wix aud. lobby	Coffee break
11:00-13:00		Parallel sessions:
	Loc. 1 on map	**Astrophysics and cosmology**
	Loc. 2 on map	**Condensed matter**
	Loc. 3 on map	**Lasers and quantum optics**
	Loc. 4 on map	**Atomic and nuclear physics**
	Loc. 5 on map	**Particles and fields**
	Loc. 6 on map	**Statistical physics and nonlinear dynamics**
	Loc. 7 on map	**Physics in medicine**
	Loc. 8 on map	**Plasma and space physics**
	Loc. 9 on map	**Physics in biology**
13:00-14:00		Lunch
13:30-14:30	Wix aud.	Poster session*
14:00-14:30	Wix aud.	IPS business meeting

14:30-16:30		Parallel sessions:
	Loc. 1 on map	**Physics teaching**
	Loc. 2 on map	**Condensed matter**
	Loc. 3 on map	**Lasers and quantum optics**
	Loc. 4 on map	**Atomic and Nuclear physics**
	Loc. 5 on map	**Particles and fields**
	Loc. 6 on map	**Statistical physics and nonlinear dynamics**
	Loc. 7 on map	**Physics in industry**
	Loc. 8 on map	**Plasma and space physics**
	Loc. 9 on map	**Computational physics**
16:30-17:00	Wix aud. lobby	Coffee break
17:00-17:45	Wix aud.	Plenary lecture:
		Prof. S. Nusseibeh, Al-Quds University
		Aspects and Prospects of Palestinian-Israeli Academic Cooperation

*Posters can be mounted from 08:30

Program
Plenary Lectures
Wix auditorium

Morning session Chair: D. Zajfman, Weizmann Institute

- 09:50-10:40 Paul Chaikin, Princeton University
  Hard Spheres in Space: Colloidal Crystals in Gravity and Microgravity

Afternoon session Chair: Y. Gefen, Weizmann Institute

- 17:00-17:45 S. Nusseibeh, Al-Quds University
  Aspects and Prospects of Palestinian-Israeli Academic Cooperation

Astrophysics and Cosmology
Feinberg Graduate School building, room 5

Morning session Chair: V. Usov, Weizmann Institute

- 11:00-11:35 J. D. Bekenstein, Hebrew University
  Adiabatic Invariance in Black Hole Physics and its Ramifications
- 11:35-12:10 D. Eichler, Ben-Gurion University
  Ground Based Gamma Ray Astronomy
- 12:10-12:45 M. Milgrom, Weizmann Institute
  The Modified Dynamics as a Vacuum Effect

Condensed Matter

Schmidt auditorium

Morning session Chair: B. Horovitz, Ben-Gurion University

- 11:00-11:30 G. Jung, Ben-Gurion University
  Coherent Vortex Motion and Josephson-like Effects in Periodically Modulated Superconducting Thin Films
- 11:30-12:00 M. Azbel, Tel-Aviv University
  Quantum Turbulence and Resonant Tunneling
- 12:00-12:30 S. Levit, Weizmann Institute
  Chaos and Interactions - Statistics of Hartree-Fock Levels in Small Disordered Systems
- 12:30-13:00 O. Agam, Hebrew University
  Nonequilibrium Effects in the Tunneling Conductance Spectra of Small Metallic Particles

Afternoon session Chair: R. Berkovits, Bar-Ilan University

- 14:30-15:00 L. Klein, Bar-Ilan University
  Itinerant Magnetism in the Limit of Strong Electron Correlations: Mainly $SrRuO_3$
- 15:00-15:30 E. Akkermans, Technion
  Hybridization of Localized and Density Modes in Superfluid Helium 4
- 15:30-16:00 S. Rotter, Soreq
  Wide Band-Gap Materials for High Power Electronics
- 16:00-16:30 D. Shahar, Weizmann Institute
  An Experimentalist's View of Quantum Phase Transitions

Lasers and Quantum Optics

Feinberg Graduate School building, room 3

Morning session Chair: M. Rosenbluh, Bar-Ilan University

- 11:00-11:30 N. Tessler, Cavendish Laboratory
  Physics of Polymer based Optoelectronic Devices
- 11:30-12:00 N. Davidson, Weizmann Institute
  New Optical Traps for Laser Cooled Atoms
- 12:00-12:30 M. Horowitz, Technion
  Noise-like Generation in Erbium-doped Fiber Lasers Due to Nonlinear Polarization Rotation in Birefringent Fibers
- 12:30-13:00 A. Arie, Tel-Aviv University
  Efficient Frequency Doubling of CW Lasers in Resonant Cavities

Afternoon session Chair: Y. Band, Ben-Gurion University

- 14:30-15:00 A. Lewis, Hebrew University
  The Quest for Three Dimensional Nanometer Functional Imaging with Light
- 15:00-15:30 S. Barad, Tel-Aviv University
  Size and Density Effects on the Magnetically-induced Fano Resonances in Semiconductors
- 15:30-16:00 A. Gover, Tel-Aviv University
  The Israeli Tandem FEL: Report on Recent Lasing Results and Options for Development of a Wide Spectral Range Radiation Source

Atomic and Nuclear Physics

Sussman building, seminar room

Morning session Chair: E. Piasetzky, Tel-Aviv University

- 11:00-11:30 A. Leviatan, Hebrew University
  On the Relativistic Origin of Pseudospin Symmetry in Nuclei
- 11:30-12:00 D. Ashery, Tel-Aviv University
  Color Explosion and the Pion Wave Function
- 12:00-12:30 E. Socol, Weizmann Institute
  CERES Results on Low-Mass Electron Pair Production in Pb–Au collisions
- 12:30-13:00 A. Gal, Hebrew University
  Nuclear Medium Effects in K and $\bar{\mathrm{K}}$ *Interactions*

Afternoon session Chair: I. Tserruya, Weizmann Institute

- 14:30-15:00 A. Wolf, Max-Planck Institut für Kernphysik, Heidelberg
  Atomic Collisions and Spectroscopy at the Heavy-ion Storage Ring TSR
- 15:00-15:30 Z. Amitay, Weizmann Institute
  Dissociative Recombination of HD^+*, State-to-State Experimental Investigation Using Fragment Imaging and Storage Ring Techniques*
- 15:30-16:00 I. Mardor, Tel-Aviv University
  New Results of Nuclear Transparency to Wide Angle Quasi-elastic Scattering
- 16:00-16:30 M. Paul, Hebrew University
  Nuclear Astrophysics with Beams of Radioactive Nuclei

Particles and Fields

Feinberg Graduate School building, room 6

Morning session Chair: A. Schwimmer, Weizmann Institute

- 11:00-11:30 A. Giveon, Hebrew University
  Brane Dynamics and Gauge Theory
- 11:30-12:00 R. Brustein, Ben-Gurion University
  Duality in String Cosmology
- 12:00-12:30 S. Bergmann, Weizmann Institute
  The Solar Neutrino Problem in the Presence of Flavor Changing Neutrino Interactions

Afternoon session Chair: A. Davidson, Ben-Gurion University

- 14:30-15:00 M. Karliner, Tel-Aviv University
  Precise Estimates of High Orders in QCD
- 15:00-15:30 E. Duchovni, Weizmann Institute
  Higgs bosons at LHC
- 15:30-16:00 Y. Rozen, Technion
  CP violation in B decays

Statistical Physics and Nonlinear Dynamics

Physics building, Weissman auditorium

Morning session Chair: E. Akkermans, Technion

- 11:00-11:30 D. Kandel, Weizmann Institute
  Polymer Induced Coiling of Membrane Tubes
- 11:30-12:00 D. Andelman, Tel-Aviv University
  Interfaces of Modulated Phases: Diblock Copolymers and Magnetic Films
- 12:00-12:30 N. Samid-Merzel, Technion
  Pattern formation in Evaporating Water Films
- 12:30-13:00 J. Fineberg, Hebrew University
  Dissipative Solitary States in Driven Surface Waves

Afternoon session Chair: D. Bergman, Tel-Aviv University

- 14:30-15:00 D. Kessler, Bar-Ilan University
  Precursors in Front Propagation
- 15:00-15:30 A. Groisman, Weizmann Institute
  Elastic Similarity in a Polymer Solution Flow
- 15:30-16:00 S. Fishman, Technion
  The Classical Limit of Quantum Evolution in Chaotic Systems
- 16:00-16:30 Y. M. Strelniker, Tel-Aviv University
  Magneto-Induced ac Electrical Permittivity of Metal-Dielectric Composites with a Two Characteristic Length Scales Periodic Microstructure

Physics in Medicine

Feinberg Graduate School building, room 4

Morning session Chair: S. Akselrod, Tel-Aviv University

- 11:00-11:30 S. Abramovich-Sivan, Tel-Aviv University
  The Generation and Modulation of the Heart Beat: A Phase Response Curve Based Model of Interacting Pacemaker Cells
- 11:30-12:00 J. Almog, Israel Police
  Scientific Methods in Criminal Investigations
- 12:00-12:30 P. R. Harvey, Elscint MRI Centre
  Twin Gradient Technology - A New Concept in MRI System Design
- 12:30-13:00 T. Flash, Weizmann Institute
  Neural Mechanical and Geometric Factors in the Control of Posture and Movement

Plasma and Space Physics

Ziskind building, room 1

Morning session Chair: S. Goldsmith, Tel-Aviv University

- 11:00-11:30 A. Zigler, Hebrew University
  Spatial and Temporal Diagnostics of Plasma Channel Waveguides for High Intensity Laser Pulses
- 11:30-12:00 E. Jerby, Tel-Aviv University
  Cyclotron-Resonance and Free-Electron Masers at Low-Voltages: Concepts, Experiments, and Applications
- 12:00-12:30 M. Gedalin, Ben-Gurion University
  Low-frequency Waves in Relativistic Pair Plasma of Pulsar Magnetospheres
- 12:30-13:00 C. Goldenberg, Soreq
  Plasma-Propellant Interaction in Electrothermal-Chemical Guns

Afternoon session Chair: L. Friedland, Hebrew University

- 14:30-15:00 Y. G. Krasik, Technion
  Observation of Downstream Energetic Electron/ion Flow and Accompanied High-power Microwave Radiation During the Opening of Submicrosecond Plasma Opening Switch

- 15:00-15:30 M. Botton, Rafael
  Numerical Simulations of Fast and Slow Microwave Sources

- 15:30-16:00 Y. Ralchenko, Weizmann Institute
  Determination of the Time-dependent Radial Distributions of the Electron Density, Electron Temperature, and Ion Charge States in an Imploding Cylindrical Plasma

- 16:00-16:30 R. Kishony, Nuclear Research Center, Beer-Sheva
  Inertial Confinement Fusion Ignition Criteria using Self-Similar Solutions

Physics in Biology

Physics building, Seminar room A

Morning session Chair: E. Braun, Technion

- 11:00-11:30 M. Elbaum, Weizmann Institute
  Biophysics of the Nuclear Shell

- 11:30-12:00 E. Ben-Jacob, Tel-Aviv University
  From Neurons to Brain

- 12:00-12:30 Y. Soen, Technion
  The Emergence of Spatial Synchronization and Periodic Temporal Rhythm in Self-assembled Heart-cell Networks

Physics in Industry

Feinberg Graduate School building, room 4

Afternoon session Chair: A. Breskin, Weizmann Institute

- 14:30-15:00 M. Brunstein, Applied Materials
  Are Physicists needed in industry?
- 15:00-15:30 N. Ben-Yosef, Hebrew University
  Multi-Spectral Imaging
- 15:30-16:00 R. Yagel, BMed, Jerusalem
  Visualization of 3D Medical Images
- 16:00-16:30 E. Finkman, Technion
  Quantum well infrared photodetectors (QWIP)

Computational Physics

Physics building, Seminar room A

Afternoon session Chair: J. Adler, Technion

- 14:30-15:00 D. C. Rapaport, Bar-Ilan University
  Simulating Granular Flow
- 15:00-15:30 R. Thieberger, Ben-Gurion University
  Cosmic Lacunarity
- 15:30-16:00 A. Hashibon, Technion
  Roughening Transitions and Surface Tension in an HCP Lattice with Higher Neighbor Interactions

Physics Teaching

Feinberg Graduate School building, room 5

Afternoon session Chair: B. Eylon, Weizmann Institute

- 14:30-14:55 B. Saering, The Israel Arts and Science Academy, and Weizmann Institute
  Using an Annotated Catalog of Websites in High School Physics
- 14:55-15:20 D. Langley, Weizmann Institute
  An Instructional Framework to Support Learning Inquiry Skills in High School Physics
- 15:20-15:45 Z. Krakover, Hebrew University
  The Motion of Charged Particles in Electric and Magnetic Fields - Learning by Simulation
- 15:45-16:10 I. Yerushalmi, Weizmann Institute
  Learning from Mistakes - a Workshop for Physics Teachers on Feedback and Control in Problem Solving
- 16:10-16:30 D. Pundak, Alperin Academic College of the Jordan Valley
  The Blossoms of Science Internet Astronomy School

ABSTRACTS

Plenary Lecture

Plenary lecture

Hard Spheres in Space: Colloidal Crystals in Gravity and Microgravity

Paul Chaikin

Princeton

Classical hard spheres have long served as a paradigm for our understanding of the structure of liquids, crystals and glasses. Suspensions of uniform polymer colloids are near ideal physical realizations of hard spheres and their thermodynamics and hydrodynamic interactions. However, gravity appears to play a significant and unexpected role in the formation and structure of these colloidal systems. Sedimenting particles set up long range flow fields reminiscent of turbulent flow (even at extremely low Reynolds number). The size, morphology, and structure of crystals grown in the m-gravity environment of the space shuttle differ from the identical samples grown in 1-g. Further, the high volume fraction "glass" samples which fail to crystallize after more than a year in 1-g, begin nucleation after several days and fully crystallize in less than two weeks on the space shuttle. Hydrodynamic and growth instabilities as well as different packing constraints of hard spheres help explain some of these experimental findings.

Astrophysics and Cosmology

Adiabatic Invariance in Black Hole Physics and its Ramifications

Jacob D. Bekenstein

Racah Institute of Physics, The Hebrew University of Jerusalem

Hawking's well known theorem [1] that a black hole's horizon's area cannot decrease has led to a folk belief that whenever *any* change occurs, the area *will* increase. But in fact there is much evidence to support the existence of an adiabatic theorem in black hole physics that would claim that adiabatic changes of a near equilibrium black hole leave the horizon's area unchanged. The precise definition of "adiabatic" is the *desideratum* of this enquiry. I will review a variety of examples that bear on the matter. These include a Schwarzschild black hole perturbed by a quasistatic scalar field (minimally or nonminimally coupled), a Kerr black under the influence of scalar radiation at the superradiance treshold, and a Reissner–Nordström black hole absorbing a charge marginally, and further examples explored by Mayo [2]. These clarify the conditions under which the conjectured theorem would be true. The adiabatic theorem would provide an important motivation for a scheme of black hole quantization based on Ehrenfest's principle [3], which I will describe briefly.

[1] S. W. Hawking Phys. Rev. Letters **26**, 1344, (1971).
[2] A. E. Mayo, publication in preparation.
[3] See for example M. Born, *Atomic Physics* (Blackie, London, 1969), eighth edition.

Ground Based Gamma Ray Astronomy

D. Eichler

Dept. of Physics, Ben-Gurion University of the Negev, Beersheva 84105

Ground based gamma ray astronomy, which measures the Cerenkov flash of the cascade that is produced when the gamma ray hits the Earth's atmosphere, is presently limited to photon energies above 200 Gev. In practice, this threshold could be lowered by about an order of magnitude, which would allow detection of blazars and millisecond pulsars at photon energies above 20 Gev. The prospects for building such a ground based gamma ray detector in Israel are reviewed.

The modified dynamics as a vacuum effect

Mordehai Milgrom

Dept. of Condensed-Matter Physics, Weizmann Institute of Science

The modified dynamics (MOND) has been propounded as an alternative to dark matter in astrophysical systems such as galaxies and clusters of galaxies. It posits a departure from conventional dynamics (law of inertia and/or gravity) in the limit of small accelerations, where the scale is set by an acceleration constant a_0. The value of a_0, as determined from the analysis of galaxy dynamics, is of the order of cH_0, evoking cosmological underpinnings for MOND: The cosmological state of the universe (expansion, curvature, cosmological constant, etc.) somehow enters local dynamics, and is represented, in an effective theory, by a_0. For example, if inertia is a derived effect, resulting from some interaction of the accelerated body with the "rest of the Universe", in the spirit of Mach's principle, then inertia might look different above and below some acceleration parameter of cosmological significance. An intriguing possibility is that MOND, and indeed the whole of inertia, is due to effects of the vacuum on an accelerated body. The vacuum might serve as the universal inertial frame because an observer can perceive its non-inertial motion by detecting the Unruh radiation: a palpable incarnation of the vacuum in non-inertial frames. (For a constant-acceleration trajectory the Unruh radiation is thermal with a temperature proportional to the acceleration.) A non-trivial state of the universe marked, e.g., by curvature, expansion, etc. also affects the vacuum and can be detected by even an inertial observer, as here too the vacuum manifests itself by detectable radiation. A non-inertial observer in a nontrivial universe will see the combined effect. So, if inertia is indeed a vacuum effect, it is conceivable that cosmology enters local dynamics through a parameter of order a_0 characterising the radiation due to cosmology alone (e.g. its temperature), which marks a break in the dynamical behaviour–as required by MOND. Without being able to offer a specific mechanism for inertia, I discuss various aspects of the problem including constraints and guiding principles that might help construct such a mechanism.

Landau-Type Wave Excitation at the Lindblad Resonances as a Mechanism for Formation of Rings in Flat Galaxies

Evgeny Griv and Michael Gedalin

Dept. of Physics, Ben-Gurion University of the Negev, Beersheva 84105

We extend the investigation which has began in [1] by studying the effects of kinetic type wave–star interaction at the Lindblad resonances in a self-gravitating disk of a highly flattened galaxy [2]. The Boltzmann kinetic and Poisson equations are used. The model of an infinitesimally thin, spatially inhomogeneous galactic disk with rare gravitational collisions between stars and giant molecular clouds is explored. The star–cloud encounters are described with the use of the exact Landau collision integral used in plasma physics [3]. By studying the dispersion relation, estimates are made for the frequencies and growth rates of the density waves which are excited/damped via a Landau mechanism at the Lindblad resonances between stars and gravitationally (Jeans-) stable perturbations (e.g., those that produced by a barlike structure, a spontaneous perturbation, and/or a companion galaxy) in the self-gravitating galactic system. We show that both axisymmetric (radial) and nonaxisymmetric (spiral) density waves may be excited effectively at the inner and outer Lindblad resonances in a weakly inhomogeneous disk. It is similar to the instability of the Doppler (Landau cyclotron) type in plasmas, and it s due to the nature of the differential rotation of the inhomogeneous galactic system: the free kinetic energy associated with the differential rotation is the only possible source for the growth of the average wave energy.

Specific astronomical implications of the present theory to actual galaxies are also discussed. In particular, we connect inner and outer rings and pseudorings already observed in a number of flat galaxies (e.g., NGC 1068, NGC 1291, NGC 1433, NGC 3081, NGC 4736, NGC 5850, NGC 6300, and M 100) to the Lindblad orbital resonances, $m(\Omega - \Omega_p) - l\kappa \approx 0$, with bars, spirals or ovals in the mass distribution. Here m is the azimuthal mode number (= number of spiral arms), $\Omega(r)$ is the local angular velocity of galactic rotation at the distance r from the center, Ω_p is the constant angular velocity of bar or spirals rotation, $l = \pm 1$, and $\kappa = 2\Omega[1 + (r/2\Omega)(d\Omega/dr)]^{1/2}$ is the ordinary local epicyclic frequency (cf. the Larmor frequency in a magnetized plasma).

The early parts of this work were carried out in the Academia's Sinica Institute of Astronomy & Astrophysics in Taiwan, the remainder of the research was granted by the Israeli Ministry of Immigrant Absorption and the Israeli Ministry of Science.

[1] E. Griv & W. Peter, Astrophys. J., **469**, 84, 99, 103, (1996).
[2] E. Griv & M. Gedalin, Astrophys. J., submitted, (1998).
[3] E. Griv and M. Gedalin, Astron. Astrophys., **328**, 531, (1997).

Dynamics of Saturn's Rings

Evgeny Griv

Dept. of Physics, Ben-Gurion University of the Negev, Beersheva 84105

Voyager 2 images of the Saturnian ring system have shown evidence of a great deal of structure [1]. The best resolution images demonstrated fine-scale, the so-called "ringlet" structures at scales of $\sim h \lesssim 100$ m, where h is the typical thickness of the system. On a small scale these ringlets have been observed to be undergo variations and oscillations with time and ring longitude. The latter probably indicates that such features are wave phenomena, and different instabilities of small-amplitude gravity perturbations may play important roles in ring's dynamics.
In the present review, the dynamics of regions in the Saturnian ring system with rare physical (inelastic) interparticle collisions is discussed. Because of a formal analogy between the collective oscillations in a self-gravitating disk of point masses and the oscillations of a one-component plasma, a particulate ring disk is treated by employing mathematical formalisms from plasma kinetic theory: kinetic theory with the Boltzmann and Poisson equations is used to obtain the eigenfrequencies of gravity oscillations propagating in the plane of the system under study. In addition, the dynamical behavior of the different models of Saturn's ring disk is studied by N-body computer simulations in order to confirm the validity of the theory. Specific astronomical implications of the study to Saturn's rings are discussed prior to rings' exploration by Cassini spacecraft that will start in 2004. The first results concerning the evolution and dynamics of Saturn's rings have already been published [2-6].

The study was supported in part by the Israeli Ministry of Immigrant Absorption and the Academia Sinica in Taiwan.

[1] A.L. Lane et al., Science, **215**, 537, (1982).
[2] E. Griv, Planet. Space Sci., **44**, 579, (1996).
[3] E. Griv, Planet. Space Sci., **46**, in press, (1998).
[4] E. Griv & T. Chiueh, Astron. Astrophys., **311**, 1033 (1996).
[5] E. Griv & C. Yuan, Planet. Space Sci., **44**, 1185, (1996).
[6] E. Griv, C. Yuan & T. Chiueh, Planet. Space Sci., **45**, 627 (1997).

N-Body Simulations of Galaxies: Modified Dynamics

Evgeny Griv, Michael Gedalin and Yehoshua Kimhi*

Dept. of Physics, Ben-Gurion University of the Negev, Beersheva 84105
**High Performance Computing Unit, Inter University Computational Center (IUCC), Tel Aviv University, Tel Aviv 69978*

We continued the study of the stability and evolution of N-body models of highly flattened galaxies of stars in light of the Modified Dynamics [1,2]. Use of the IUCC 32-processor IBM SP2 concurrent computer has enabled us to make long runs using a sufficiently large number of model stars, $N \gtrsim 25\,000$, in the direct summation code and thus simulate model regimes not previously studied. The simulation clearly shows the remarkable resemblance of the planar and vertical structures that seen in computer models and the ones in actual galaxies. As an example, in this figure a series of face-on view snapshots from a simulation run is shown; a time $t = 1$ is taken to correspond to a single revolution of the initial disk.

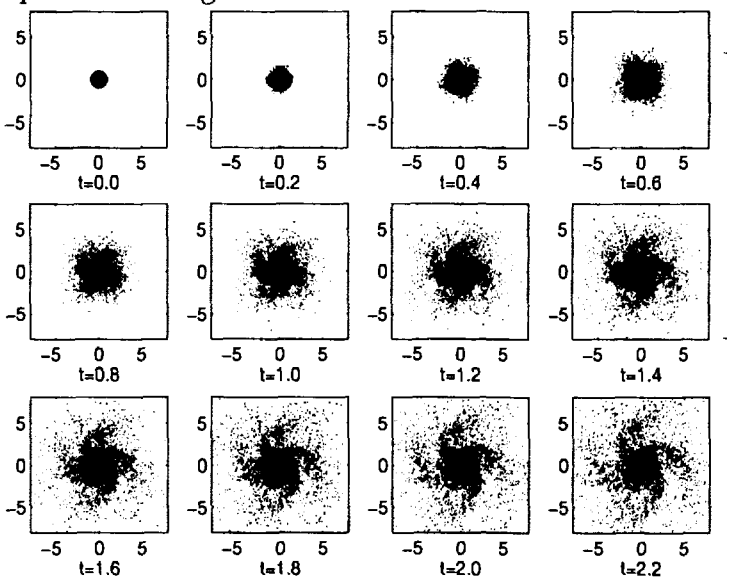

[1] M. Milgrom, Astrophys. J., **270**, 366, 371, (1983).
[2] E. Griv and V. V. Zhytnikov, Astrophys. Space. Sci., **226**, 51 (1995).

Local Stability Criterion for a Disk of Stars

Evgeny Griv, Baruch Rosenstein* and Tzi-Hong Chiueh**

Dept. of Physics, Ben-Gurion University of the Negev, Beersheva 84105
**Electrophysics Dept., National Chiao Tung University, Hsinchu 300, Taiwan*
***Institute of Astronomy, National Central University, Chung-Li 320, Taiwan*

The analysis of the stability of small-amplitude gravity oscillations in disk-shaped galaxies of stars is the first step towards an understanding of the phenomena of spiral structure of ours and other galaxies. Here, the linear stability theory of small oscillations of a highly flattened, rapidly rotating stellar disk of spiral galaxies is refined [1]. The criterion which guarantees the lack of arbitrary gravitationally (Jeans-) unstable perturbations in such a disk is rederived by using a plasma theory method of particle dynamics or particle orbit theory, and for the first time in stellar dynamics the advantages of this purely Langrangian method were realized. The criterion for stabilizing the disk by means of random motion of stars generalizes the well-known Toomre's [2] marginal stability criterion. The fact that the *nonaxisymmetric* (spiral) perturbations in the *differentially* rotating system are more unstable than the *axisymmetric* (radial) ones has taken into account in this criterion. The latter is due to the nature of the differential rotation of the spatially inhomogeneous galactic system: the free kinetic energy associated with the differential rotation is the only possible source for the growth of the perturbation energy.
In order to determine the range of validity of the generalized local stability criterion, we simulate numerically disks of many mutual-gravitating stars. The dynamical behavior of the different computer models of an infinitesimally thin, inhomogeneous, and practically collisionless stellar disk is studied by applying the numerical method of local simulations or N-body simulations in Hill's [3,4] equations context. The main thrust of our work is to dispute Toomre's [3] explanation of streakiness in these local simulations as swing amplified particle noise. We advocate an alternate way to describe the rapidly evolving structures, such as those reported in the simulations, in terms of local true instabilities of spiral Jeans-type perturbations. The simulations clearly confirm the qualitative picture and moreover are in fair quantitative agreement with the simplified theory, developed in the current study. Certain applications of the theory and the N-body simulations to actual spiral galaxies are discussed as well.

The early part of this work was carried out in the Astrophysics Institute, Dushanbe, in the former Soviet Union. E.G. would like to thank Alexei M. Fridman and Muzafar N. Maksumov for the informative discussions during that period.

[1] E. Griv, B. Rosenstein & T. Chiueh, Astron. Astrophys, submitted, (1998).
[2] A. Toomre, Astrophys. J., **139**, 1217, (1964).
[3] A. Toomre, in *Dynamics and Interactions of Galaxies*, p. 292, ed. R. Wielen, Springer-Verlag, Berlin, (1990).
[4] E. Griv, Planet. Space Sci., **46**, in press (1998).

First Results of the Solar Observations by the Solar Radio Telescope RT-2.5 of the Sea of Gallilee Astrophysical Observatory of the Jordan Valley College: Prefalre Bursts - Precursors of Solar Flares

D.Pundak, L.A.Pustil'nik, S.V.Pustil'nik, V.M.Bogod *., V.Shatilov *

Sea of Gallilee Astrophysical Observatory of the Jordan Valley Academic College, 15132, ISRAEL; lev@yarden.yarden.ac.il

* *RATAN-600, Special Astrophysical Observatory of the Russian Science Academy, N.Arkhyz, Karachay-Cherkessia, 357147, RUSSIA; vbog@ratan.sao.ru*

We present first results of flare activity investigations with the new solar radio telescope RT-2.5 of the Sea of Gallilee Astrophysical Observatory of the Jordan Valley College, Israel. Principal scheme of the fast multichannel narrow- band receiver-polarimeter and registration method are adduced.

Main specific of our complex caused by using of multichannel narrow band fast receiver/polarimeter which is able to detect propagation through solar atmosphere compact beams of accelerated particles. Cyclotron resonance origin of the solar radio emission in used wavelengths 4.8-5.2 cm provide very high sensitivity of our system to possible effects of pulse -like energy release preceded to flare itself.

We demonstrate observational examples of the short time preflare bursts - precursors for two extreme cases of flares: very strong flare July 09, 1996 and weak flare 25.11.1996. We show that manifestations of these kind of preflare behavior in the spectra slope and/or polarization in narrow spectral bands have much more higher amplitudes and confidence level then in standard method with flux measuring only. It caused by gyroresonance character of microwave radio emission from corona and transition layer above solar spots with its extreme high sensitivity to any inhomogeneous and fronts of hot plasma density or beams of accelerated particles.

For the case of very strong flare July 09, 1996 we demonstrate existence of some universal sequence of flare energy release both in two precursors, preceded flare (15 min and 30 min before flare) and in the flare itself: "main" strong pulse - weak "echo" pulse - shower of the weak pulses. This sequence is repeated both in precursors and flare with the same temporary characteristics in spectral slope and polarization. This universality may be result of manifestation the same chain of processes in turbulent current sheet during its transition from preflare equilibrium to the flare's one with some "false-starts" during the preflare rebuilding.

Additional Charged Particle Acceleration in Space Plasma With Two Types of Scatterers: Applications to Some Astrophysical Objects

Lev Dorman[1], Vjacheslav Shogenov[2]
[1] *Technion and ICRC, affiliated to TAU, Israel*
[2] *Kabardino-Balkar State University, Russia*

We develop our model [1] of space plasma consisted from two types of charged particle scatterers: 1-background plasma moved with some velocity $\overrightarrow{U}_1$ with frozen in magnetic inhomogeneities characterized by transport path $L_1(R)$, where R is the rigidity of charged particles;
2- magnetic clouds, high speed streams, shock waves (considered only as scatterers) moved with some average velocity $\overrightarrow{U}_2$ and characterized by transport path $L_2(R)$. We suppose that $\overrightarrow{U}_1$ and $\overrightarrow{U}_2$ contain regular parts $\overrightarrow{U}_{10} = \left\langle \overrightarrow{U}_1 \right\rangle$, $\overrightarrow{U}_{20} = \left\langle \overrightarrow{U}_2 \right\rangle$ and fluctuated parts $\overrightarrow{U}_1 - \overrightarrow{U}_{10}$, $\overrightarrow{U}_2 - \overrightarrow{U}_{20}$. ¿From the collisional Boltzmann equation we derive the diffusion approximation described the propagation and acceleration of charged particles which coincide with usually used at $\overrightarrow{U}_{10} = \overrightarrow{U}_{20}$. Particle acceleration in this system will be determined by diffusion coefficient in momentum space $D = D_1 + D_2 + D_{12}$. Here $D_1 = p^2 \left\langle \Delta \overrightarrow{U}_1^2 \right\rangle /3vL_1(R)$,where v is the velocity of particles and $\left\langle \Delta \overrightarrow{U}_1^2 \right\rangle = \left\langle \overrightarrow{U}_1^2 \right\rangle - \overrightarrow{U}_{10}^2$ described usual Fermi acceleration by inhomogeneities in background plasma. Coefficient $D_2 = p^2 \left\langle \Delta \overrightarrow{U}_2^2 \right\rangle /3vL_2(R)$ described Fermi acceleration by scatterers of second type. Coefficient $D_{12} = p^2 \left(\overrightarrow{U}_{10} - \overrightarrow{U}_{20} \right)^2 /3v\left(L_1(R) + L_2(R)\right)$ described additional acceleration (when $\overrightarrow{U}_{10}$ and $\overrightarrow{U}_{20}$ are not equal). In some cases, when $\overrightarrow{U}_{10}$ and $\overrightarrow{U}_{20}$ have opposite directions, the additional acceleration can be much faster than usual first two: $D_{12} >> D_1 + D_2$. We show that additional acceleration will be important in the Heliosphere in periods of high solar activity (for small energy particles) and in stellar winds, in binary systems and accretion disks, in the Galaxy with galactic wind driven by cosmic rays or/and driven by supernova explosions and great stellar winds, in regions of galaxies collisions, and other astrophysical objects.

[1] L.I. Dorman, V.Kh. Shogenov, Zh. Eksp. Teor. Fiz., **89**, 1624, (1985).

On a possible cyclical activity of the flare star EV Lac.

G.Roizman, G.Sigal, D.Pundak.

Sea of Galilee Astrophysical Observatory, Jordan Valley Academic College

Results of the EV Lac spotted variability observations carried out during the summer 1995 at the Israel Sea of Galilee Astrophysical Observatory are discussed. The observations have been carried out with a 16" Schmidt-Cassegrain MEADE telescope equipped with the ST-6 CCD-camera and the BVR set of filters. An amplitude of the EV Lac brightness variability in V-band was about 0.025 mag. No real changes of B-V and V-R color-indexes were found, nor real deviations of the observed light curves from a sine function with a confidence probability of 99Nevertheless, there is a significant distinction between the standard deviation of the EV Lac magnitude measurements and the standard deviation of the comparison stars magnitudes measurements. This difference may be the result of real microflare fast variability of EV Lac or, more probably, it may be the result of a rough fitting of really very complicated light curve by a simple sinus function. Analysis of the brightness variations and the internal variances of the nightly averaged measurements in the BVR-bands suggests an existence of additional blue non-flare radiation, probably due to an emission of bright active regions in the chromosphere of EV Lac. As a result the star may be brighter than when it is in a quiet state and its brightness is not disturbed by small fast flares. The Julian dates of EV Lac brightness minima collected from different sources during 1970-1995 are presented. The O-C deviations of the minima times give the evidence of being a periodic function of time with about 3.5-years period of variability, probably due to the latitudinal drift of starspots during an activity cycle on the differentially rotating star. Since the most spotted area moves from high latitudes to the equator, so the period of spotted variability decreases because velocity of differential rotation increases forward to the equator. As a result of this process, the systematic O-C variations appear. With a new activity cycle, the process repeats itself.

Condensed Matter

IL9905610

Coherent Vortex Motion and Josephson-like Effects in Periodically Modulated Superconducting Thin Films.

Grzegorz Jung

Dept. of Physics, Ben Gurion University of the Negev, Beer Sheva

Josephson effects with pure sine current-phase relationship persist only in weak-links having dimensions of the order of the superconducting coherence length. Voltage states observed in experimentally achievable high-T_c bridges are not related to the Josephson effects but to the dissipation caused by movements of Abrikosov vortices. Vortices of opposite sign nucleate at strip borders move toward the bridge center and annihilate. In bridges smaller than the effective penetration depth of magnetic field interactions between vortices cause highly coherent vortex motion resulting in appearance of Josephson-like effects. With increasing bridge size vortices start to penetrate simultaneously at different positions along the macrobridge edges. Non-homogeneity and intrinsic pinning lead to differences of velocities along different channels of vortex motion and coherence in vortex motion breaks down.

Artificial pinning proved to be extremely useful technique in studies of vortex matter dynamics. The commonly exercised way of changing the pinning properties consists in introducing additional quenched disorder to the specimen. Recently the general interest shifts towards effects of ordered artificial periodic pinning structures. Current driven vortices interacting with periodic pinning exhibit a number of novel plastic flow phases not observed in random pinning. Most importantly, the periodic pinning is capable to enforce coherence in current driven vortex motion. Quasi Josephson effects may be thus employed as an efficient tool for probing vortex matter dynamics, while a system of Abrikosov vortices current driven across a periodic potential structure can offer a possible alternative for weak-link Josephson devices operating at liquid nitrogen temperatures.

Shapiro-like steps in quasi-Josephson effects result from locking of the vortex flow to the frequency of externally applied ac signal. In a system with periodic pins one should possibly observe similar effects even in the absence of any applied signal. Self-induced current steps on samples I-V characteristics should appear whenever vortex creation frequency matches any harmonics of the self-frequencies of the system set by the time of flight across the magnetic period and the time of flight across the sample width.

In the talk we shall report on investigations of self induced Shapiro-like steps in vortex motion across reversible and controllable periodic pinning structures imposed by spatially non-homogeneous magnetic field of a pre-recorded magnetic tape placed on a surface of the superconductor. The pinning strength and periodicity are controlled by the frequency and amplitude of the pre-recorded signal. We provide experimental evidence for self-induced Shapiro-like steps and provide a theoretical picture describing the experimentally observed phenomena.

IL9905611

Quantum Turbulence and Resonant Tunneling

Mark Ya. Azbel'

School of Physics and Astronomy,
** Tel Aviv University, Tel Aviv*

Tunneling of the Hartree liquid through opaque potential barriers separated by a well is considered. It is always unstable and is related to three distinctly different time scales. The shortest one is the period of classical oscillations in the well. It determines the period of tunneling current oscillations. Instability and specifically quantum turbulence develop on the scale of the quantum dwell time in the well. Dissipation yeilds the largest time scale. Analytical and numerical solutions are presented, and possible experiments are discussed.

IL9905612

Chaos and Interactions : Statistics of Hartree-Fock Levels in Small Disordered Systems

Roi Hadar, Shimon Levit, Dror Orgad

Dept. of Condensed Matter Physics, The Weizmann Institute of Science

We study the statistics of quasiparticle and quasihole levels in small disordered systems with interactions. In the Hartree-Fock approximation the distribution $P(s)$ of energies of the lowest particle-hole pair (level spacings of the Hartree-Fock levels on both sides of the Fermi energy) deviates drastically from the predictions of the Random Matrix Theory. We present theoretical considerations and numerical investigation of these deviations. We pay special attention to the spin and exchange effects in the unrestricted Hartree-Fock theory and make comparison with the exsisting data on the statistics of the Coulomb blockade peaks.

[1] S. Levit and D. Orgad, manuscript in preparation.
[2] R. Hadar, S. Levit and D. Orgad, work in progress.

IL9905613

Nonequilibrium Effects in the Tunneling Conductance Spectra of Small Metallic Particles

Oded Agam

The Racah Institute of Physics, The Hebrew University, Jerusalem 91904

Recent experiments on the tunneling spectra of small metallic grains revealed an unusual structure of the differential conductance peaks. The peaks appear in clusters, or develop a substructure as the gate voltage changes. These features are manifestations of nonequilibrium behavior. Electron-electron interactions play an important role in determining the magnitude and the energy scales of the phenomenon. For normal grains, each cluster of resonances is identified with one excited single–electron state of the metal particle, shifted as a result of the different nonequilibrium occupancy configurations of the other single–electron states. Assuming the underlying classical dynamics of the electrons to be chaotic, the typical shift is δ/g where δ is the single particle mean level spacing and g is the dimensionless conductance of the grain. For superconducting grains in the odd charging state, the substructure of the first resonance is explained by nonequilibrium "gapless" excitations associated with different energy levels occupied by the unpaired electron. These excitations are generated by inelastic cotunneling.

Condensed Matter IL9905614 *Invited*

Itinerant Magnetism in the Limit of Strong Electron Correlations: Mainly $SrRuO_3$

Lior Klein

Dept. of Physics, Bar-Ilan University, Ramat Gan 52900

A central challenge in solid-state physics is elucidating the properties of metals with strong electron correlation; particularly, when the correlations are strong enough to destroy the effectively free electron state of a typical metal, as described by Fermi liquid theory. A well known manifestation of electron correlations is itinerant magnetism (i.e., magnetism of the conduction electrons); hence, itinerant magnets are a natural choice for studying effects of strong electron correlations. Hitherto, however, much effort has been focused on studying itinerant magnets that (despite the electron correlations) maintain their Fermi liquid state (e.g., Fe, Ni, Co), while very little has been done to identify and study itinerant magnets in which the electron correlations are sufficiently strong to cause a non-Fermi liquid behavior.
In my talk I will concentrate on the recent study of the itinerant ferromagnet $SrRuO_3$. I will present transport[1], magnetization[1], optic[2], and magneto-optic[3] data and discuss the possibility that $SrRuO_3$ is an example of an itinerant ferromagnet driven to non-Fermi liquid behavior by strong electron correlations. I will also address implications to other "suspected" non-Fermi liquid metals such as the high-T_c superconductors.

[1] L. Klein, J. S. Dodge, C. H. Ahn, G. J. Snyder, T. H. Geballe, M. R. Beasley, and A. Kapitulnik, Phys. Rev. Lett. **77**, 2774 (1996); L. Klein, J. S. Dodge, C. H. Ahn, J. W. Reiner, L. Miéville, T. H. Geballe, M. R. Beasley, and A. Kapitulnik, J. Phys. Condens. Matter **8**, 10 111 (1996); L. Klein, J. S. Dodge, T. H. Geballe, A. Kapitulnik, A. F. Marshall, L. Antognazza, and K. Char, Appl. Phys. Lett. **66**, 2427-9 (1995).
[2] P. Kostic, Y. Okada, Z. Schlesinger, J. W. Reiner, L. Klein, A. Kapitulnik, M. R. Beasley, and T. H. Geballe (preprint).
[3] J. S. Dodge, L. Klein, C. H. Ahn, J. W. Reiner, L. Miéville, T. H. Geballe, M. R. Beasley, A. Kapitulnik, H. Ohta, Yu. Uspenskii, S. Halilov, and E. Kulatov (submitted).

Hybridization of localized and density modes in superfluid Helium 4

Nir Gov and Eric Akkermans

Physics Department, Technion, Haifa

We present a new approach for studying the energy spectrum of superfluid Helium 4. It is based on the assumption that there exist localized modes in addition to the usual Feynman density fluctuations (phonons). They correspond to the short range behaviour in the liquid where effects of quantum statistics are important. We describe in a phenomenological way the hybridization of those two kinds of excitations and we compare the resulting energy spectrum with experimental results, e.g. the structure factor and the single excitation scattering intensity. We also predict the existence of another type of excitation interpreted as a vortex loop. The energy of this mode agrees both with the Raman scattering data and critical velocity experiments of Varoquaux et al..

IL9905616

Wide Band-Gap Materials for High Power Electronics

Shlomo Rotter

A. R. T. Division, Soreq NRC, Yavnel 81800

The wide-gap semiconductors are the basis for the third generation of microelectronics and specially for the high end of the temperature range. In this presentation we will review the prospects and status of two members of this group: Diamond and Silicon Carbide (SiC). The two are at different stages of technological development and their respective modes of application at present are quite different. SiC devices can operate at up to 1050C! High power and high frequency devices have been demonstrated. Diamond is not yet ready for real electronic devices but its many extreme properties find their applications in several cases. The prospects of the future applications will be described in view of the semiconducting characteristics of these materials.

An Experimentalist's View of Quantum Phase Transitions

Dan Shahar

Dept. of Condensed Matter Physics, Weizmann Institute of Science

A careful investigation of the transport near quantum Hall transitions and near the new metal-insulator transition in two-dimensional systems reveals possible flaws in the basic theoretical framework with which we perceive these transitions. I will present a summary of our results, emphasizing their implications on the quantum-critical theoretical approach, and also on our understanding of the phases involved.

Duality Transformation in a Three Dimensional Conducting Composite with Two Dimensional Periodic Columnar Microstructure and an In-Plane Magnetic Field

David J. Bergman and Yakov M. Strelniker

School of Physics and Astronomy, Raymond and Beverly Sackler Faculty of Exact Sciences, Tel Aviv University, Tel Aviv 69978, Israel

Not long ago, it was first predicted that composites made of a periodic array of inclusions embedded in a conducting host would exhibit a strongly anisotropic dependence on a uniform applied magnetic field **B**, when that field is strong enough [1]. Such behavior, which appears as soon as the Hall resistivity of the host exceeds its Ohmic resistivity, was recently observed for the first time in a thin semiconducting film, in which a periodic array of mesoscopic holes were etched, when a strong magnetic field was applied in the film plane [2]. Nevertheless, many aspects and ramifications of this newly discovered phenomenon have not yet been explored. One of those is the fact that the effect is much stronger in 2D microstructures than in 3D microstructures. The physical reasons for this are now explained using a classical duality transformation which is based upon the fact that a two dimensional (2D) curl-free vector field becomes divergence-free when it is rotated by 90° in the plane, while a 2D divergence-free vector field becomes curl-free when it is similarly rotated. Three dimensional (3D) vector fields usually lack these properties. We show that, for the special case of electrical conduction in a 3D system with a 2D heterogeneity, a non-trivial duality transformation does exist. We use this transformation in order to gain insight about the magneto-transport properties of a two component composite medium of the above mentioned type, and find some surprising results, which are compared with numerical computations on such systems. Finally, instead of inclusions that are *perfect insulators*, we also consider the other extreme situation, namely, a 2D array of *superconducting* rods (with either square or circular cross-section), again embedded in a free electron host. For both types of periodic columnar inclusion arrays, i.e., inclusions that are either perfect insulators or perfect conductors, we find that in a strong magnetic field, the current distributions and angular dependence of the magneto-resistance have a surprisingly rich behavior. In some cases, duality enables us to obtain closed form expressions for the local current distribution and the bulk effective magneto-resistance when $|\mathbf{B}| \to \infty$—all in good agreement with numerical computations.

[1] D. J. Bergman and Y. M. Strelniker, Phys. Rev. B **49**, 16256 (1994).
[2] M. Tornow, D. Weiss, K. v. Klitzing, K. Eberl, D. J. Bergman, and Y. M. Strelniker, Phys. Rev. Lett. **77**, 147 (1996).

Adsorption of Polyelectrolytes and Inter–Colloidal Forces

Itamar Borukhov, David Andelman, Henri Orland*

School of Physics and Astronomy, Tel Aviv University
** Service de Physique Théorique, CE-Saclay, France*

The effect of charged polymers on the interactions between charged surfaces in solution is investigated theoretically. We use mean field theory to derive a self consistent field equation for the polymer order parameter, and a modified Poisson Boltzmann equation for the electrostatic potential [1,2]. The two differential equations together with the appropriate boundary conditions are solved numerically. We use simple scaling arguments to investigate the adsorption characteristics to a single surface in the strong electrostatic regime. We obtain simple expressions for the dependence of the adsorbed amount Γ on the charge fraction p and the salt concentration c_b [3], in good agreement with experiments. Concentration profiles between two charged surfaces are calculated as well and the inter–surface forces are calculated using a generalized contact theorem [4]. We obtain repulsion as well as attraction between equally charged surfaces. The single surface scaling arguments can be generalized for two interacting surfaces. Simple expressions are derived for the polymer contribution to the interaction energy. These expressions agree qualitatively with the numerical results.

[1] Borukhov I., Andelman D. and Orland H., *Europhys. Lett.* **32**, 499, (1995).
[2] Borukhov I., Andelman D. and Orland H., *submitted to Eur. Phys. J. D*
[3] Borukhov I., Andelman D. and Orland H., *Macromolecules*, (in press).
[4] Borukhov I., Andelman D. and Orland H., (in preparation).

IL9905619

NUCLEAR MAGNETIC RESONANCE STUDY of FLUORINE-GRAPHITE INTERCALATION COMPOUNDS

A. M. Panich, S. D. Goren, T. Nakajima*, H.-M. Vieth**, A. Privalov**

Dept. of Physics, Ben-Gurion University, Beer Sheva
** Division of Polymer Chemistry, Kyoto University, Japan*
*** Institute of Experimental Physics, Free University, Berlin, Germany*

To study the origin of semimetal-metal and metal-insulator transformations, localization effects and C-F bonding in fluorine-intercalated graphite C_xF, ^{13}C and ^{19}F NMR investigations have been carried out for a wide range of fluorine content, $3.8 < x < 12.7$. Fluorine spectra for small fluorine content, $x > 8$, are attributed to mobile fluorine acceptor species which are responsible for the increase of electric conductivity in the dilute compound. When increasing the fluorine content to $x \sim 8$ corresponding to the maximum electric conductivity, covalent C-F bonds start to occur. The number of these bonds grows with fluorine content resulting in the decrease in conductivity which is caused by a percolation mechanism rather than by a change in bond length. A difference in ^{19}F chemical shift for fluorine-intercalated graphite C_xF and covalent graphite fluoride $(CF)_n$ has been observed and is attributed to different C-F bonding in these compounds.

The Isothermal Dielectric Relaxation of a Model System of Interacting Dipoles.

V. Halpern

Department of Physics, Bar-Ilan University, Ramat-Gan, Israel.

The properties are examined of a system of dipoles which can be randomly in one of two states, which are called slow or fast according to the rate at which the dipoles in them change their orientation, and in one of two orientations. There is a local interaction between the dipoles such that the rotation of a dipole has fixed probabilities of changing the state of its neighboring dipoles from slow to fast or vice versa. The isothermal relaxation of the system was studied mainly in a mean field approximation, and also by computer simulations. The results show that the non-exponential decay of the system's response function is associated with the fact that initially the decay is due mainly to the depolarization of the dipoles in fast states, while the later stages are associated mainly with the transfer of polarized dipoles from slow to fast states and their subsequent depolarization. This could be a quite general mechanism for non-exponential dielectric relaxation. A comparison between the relaxation of systems for which the populations of the two types of state was and was not initially in equilibrium shows that a time dependent transition rate is not a very useful concept.

Multiquantum Vortices in Conventional Superconductors with Collumnar Defects Near the Upper Critical Field

Gregory M. Braverman, Sergey A. Gredeskul, and Yshai Avishai

Dept. of Physics, Ben-Gurion University of the Negev, Beer-Sheva 84105 ISRAEL

Mixed state or Shubnikov phase of type II superconductors is characterized by penetration of vortices into the sample each one carrying the superconducting flux quantum. Near the upper critical field H_{c2} these vortices form a triangular Abrikosov lattice [1]. A single strong defect is able to pin a vortex. Columnar defects produced with the usage of heavy ion irradiation [2] can serve as such strong pinning centers. The columnar defect is called a short-range one if its radius is less than the Abrikosov lattice constant.

Strong columnar defects may lead to the formation of multiquantum vortices in high temperature superconductors [3]. Such vortices were observed experimentally on submicron artificial holes in mutlilayers Pb/Ge [4]. Multiquantum vortices can also be formed at large pinning centers with radius of order of the penetration length [5].

We show here that columnar defects can also strongly affect the properties of conventional type II superconductors. In such superconductors near the upper critical field even the *short-range* columnar defects cause a strong local deformation of the vortex lattice due to its softening and as a result to the formation of multiquantum vortices.

We consider mainly a superconductor containing a single short-range columnar defect. When the magnetic field approaches to H_{c2} the strength of the defect effectively increases resulting in strong lattice deformation in its vicinity. Initially the Abrikosov lattice is triangular. Therefore the local deformation belongs to one of the two possible symmetry types – C_6 or C_3. In the case of an attractive defect, the vortices can collapse onto this defect with increasing of a magnetic field. As a result, reentering transitions between two local symmetries are possible. For example, at some external field the local vortex configuration C_6 with a single vortex pinned by a defect is preferred over the C_3 configuration with the defect placed at the center of a triangle. But with increasing of a magnetic field the closest three vortices in the C_3 configuration could collapse onto the defect and a C_6–C_3 transition occurs. Now the mostly preferred local configuration is of C_3 type, with a three-quantum vortex on the defect. Further increasing of a magnetic field results in a C_6 type configuration with a seven-quantum vortex at the defect and so on.

In the case of a small concentration of defects (which was realized e.g. in an experiment [2]) these transitions manifest themselves as jumps of magnetization and discontinuties of the magnetic susceptibility curve.

[1] A. A. Abrikosov, Sov. Phys. JETP, **5**, 1174, (1957);
[2] L. Civale, A.D.Marwick, M.W. McElfresh, T.K. Worthington, A.P. Malozemoff, F.H. Holtzberg, J.R. Thompson, M.A. Kirk, Phys. Rev. Lett. **65**, 1164 (1990);
[3] A.I. Buzdin, Phys. Rev. B **47** 11416 (1993);

[4] M. Baert, V.V. Metlushko, R. Jonckheere, V.V. Moshchalkov, Y. Bruynseraede, Phys. Rev. Lett. **74**, 3269 (1995);
[5] I.B. Khalfin, B.Ya. Shapiro, Physica C **202**, 393 (1992).

A Model Ground State of Polyampholytes

Shay Wolfling, Yacov Kantor

School of Physics and Astronomy, Tel Aviv University, Tel Aviv 69978, Israel

The ground state of randomly charged polyampholytes (polymers with positive and negatively charged groups along their backbone) is conjectured to have a structure similar to a *necklace*, made of weakly charged parts of the chain, compacting into globules, connected by highly charged stretched 'strings'[1,2]. Kantor and Ertaş [3] attempted to quantify the qualitative necklace model, by suggesting a zero approximation model, in which the longest neutral segment of the polyampholyte (PA) forms a globule, while the remaining part will form a tail. Expanding this approximation, we suggest [4] a specific necklace-type structure for the ground state of randomly charged PA's, where all the neutral parts of the chain compact into globules: The longest neutral segment compacts into a globule; in the remaining part of the chain, the longest neutral segment (the 2nd longest neutral segment) compacts into a globule, then the 3rd, and so on.
A random sequence of charges is equivalent to a random walk (RW), and a neutral segment is equivalent to a loop inside the RW. We use analytical and Monte Carlo methods to investigate the size distribution of loops in a one-dimensional RW. We show that the length of the nth longest neutral segment in a sequence of N monomers (or equivalently, the nth longest loop in a RW of N steps) is proportional to N/n^2, while the mean number of neutral segments increases as $\sqrt{N}$. The PA in the ground state within our model is found to have an average linear size proportional to $\sqrt{N}$, and an average surface area proportional to $N^{2/3}$.

[1] Y. Kantor and M. Kardar, Phys. Rev. E **51**, 1299 (1995).
[2] Y. Kantor and M. Kardar, Phys. Rev. E **52**, 835 (1995).
[3] D. Ertaş and Y. Kantor, Phys. Rev. E **53**, 846 (1996).
[4] S. Wolfling and Y. Kantor, Phys. Rev. E, in press (1998).

IL9905623

Density of States in NS Interface With a Barrier and Reflectionless Tunneling

M. Schechter, Y. Levinson, Y. Imry

Dept. of Condensed Matter Physics, Weizmann Institute of Science

We consider a disordered NS junction with a barrier with transmission probability $\Gamma \ll 1$ at the interface. We calculate the local density of states in the system with and without magnetic field, as well as the conductance of the junction. It is shown that in all the above cases the barrier is effective if $\Gamma \ll l_n/\xi \ll 1$, where l_n is the elastic mean free path and ξ is a characteristic length which is energy, ϵ, and magnetic field, H, dependent, and defines the distance from the interface, at which electrons and holes are still coherent. In the opposite limit ($l_n/\xi \ll \Gamma \ll 1$) the barrier, though large, is effectively transparent. We explain this result using path integral picture. We show that the criterion for the barrier to be effectively transparent, is that trajectories that reflect from the interface more than Γ^{-1} times before electron-hole coherence is lost are dominant.This criterion can be applicable to other systems as well, including special cases of ballistic systems.

STM Studies of Superconductor Proximity Systems

Yair Levi and Oded Millo

Racah Institute of Physics, The Hebrew University, Jerusalem 91904

Scanning tunneling microscopy and spectroscopy are employed in order to investigate with nanometer spatial resolution the superconductor proximity effect. The samples are novel superconducting wires consisting of ordered arrays of sub-micron diameter normal metal (N) filaments, either Cu or Ni, embedded in a superconducting (S) NbTi matrix. Two main issues are addressed: 1) The evolution of the superconductor gap as a function of distance from the N/S boundary. We focus on the extent of penetration of superconductivity into N and on the recovery of the gap in S, which is found to occur on a scale much larger than expected. 2) Effects resulting from multiple Andreev reflections at the boundaries between the different constituents, namely, quasi-particle bound states and Tomasch oscillations. Such effects have not been previously studied in a geometry where tunneling takes place in parallel to the N/S interfaces.

Fermi Liquid Properties of a Two Dimensional Electron Liquid Near Van-Hove Singularities

D. Menashe and B. Laikhtman

Racah Inst. of Physics, Hebrew University

In this work we use a standard diagrammatic approach to study Fermi liquid properties of a two dimensional electron system where the Fermi level is near a van-Hove singularity. Contrary to previous works [1], we find that the physics near the Fermi level does not differ much from that of a regular Fermi liquid. Specifically, we find for the imaginary part of the self energy, $\mathrm{Im}\Sigma(\mathbf{k},\omega) \propto \omega/\ln^4\frac{\epsilon_c}{|\omega|}$, where ϵ_c is an ultraviolet cutoff, typically the bandwidth, and ω is measured relative to the Fermi energy. This implies that quasiparticles close to the Fermi level are well defined, just as in the case of a regular Fermi liquid. Furthermore, we find that the quasiparticle weight and the energy spectrum are not renormalized due to the van-Hove singularity, and that the electron-electron interaction is strongly screened. We also discuss the effect of two van-Hove singularities near the Fermi surface, which applies to the cuprate superconductors [2], and find that except for the case of perfect nesting, the above results still apply. The relevance of our work to the physics of high temperature superconductivity is also discussed.

[1] C.C. Tsuei *et al*, Phys. Rev. Lett. **65**, 2724 (1990); C.C. Tsuei *et al*, Phys. Rev. Lett. **69**, 2134 (1992); J. Gonzalez, F. Guinea and M.A.H. Vozmediano, Europhys. Lett. **34**, 711 (1996);
[2] D.H. Lu *et al*, Phys. Rev. Lett. **76**, 4845 (1996) and references therein.

Electron-Electron Scattering Time in General Two Dimensional Electron Systems

D. Menashe and B. Laikhtman

Racah Inst. of Physics, Hebrew University

We present a general method for calculating the electron-electron scattering rate in two dimensional electron systems with arbitrary energy spectrums. When the test electron is near the Fermi surface, and the temperature is small compared to ϵ_F, it is possible to show that the main contribution to the scattering rate comes from selected scattering processes, rather than all processes allowed by momentum and energy conservation. This observation allows us to receive an expression for the scattering rate based only on the geometry of the Fermi surface. We consider different types of Fermi surface geometries and derive the energy and temperature dependence of the scattering rate for each case. If the test electron is near a region of the Fermi surface which has a finite curvature, then the scattering rate is similar to that of a uniform two dimensional electron system. In all other cases the scattering rate is generally much higher. We also consider the scattering rate averaged over all electrons near the Fermi surface. As an example of the application of this method, we consider the scattering rate in a multiple subband quantum well and in a one dimensional surface superlattice.

IL9905627

Influence of paramagnetic centers on the nuclear spin lattice relaxation in NQR experiments

G.B.Furman, S.D.Goren, A.M.Panich, and A.I.Shames
Dept. of Physics, Ben-Gurion University of the Negev, Be'er Sheva

We investigated the influence of paramagnetic centers (PC) on the nuclear spin relaxation in NQR experiments. ^{35}Cl NQR spectra, spin-lattice relaxation times in laboratory and rotating frames T_1 and T_{1e} and spin-spin relaxation time T_2 in $NaClO_3$ have been measured at 77 K for a large range of PI concentration. Paramagnetic centers were developed by g-irradiation with doses of 0.2, 1, 3, 5, 10, 20 and 50 $Mrad$. Nonirradiated $NaClO_3$ sample has been also studied. The amount and origin of PI were controlled by ESR measurements. NQR frequency and line width in nonirradiated sample at 77 K were found to be 30.63245 MHz and 1.2 kHz, respectively. Line width shows linear dependence on the dose of irradiation in the whole range of irradiation, while larger doses result in a deviation of line shift from the linear law. These frequency and line width variations result from the distortion of electric field gradient (EFG); a static broadening may be also caused by the dipole-dipole interaction between the unpaired magnetic moments of the PCs and the magnetic moments of the resonant nuclei. The value of spin-spin relaxation time T_2=0.8 ms does not vary with irradiation within the accuracy of the experiment. Spin-lattice relaxation time T_1 shows no visible changes up to 3 $Mrad$. By fitting the M(t) decay with a stretched exponent given by the expression $M_0\,[1 - Bexp(-(t/T_1)^{\alpha})]$, we found the parameter a around 0.83 [1]. However, further irradiation reduces both T_1 and α. These changes are attributed to the influence of PC and may be explained in the frames of the theory of relaxation via PC in the absence of spin diffusion. Measurements of T_{1e} show that magnetization decay is two-exponential for the delay between pulses > 50 ms and becomes close to one-exponential when reduce the delay < 50 ms. Analysis of one-exponential decay with a stretched exponent shows visible dependence of T_{1e} and α on the dose of irradiation which are attributed to the influence of PI and may be explained in the frames of a theory of relaxation via PC in the presence of spin diffusion. The contribution of spin diffusion is predominating at longer times (t >150 ms) of the M(t) curve. This part of M(t) curve may be fitted by a stretched exponent with α =1 and be regarded to the spin diffusion contribution.

[1]G.B.Furman et al, Phys. Rev. B, **52**, 10814, (1995).

Spin-Locking in One Pulse MNR Experiment

Gregory B. Furman, Alex M. Panich , Shaul D. Goren
Dept. of Physics, Ben-Gurion University, Be'er-Sheva

The response of a nuclear spin system to a long (in comparison to spin spin relaxation time T_2) radiofrequency pulse has been stusied. We observed that the magnetization after the long pulse does not fall to zero at time $t \gg T_2$ for both on-resonance and off-resonance conditions [1]. The dependencies of the magnetization on frequency offset, linewidth, and radiofrequency power are investigated , both theoretically and experimentally. In addition, we also obtain the direction and the value of the effective field, along which the magnetization is locked.

[1] G.B.Furman, A.M.Panich, S.D.Goren, Solid State Nucl.Magn. Res., to be publ.,(1998).

Spin Diffusion and Spin Lattice Relaxation of Dipolar Order in Solids Containing Paramagnetic Impurities

Gregory B. Furman and Shaul D. Goren
Department of Physics, Ben-Gurion University

The phenomena of spin diffusion and spin lattice relaxation of nuclear dipolar order in solids containing paramagnetic impurities (PI) is considered. We show that at the beginning of the relaxation process the diffusion vaninshing regime realizes with non-exponential time dependence [1] , $R(t) \sim \exp\left[-\left(\frac{t}{T_{1d}}\right)^{\alpha}\right]$, where $T_{1d} \sim C_p^{-1/\alpha}$, C_p is PI's concentration. For a homogeneous distribution of PIs and nuclear spins, $\alpha = Q/6$, where Q is the sample dimensionality; for an inhomogeneous distribution, the sample is divided into q-dimensional subsystems, each containing one PI, yielding $\alpha = (Q+q)/6$.This result coincides with experimental data for CaF_2 doped with $0.8 \cdot 10^{-3}$ wt % of Mn^{2+}, where the non-exponential decay of the dipolar signal with $\alpha = 0.83$ has been observed [3]. Fitting the experimental data [3] yields a good agreement with $T_{1d} = 66$ ms . For another independent check of the obtained results we use dependence of the relaxation time on impurities concentration. In accordance that $1/\alpha = 1.2$, we have $T_{1d} \sim C_p^{-1.2}$. Exactly this dependence on impurity concentration of the relaxation time has been found in the experiment [2]. Then the relaxation regime starts as a non-exponential time dependent, proceed asymptotically to an to an exponential function of time, to so called diffusion limited relaxation regime with relaxation time T_{1d}^D is inversely depends on impurities concentration. This kind of relaxation behavior of the dipolar order takes place in the experiment [2]. Using experimental results [2] from this two regime we can estimate the diffusion coefficient of the nuclear dipolar order in CaF_2 , which gives for typical values of impurity concentration $C_p \sim 10^{18}$ cm^3 the diffusion coefficient of dipolar order in the interval $D \sim 10^{-11} \div 10^{-12}$ $\frac{cm^2}{\text{sec}}$, which is coincide to the case of Zeeman energy spin diffusion.[3].

[1] G.B.Furman *et al*, Phys. Rev. B **55**, 439, (1997).
[2] L.J.Humphries and S.M.Day, Phys. Rev. B **12**, 2601, (1975).
[3] G.R.Khutsishili, Sov. Phys. Uspekhi **11**, 802, (1969).

IL9905630

Conductivity and magnetoconductivity below 1K in films of poly(3,4-ethylenedioxythiophene) doped with CF_3SO_3

M. Levin, I. Shlimak, A.N. Aleshin*, R. Kiebooms*, H. Yu*

Jack and Pearl Resnick Institute of Advanced Technology, Department of Physics Bar-Ilan University, Ramat-Gan, 52900, Israel

* *Institute for Polymers and Organic Solids, University of California at Santa Barbara, Santa Barbara, CA 93106, U.S.A.*

The temperature dependence of the electrical conductivity $\sigma(T)$ and the magnetoconductivity $\sigma(B,T)$ of poly(3,4-ethylenedioxythiophene) - PEDOT films heavily doped with CF_3SO_3 has been measured down to 150 mK in magnetic fields up to $B = 9$ T. It is shown that below 1K, $\sigma(T) \propto \ln T$ and $\sigma(B,T)$ depends significantly on the orientation of B parallel or perpendicular to the film surface. These facts are interpreted as a manifestation of two-dimensional character of electron transport in highly doped PEDOT films because of the possible formation of strongly graphitized layers with plane structure of polymer chains or fibrills.

Geometrically-based free-energy functional for confined hard-spheres, and the density functional theory for simple classical systems

Yaakov Rosenfeld

Physics Department, Nuclear Research Center Negev
** P.O.Box 9001, Beer-Sheva 84190*

Some recent developments in classical density functional theory are reviewed briefly, concerning mainly dimensional cross-over, close packed configurations, symmetry breaking, and the freezing transition. The so called Fundamental-Measure Functionals [1]-[3] are based on the fundamental geometric measures of the *individual* hard particles. They were originally derived by seeking an interpolation between the ideal gas and *idea – liquid* limits. Their general behavior depends crucially on their *singularity* at local packing fraction $\eta(\mathbf{r}) = \int d\mathbf{r}'\rho(\mathbf{r}')\theta(R - |\mathbf{r} - \mathbf{r}'|)$ equal one, $\eta(\mathbf{r}) = 1$, where $\theta(x)$ is the Heaviside step function. Several very recent analyses [1]-[3] revealed that the fundamental measure functionals, due to their singularity and their unique structure, have many of the basic physical properties expected from the exact (but unknown!) free-energy functional when applied to densely packed hard-spheres. These properties are important also for applications to continuous ("soft") interactions [4].

[1] Y. Rosenfeld, Phys.Rev.Lett. **63**, 980 (1989); J.Phys.:Cond.Matter **8**, L795, 9289 (1996).
[2] Y. Rosenfeld, et al., J. Phys.: Cond. Matter **8**, L89, L577 (1996); Phys.Rev.E. **55**, 4245 (1997).
[3] P. Tarazona and Y. Rosenfeld, Phys.Rev.E **55**, R4873 (1997).
[4] Y. Rosenfeld and P. Tarazona, Molec.Phys. (the John Barker issue), 1998, in print.

IL9905632

Calculation of critical currents in Josephson Junctions

Ofer Nesher, Eugene Gershnik, Erez N. Ribak
Department of Physics, Technion, Haifa

We were able for the first time to calculate the critical current in a Josephson junction, under the influence of a magnetic field. This was accomplished for the general case and without any preliminary assumptions on the self-induced field. Based on these calculations, we were also able to retrieve the spatial distribution of the critical current in the junction, given its magnetic field dependence [1]. The junction size can be large compared to the global penetration depth λ_J, and the self induced field does not have to be neglected.
The calculation of the critical current as a function of the external magnetic field, $I_c(H)$, is based on the DC Josephson effect. Here the phase difference across the junction is related to the magnetic field [2]. If the spatial distribution of the critical current, $j_c(x)$, is known, then

$$I_c(H) = \left| \int_{-\infty}^{\infty} \mathrm{d}x \; j_c(x) \exp\{2\pi i \; F[j_c(x)]\} \right|$$

We can now calculate numerically a sample of critical currents for simulated distributions. Results can be compared very favourably with calculations made by others [2] under the assumption of a global penetration depth λ_J. In addition, we use the spatial dependence of the penetration depth to yield more accurate results.

[1] O. Nesher and E. N. Ribak, Appl. Phys. Lett. **71**, 1249 (1997).
[2] A. Barone and G. Paterno, *Physics and applications of the Josephson effect*, Wiley (1982).

IL9905633

Metal-Insulator Crossover at B=0 in a Two-Dimensional Hole System

Y. Hanein[1,2], U. Meirav[1], D. Shahar[1,2], H. Shtrikman [1], C.C. Li[2], and D.C. Tsui[2]

[1] *Dept. of Condensed Matter Physics, Weizmann Institute, Rehovot 76100, Israel*
[2] *Dept. of Electrical Engineering, Princeton University, Princeton, New Jersey 08544*

In contrast to the widespread notion that two-dimensional electrons are always localized at zero temperature (T), Kravchenko *et al.*[1] showed that in low-density, high-mobility, two-dimensional electron system in Si-MOSFET's it is possible to observe a transition from an insulating to a metallic behavior. This result was later supported by other experiments on various Si-based structures. We have used variable-density, two-dimensional, hole system in GaAs and investigated its behavior at low T. We found, for the first time in GaAs-based materials, a crossover from an insulating behavior at low-density, to a metallic-like behavior at high-density, in qualitative agreement with the results obtained from Si-based materials. This agreement rules out explanations of the data that are material dependent and implies that a common mechanism to the two systems may be responsible to the observed behavior.
Following a suggestion of Pudalov[2], we explicitly showed[3] that the data in the high-density, metallic-like, range can be fitted with the empiric formula $\rho = \rho_0 + \rho_1 exp(-T_0/T)$. Upon reducing the density this behavior crosses-over to an intermediate regime which is followed, at yet lower density, by insulating behavior.

[1] S. V. Kravchenkoet *et al.*, Phys. Rev. B **50**, 8039 (1994).
[2] V. M. Pudalov, JETP Lett. **66** (1997).
[3] Hanein *et al.*, Phys. Rev. Lett. **80**, 1288 (1998).

IL9905634

Coulomb drag in the quantum Hall $\nu = \frac{1}{2}$ state

Iddo Ussishkin and Ady Stern

Dept. of Condensed Matter Physics, The Weizmann Institute of Science, Rehovot

We consider the Coulomb drag between two two-dimensional electron gas layers subject to a perpendicular magnetic field, with Landau level filling factor being $\frac{1}{2}$. In the limit of weak coupling between the layers, the unique dependence of the single-layer longitudinal conductivity on wavevector leads to a very slow decay of density fluctuations. As a result, the transresistivity ρ_D is much larger than at zero magnetic field (a factor of 10^4 at 1^0K), and has a temperature dependence of $T^{4/3}$ in the clean limit [1]. Within a semiclassical approximation, the transresistivity is slightly decreased when disorder is introduced [2]. In the composite fermion language, the interlayer interaction between transverse current components of the composite fermions is attractive for fermions of opposite momentum. Interlayer pairing is thus expected at low temperatures, and may provide an explanation for the finite drag observed experimentally when the temperature approaches zero [3]. By modeling the interaction by a BCS constant interlayer interaction, we study the contribution of pairing fluctuations to the transconductivity, including both Aslamasov-Larkin and Maki-Thompson like contributions.

[1] I. Ussishkin and A. Stern, Phys. Rev. B **56**, 4013 (1997).
[2] A. Stern and I. Ussishkin, Physica E **1**, 176 (1997).
[3] M. P. Lilly *et al.*, preprint cond-mat/9710041.

IL9905635

DC voltage increment due to AC coupling in a high-TC superconducting coil

N. Shaked, I.A. Al-Omari*, A. Friedman, Y. Wolfus, M. Sinvani, and Y. Yeshurun

Institute for Superconductivity, Department of Physics, Bar-Ilan University, Ramat-Gan 52900, ISRAEL

* *Department of Applied Physical Sciences, Jordan University of Science and Technology, P.O.Box 3030, Irbid, JORDAN*

In this work the interplay between AC and DC currents is investigated in a High-TC Superconducting (HTS) coil. The coil, made of multifilamentary silver-sheathed Bi- 2223 tape, stores energy of 4.2J at 77K where the critical current is 22.2A. We observed that the application of a sinusoidal current component in the frequency range of 50-500Hz into the coil, while it is already carrying DC current in the range of 16- 22.5A, caused an increase in the coil DC voltage. The DC voltage increment due to AC application is found to increase linearly with frequency and quadratically with amplitude. This phenomenon might be caused by the enhancement of flux creep in the HTS filaments due to excitation of pinned vortices by the AC current. The DC voltage increment increases as the coil current grows towards its critical value. A relative increment of 24and 205Hz at the critical current. Clearly, the DC power loss in the coil increases in the same proportion. This result can be important in power applications based on HTS coils driven by a subcritical DC current and loaded by a relatively small AC current such as SMES and FCL.

This research has been supported by the Ministry of Infrastructure, grant 95-11-09. A.F. acknowledges a support from the ministry of science. I.A.A. acknowledges the support from Jordan University of Science and Technology.

Effect of surface and bulk pinning on the distribution of transport current in superconducting film

L.Burlachkov*,V.Ginodman and I.Shlimak

*Institute of Superconductivity, Department of Physics, Bar-Ilan University, Ramat-Gan 52900, Israel

Jack and Pearl Resnik Institute of Advanced Technology, Department of Physics, Bar-Ilan University, Ramat-Gan 52900, Israel

We show, both experimentally and theoretically, that the inhomogeneous distribution of transport current produced by two contacts located at the opposite corners of a square film changes significantly as the film becomes superconducting. We analyze two possible sources for such a re-distribution: (1) the nonlinear dependence of the resistivity on the current density and (2) the effect of surface barriers. In the above geometry these sources have the opposite effect and compete with each other. This technique can be easily modified for various sample/contact geometries and is useful for the analysis of surface and bulk pinning of vortices.

IL9905637

Electrical Field Effect Dependence of Hall Constant in Bi-films

A. V. Butenko, V. Sandomirsky, Y. Schlesinger, and Dm. Shvarts

The Jack and Pearl Resnick Institute for Advanced Technology
Department of Physics, Bar-Ilan University, Ramat-Gan 52900

The Electrical Field Effect (EFE) was investigated on the capacitive structure Au - mica (≈ 10 μm) - Bi films (L $\sim 350 \div 500$ Å) in the temperature region 15 - 100 K. The thicknesses of Bi films lay in the region of the Quantum Size Effect (QSE). The transverse electric fields reach the value of 10^6 V/cm. The corresponding surface carrier concentrations are $n_s \approx 10^{13}$ [e]/cm^2, i.e. the average change of carrier concentration in the 500 Å film is $n_s/L \approx 10^{17}$ cm^{-3}. The latter value is comparable with the original carrier concentration in Bi film, $3 \cdot 10^{17}$ cm^{-3}. However, EFE, the film resistance change ΔR is 0.5 %. On the other hand EFE change of Hall constant (ΔR_H), that was observed for the first time in this work, is 5 - 30 % (depending on the film thickness). These results point to a small carrier mobility and to an essential change of carrier concentration in the EFE influence region (of the order of the screening length). The interpretation takes into account both classical and quantum versions of Bi film behavior under EFE conditions. A procedure to determine the surface charge carrier mobilities and concentrations from EFE-data (both ΔR and ΔR_H) is proposed.

IL9905638

Investigation of the magnetoresistance behavior in high pulsed magnetic fields up to 35T in thick films YBa2Cu3Ox and YBa2Cu3Ox (5%Ag-doped) near by superconductivity transition

Efim Broide* and Mikhail Yakunin

**Building 3,Kiryat Weizmann ,Ness Ziona ,70400, "Separator Ltd" Technological Incubator ,Israel*

Institut of Metal Physics ,Russian Acad.of Science, Ekatirinburg,Russia

The influence of pulsed magnetic fields up to 35T on samples YBa2Cu3Ox and YBa2Cu3Ox (5% Ag-doped) thick films produced after electromagnetic separation HTSC1-2-3 powders was investigated. The field was generated in the multiturned copper wire coil with a semisinusoidal pulse duration of about 10 ms.To measure the magnetoresistivity the sample voltage under the constant current regime was made to an accuracy of $0.5x10^{-6}$ V and minimal time interval of 100 ns. To extract the true signal from the spurious background voltage generated by the pulsed magnetic field ,the previously recorded signals for zero current were subtracted with high precision from the nonzero current signals. After a series of pulses the zero field resistivities as a function of temperature were compared with the initial date to reveal the irreversible changes in samples.

We discovered a non linear behavior in the magnetoresistance of YBa2Cu3Ox after measurements with current greater than $1A/cm^2$ at the temperature 67.4K. However in the specimens with 5% Ag+YBa2Cu3Ox we observed a linear plot of magnetoresistivity and magnetic field at currents less than 20 A/cm^2 at the 77K. In our view the difference in behavior of the two types of samples is a function of the resistivity of granular contacts in polycrystal thick films YBa2Cu3Ox and YBa2Cu3Ox(5% Ag doped).

[1] P.J.M. van Bentum ,H. Van .Kempen .et al. Physica B 155 (1989) 160-163

[2] C.Van .Haesendonck,J,P.Locquet,et al. Physica B155 (1989) 149-155

[3] P.Rodrigues Jr.Ghivelder,P.Pureur and S Reich Physica C 211 (1993) 13-21

Isomers of $(Ca_{0.1}La_{0.9})(Ba_{1.65}La_{0.35})Cu_3O_y$ Superconductor Having Different T_c

A. Knizhnik, G.M. Reisner, A. Men and Y. Eckstein

Dept. of Physics and Crown Center for Superconductivity, Technion, Haifa

$(Ca_{0.1}La_{0.9})(Ba_{1.65}La_{0.35})Cu_3O_y$ is a YBCO like superconductor but tetragonal for any y, i.e. without ordered chains. Its T_c vs y plot has no intermediate plateau and is a nearly straight line in the underdoped region[1]. Different oxygen contents were obtained by oxygenation at various temperatures under 1 atm O_2 followed by quench in liquid nitrogen. This type of oxygenation leads to samples where the oxygen content corresponds to the thermodynamic equilibrium with the gas phase because the form of attaining the oxygenation temperature (from higher or lower temperature) and time (over 10h) of oxygenation do not change y and T_c.
Changing of the firing temperature (we used the usual carbonate-oxide preparation which included 3 firings in powder, pelletization, sintering and oxygenation [1]) changes T_c at the same y. The increase of the firing temperature by 40°C increases T_c by 7-10K while y remains unchanged. Increases of the temperature of sintering virtually do not change T_c which shows that low and high T_c compounds are formed during the first stages of preparation and that there is no thermodynamic equilibrium between them. The low T_c compounds cannot be transformed into high T_c ones by raising the temperature.

temperatures °C of:		oxygenation at 450°C		oxygenation at 380°C	
firings	sinterings	y	$T_c(R)$	y	$T_c(R)$
925	935	6.985	24.7	7.037	40.9
925	965	6.988	26.3	7.031	41.5
935	965	6.981	28.2	7.033	42.3
950	965	6.993*	30.9	7.034	42.6
965	965	6.983	34.3	7.034	48.0

* oxygenated at 440°C

X-ray and neutron powder diffraction showed the compound to be pure with no Ca on the Ba-site[2]. Theoretical calculations showed that isomers with different ratios of the following unit cells: $LaBa_2Cu_3O_y$, $La(BaLa)Cu_3O_y$, $LaLa_2Cu_3O_y$, $CaBa_2Cu_3O_y$, $Ca(BaLa)Cu_3O_y$ and $CaLa_2Cu_3O_y$ may be present in our samples and cause differences up to 22K in T_c.
This research was supported by the Israel Science Foundation administered by the Israel Academy of Sciences and Humanities and by the Center of Absorption in Science, Ministry of Immigrant Absorption, State of Israel.

[1] D. Goldschmidt, A. Knizhnik, Y. Direktovitch, G.M. Reisner, and Y. Eckstein Phys. Rev. **B52**, 12982, (1995) [2] J. Jorgensen. Private communication

A New Method of Preparation of Isomers of the $(Ca_{0.1}La_{0.9})(Ba_{1.65}La_{0.35})Cu_3O_y$ Superconductor with Predicted Maximal T_c

A. Knizhnik, G.M. Reisner, A. Men, and Y. Eckstein

Dept. of Physics and Crown Center for Superconductivity, Technion, Haifa

The 123 superconductor $(Ca_{0.1}La_{0.9})(Ba_{1.65}La_{0.35})Cu_3O_y$ (c) has been prepared by the usual carbonate-oxyde method. After oxygenation to the optimal oxygen doping of y=7.135, the maximal T_c=57K. We prepared (c) also via reaction (1): $0.75La(La_{0.25}Ba_{1.75})Cu_3O_{6.782}+0.25Ca_{0.4}La_{0.6}$ $(La_{0.65}Ba_{1.35})Cu_3O_{6.806}$ + $0.033O_2$ = $(Ca_{0.1}La_{0.9})(Ba_{1.65}La_{0.35})Cu_3O_{6.854}$ (1)

The initial reagents are also superconductors. The first (a) has a maximal T_c=57K, second (b) - 81K. In reference [1] we have shown that several isomers having the same general formula (c), may exist each having different ratios of the following possible unit cells: $LaBa_2Cu_3O_y$, $La(BaLa)Cu_3O_y$, $LaLa_2Cu_3O_y$, $CaBa_2Cu_3O_y$, $Ca(BaLa)Cu_3O_y$,$CaLa_2Cu_3O_y$. These isomers are formed at different temperatures of the preparation of (c) by carbonate-oxyde method [1]. After the formation of compound (c) has been completed, further heating, even to higher temperatures, cannot change one isomer into another. Thus, there is no equilibrium between the (c) isomers and, if there also is no equilibrium in the cases of both isomers (a) and (b), then reaction (1) should not change the ratio of the unit cells. Each cell (i), which is present in (a) in concentration q_i(a), should be present in (c) in concentration $0.75q_i$(a); analogously, each cell (i) which is present in (b) in concentration q_i(b) should be present in (c) in concentration $0.25q_i$(b). According to the cluster component method, [2], $T_{c,max} = \Sigma q_i T_i$, where T_i is $T_{c,max}$ of such a hypothetical sample, which contains cells (i) only. Thus the expected $T_{c,max}$ of (c), prepared via reaction (1), is: $\Sigma 0.75q_i(a)T_i + \Sigma 0.25q_i(b)T_i = 0.75 \times 57 + 0.25 \times 81 = 63$K, i.e. higher by 6 degrees than the T_{cmax} of (c) prepared by the usual method.

We studied reaction (1) via X-ray diffraction. XRD spectra showed that the intensity of the reagents peaks decrease with the time of the reaction and after 100 hours at 950°C only peaks of (c) remain (having the same width as the peaks of (c) prepared via the usual method). After oxygenation to the optimal oxygen doping ($y = 7.137$) we found that its maximal T_c was 63K as predicted.

This research was supported by the Israel Science Foundation administered by the Israel Academy of Sciences and Humanities and by the Center of Absorption in Science, Ministry of Immigrant Absorption, State of Israel.

[1] A. Knizhnik, G.M. Reisner, A. Men, and Y. Eckstein. Isomers of $(Ca_{0.1}La_{0.9})(Ba_{1.65}La_{0.35})Cu_3O_y$ superconductor having different T_c. Submitted to IPS98. [2] A.N. Men, M.P. Bogdanovich, Yu. P. Vorobiev, R.Yu. Dobrovinsky, V.M. Kamishev, V.B. Fetisov. Composition-property of defect solid phases. Cluster component method. Nauka, Moscow, 1977 (Russ.).

IL9905641

Mechanism of Oxygenation of $Hg_nBa_2CuO_{3+n+x}$

A. Knizhnik, G.M. Reisner, Y. Direktovich, D. Goldschmidt and Y. Eckstein

Dept. of Physics and Crown Center for Superconductivity, Technion, Haifa

We prepared pure Hg1201 with some deficiency in Hg (n=0.96-0.97) and $x = 0.030 - 0.034$ by the reaction of dry oxides in the 121 ratio in an ampoule. At 1 atm O_2 oxygenation the deficiency of Hg in the sample increases, but in the 1201 phase it remains nearly constant due to the decrease of the phase content through BaO_2 formation. The content of peroxide (determined by calibrated X-ray powder diffraction and Rietveld calculations [1]) increases with the temperature of oxygenation. No other impurities (up to 620°C) were detected. Thus, the Cu content is > 1 in the phase (this was also confirmed by Rietveld [1]). The equation of the reaction is: $Hg_nBa_2CuO_{3+n+x}$+ 0.5 $(z - 0.5zw + m + w - n - x)O_2 = (n - m)$Hg+$z$ BaO_2 + $(1 - 0.5z)Hg_{m/(1-0.5z)}$ $Ba_2Cu_{1/(1-0.5z)}O_{2+((1+m)/(1-0.5z))+w}$ The Cu and oxygen contents x and w were determined by iodometric microtitration. The presence of peroxide requires, in addition to the usual titrations of type A and B [2], further titration after the decomposition of the peroxide by $KMnO_4$ and the decomposition of the excess of $KMnO_4$ by heating with HCl. The oxygen and Cu contents in YBCO, determined in the mixture of YBCO and BaO_2 (up to 0.06 BaO_2 per 1 Cu), were in good agreement with those determined without BaO_2. The Hg content, found by the recalculation of the Cu content, was close to that obtained from Rietveld [1]. The superconductive transitions were sharp and single (only for the first sample a small step on the χ' vs T graph was observed). $dT_c/dV = 340$ was obtained from T_c vs w graph ($V = 2 + 2w$ is the average copper valence). It is near to the values of 370-460 for the tetragonal 123 superconductors CLBCO [3]. In the table: t°C-temperature of oxygenation, ρ is in $m\Omega$·cm, S - thermopower at 290-295K, μV/K; subscript k - for magnetic susceptibility

No.	t°C	m/ (1-0.5z)	z	w	$T_c(R)$	ΔT_c	T_0	ρ	T_k	ΔT_k	S
1	360	0.96	0.007	0.073	97.8	1.0	96.4		96	1	1.3
2	380	0.96	0.01	0.073	95.2	0.7	94.5	2.1	95.1	1	3.6
3	450	0.96	0.025	0.057	89.4	0.8	88.6	2.0	88.1	0.3	7.5
4	520	0.95	0.025	0.048	81.4	1.1	79.8	3.2	79.7	1.5	14.4
5	620	0.96	0.046	0.039	76.0	2.2	73.8	3.2	73.8	2.2	20.8
6	620*	0.92	0.065	0.045	76.1	1.6	74.5	3.0	75.4	3.7	19.6

* - long time of oxygenation.

The lattice constants were practically constant for the series of compounds studied: No. 1: $a = b = 3.883$; $c = 9.535\AA$. No. 2: $a = b = 3.881$; $c = 9.529\AA$. No. 5: $a = b = 3.884$; $c = 9.536\AA$. No. 6: $a = b = 3.883$; $c = 9.533\AA$

[1] E. Gartstein and D. Mogiljanskij. Private communication [2] A. Knizhnik, Y. Direktovich, D. Goldschmidt, and Y. Eckstein. Supercond. Sci. Technol. **6**, 209 (1993) [3] D. Goldschmidt, A. Knizhnik, Y. Direktovitch, G.M. Reisner, and Y. Eckstein. Phys. Rev. **B52**, 12982, (1995)

IL9905642

Josephson, von Klitzing and reformulation of SI in terms of VAms

S.I. Ben-Abraham

Department of Physics, Ben Gurion University,
POB 653, IL-84105 Beer-Sheba, Israel

The International System of Units (SI) comprises at present seven base quantities and their units. (1) length meter (m); (2) mass - kilogram (kg); (3) time - second (s); (4) electric current - ampere (A); (5) thermodynamic temperature kelvin (K); (6) amount of substance - mole (mol); (7) luminous intensity candela (cd). The choice of base quantities and units is a matter of convenience, convention and compromise. Temperature could be measured in units of energy. The mole is, in fact, a number. The candela is a concession to photometry and is defined in terms of the first four units to which I confine myself. They are all defined by natural standards except for the kilogram which is still based on an artificial prototype and has an anomalous name comprising a multiplicative prefix.

The discoveries of the Josephson and Quantum Hall Effects opened up new avenues to the definition of base units in terms of fundamental constants. When the Josephson and von Klitzing constants achieve a precision surpassing that of comparing weights the SI base units will have to be redefined and the traditional kilogram abandoned. I propose to choose as base units the quadruple: **volt (V), ampere (A), meter (m), second (s)**. My reasons are as follows. Geometry involves only powers of length, hence its base unit is the meter. Kinematics introduces time and thus adds the second. Dynamics comprises mass, force, energy, power etc. The appropriate units can be conveniently defined in terms of the volt and ampere, the watt providing the bridge: W := V·A. In all of mechanics V and A always occur only in the combination (VA). The great advantage of this scheme comes to light in electromagnetics. The electromagnetic duality ($\vec{E} \leftrightarrow \vec{H}, \vec{B} \leftrightarrow \vec{D}$, etc.) is simply expressed by the interchange V↔A

The primary unit should remain the **second** as defined by the cesium (or any improved) atomic clock. The ac Josephson effect allows to define the **volt** via the Josephson constant whose agreed value at present is $K_{J-90} = 4,835979 \times 10^{14}$ Hz/V. The integral quantum Hall effect defines directly the **ohm** in terms of the von Klitzing constant K_{K-90} 25812, 807Ω. However, it is preferable to define as base unit the **ampere** by A:=3D $V/\Omega = (\{K_J\} \cdot \{K_K\})/(K_J \cdot K_K s)$. There can be no objection to this oblique definition. Even the **meter** is defined indirectly through the second and the speed of light in vacuum c.

A variant of this scheme might utilize the weber (Wb≡Vs) and the coulomb (C≡As) rather than the volt and the ampere. The weber would then be given directly by the inverse Josephson constant while the coulomb would be the inverse product of both K_J and K_K. This might be more appealing from a fundamental point of view since the base quantities would be the magnetic and electric charges (or fluxes) making the action their simple product. Yet I maintain that the **VAms** scheme is the simplest and most advantageous from a practical point of view.

IL9905643

Local Magnetization Measurements in High-T_c Superconductors

D. Giller, Y. Abulafia, R. Prozorov, Y. Wolfus, A. Shaulov, and Y. Yeshurun
Institute of Superconductivity, Department of Physics, Bar Ilan University, Ramat Gan, 52900 Israel

We present measurements of the local magnetization in high-temperature superconductors, focusing attention to dynamic and thermodynamic transitions in their magnetic phase diagram. In particular, *local* electric field vs. current density (E-j) curves were measured in $YBa_2Cu_3O_{7-d}$ and $Nd_{1.85}Ce_{0.15}CuO_{4-d}$ single crystals using a miniature Hall-sensors array. Measurements in the field range corresponding to the anomalous magnetization peak in these crystals, reveal remarkably different E-j characteristics below and above the peak, indicating a crossover in the flux creep mechanism. Similar E-j behavior, as observed here in $YBa_2Cu_3O_{7-d}$ and $Nd_{1.85}Ce_{0.15}CuO_{4-d}$, is expected universally in every superconductor exhibiting the anomalous peak.

IL9905644

Spin Glass State in Pure SrRuO3

S. Reich, Y. Tsabba and G. Cao*
Dept. of Materials and Interfaces, Weizmann Institute of Science, Rehovot, 76100 Israel
National High Magnetic Field Laboratory, Tallahassee, Florida

The magnetic interactions in ternary ruthenium oxides were studied in details by Ward and co-workers in 1966 [1]; already at that time it was recognized that the ferromagnetism of SrRuO3 is interesting and rather unexpected since the other homologues, namely CaRuO3 and BaRuO3, are not ferromagnetic. It has become clear that there are strong d-p hybridization and that oxygen plays an unusually important role in magnetic properties of SrRuO3.
AC and DC magnetization measurements performed on pure SrRuO3 single crystals suggest a spin glass behaviour below Tf = 163K. This character of SrRuO3 may be due to the strong Ru(4d) - O(2p) hybridization which requires part of the magnetic moment to reside on oxygen sites [2]. The involvement of the oxygen results in frustration, which, in turn, leads to glassy behaviour.

[1] A. Callaghan, C. Moeller and R. Ward, Inorg. Chem. 5, 1572 (1966).
[2] S.E. Nagler and B.C. Chakoumakos, Bull. Am. Phys. Soc. 42, 551 (1997).

Laser and Quantum Optics

Physics of Polymer based Optoelectronic Devices

Nir Tessler

Dept. Of Physics, Cavendish Laboratory
** University of Cambridge, Cambridge CB3 0HE, UK*

Polymers in general and light emitting polymers in particular are now being considered for a wide range of devices. The progress that has been made in the synthesis of these materials and in the understanding of the handling procedure of them, brought us to the point where we can study intrinsic polymer properties in an optoelectronic device. A clear evidence for the material quality was demonstrated when the first polymer based laser was realised using a very simple, and lossy, structure [1]. Another evidence was found in the report of high peak currents ($1KA/cm^2$) and output powers (5mw) of green polymer LED [2]. It was also demonstrated [2] that the polymer was trap free and exhibited the properties predicted [3] for disordered materials.
In this talk, intrinsic polymer properties will be presented as measured in a "running" optoelectronic device and under various experimental conditions/set-ups. Among the experimental results I will describe time resolved optical pump-probe measurements of gain, absorption, and refractive index. To complement the optical-excitation measurements we performed time resolved current induced measurements of the above properties. These two set of measurements allow us to establish the controversial nature of the excited state absorption band in PPV. We support our conclusions through photo-current measurements excited with sub-ps pulses in a wide range of excitation densities.
Finally, we show how better device making procedure can be applied also to polymer based FETs and demonstrate an integrated circuit of polymer transistor driving a polymer LED [4].

[1] N. Tessler, G. J. Denton, and R. H. Friend, Nature 382, 695-697 (1996).

[2] N. Tessler, N. T. Harrison, and R. H. Friend, Adv. Mat. 10, 64-68 (1998).

[3] H. Bassler, G. Schonherr, M. Abkowitz, and D. M. Pai, Phys. Rev. B - Cond. Matt. 26, 3105-3113 (1982).

[4] H. Sirringhaus, N. Tessler, and R.H. Friend, submitted.

New optical traps for laser cooled atoms

Nir Davidson, Roee Ozeri, and Lev Khaykovich
Dept. of Physics of Complex Systems, Weizmann Institute of Science
Rehovot 76100, Israel

We propose and demonstrate a new blue-detuned dipole trap for atoms. A dark ellipsoid completely surrounded by light is created by passing the center of a Gaussian 1 watt Ti-Sapphire laser beam through a holographic phase plate, followed by a focusing lens. Destructive interference creates in the focal plane and along the optical axis a dark region with a diameter of 50 μm and length of 1 mm. This trap was loaded with cold Rubidium atoms released from a Magneto Optical Trap. At a detuning of +1 nm from resonance (with the D_2 line), 10^5 atoms are loaded into the trap. Trap length was measured to be 1 mm, and by time-of-flight techniques the atoms temperature was measured to be 25 μK.
In blue-detuned traps atoms spend most of their time at zero potential. They are thus less exposed to perturbation of the atomic energy levels and to spontaneous emission, in particular for large detunings of the trapping laser [1]. The combination of these factors allows long atomic coherence times and high precision spectroscopy in such traps. As opposed to existing blue-detuned traps [1,2] our new trap uses only one laser beam and is not gravity assisted. Adiabatic changes to the trap geometry and position are therefore simplified.

[1] N. Davidson et. al. ,Phys. Rev. Lett. **74**, 1311 (1995)
[2] T. Kuga, Y.Torii, N. Shiokawa, and T. Hirano, Phys. Rev. Lett. **78** 4713 (1997).

Noise-like Generation in Erbium-doped Fiber Lasers due to Nonlinear Polarization Rotation in Birefringent Fibers

Moshe Horowitz, Yaron Silberberg*

Dep. of Electrical Engineering, Technion, Haifa
** Dept. of Physics of Complex Systems, Weizmann Institute of Science*

Nonlinear polarization rotation in optical fibers can be used to form artificial saturable absorbers, which promote passive mode locking in fiber lasers [1]. In this work we show that when the birefringence in the optical fiber becomes significant, the effect of nonlinear polarization rotation can be used to form a nonlinear optical derivator [2]. When this new nonlinear element is placed inside a laser cavity, it produces new and useful pulsed laser characteristics with a smooth and broad spectrum and a narrow intensity autocorrelation trace. The noise-like mode has significant advantages over the conventional pulsed mode and it may become important in many applications that require bright and broad spectrum sources with low coherence.

[1] M.E. Fermann, Appl. Physics B. 58, 197 (1994).

[2] M. Horowitz and Y. Silberberg, Opt. Lett. 23, 1760 (1997).

Efficient frequency doubling of CW lasers in resonant cavities

Ady Arie

Dept. of Electrical Engineering - Physical Electronics,
** Tel-Aviv University, Tel-Aviv, Israel 69978*

The doubling efficiency of continuous wave lasers can be improved significantly by placing the nonlinear doubling crystal in an external enhancement cavity and locking the laser to the cavity resonance frequency [1]. This technique is suitable in particular for monolithic lasers - e.g. diode lasers, microchip lasers and non-planar ring solid state lasers. Higher efficiencies, new wavelength bands and novel cavity configurations are enabled by the recent development of engineered non- linear crystals such as periodically-poled Lithium Niobate (PPLN) and periodically poled KTP (PPKTP). As an example [2], we recently doubled a 225mW CW monolithic Nd:YAG laser in an external enhancement cavity containing PPKTP crystal with conversion efficiency of 53the single pass efficiency by a factor of 180. In this talk, I will describe the method of resonant doubling as well as the crystal, cavity and servo requirements and will discuss novel configurations for using periodically- poled materials in resonant doubling cavities.

[1] W. J. Kozlovsky, C. D. Nabors and R. L. Byer, IEEE Journal of Quantum Electronics **24**, 913, (1988).
[2] A. Arie, G. Rosneman, A. Korenfeld, A. Skliar, M. Oron, M. Katz and D. Eger, Optics Letter **23**, 28, (1998).

The Quest for Three Dimensional Nanometer Functional Imaging with Light

Aaron Lewis

Division of Applied Physics, The Hadassah Laser Center and The Center for Neural Computation, The Hebrew University of Jerusalem, Jerusalem, Israel

The requirement to functionally probe with ever increasing selectivity and super-resolution biological and other structures is a frontier area in microscopy. Many critical problems today face the same wall of optical resolution that limits optical imaging in various areas of science and technology. These areas include diverse problems from technologial areas, such as microelectronics and information storage to fundamental problems in neurobiology.

Our research efforts over the past decade have been concentrated on trying to develop two optical microscopic techniques that have the potential to resolve with nanometer resolution the morphology, the movement and the function of interfaces associated with biological and non-biological systems. The two super-resolution methods that we have developed are both based ultimately on what is called the optical near-field [1]. All optical microscopes work in the far-field, where the optical element is held many wavelengths away from the object that is to be imaged. The near-field, on the other hand, is a few nanometers from the point in the object that has to be imaged and near-field imaging requires an optical probe of nanometer dimensionality to be brought within the spatially confined region that is to be interogated. The use of such near-field probes in imaging with linear [1-4] and non-linear [5-8] optical processes will be discussed.

The object of this lecture is to show that we are in an age where it is possible to monitor the spatial alterations in systems with the nanometer resolutions that underlie the functionality of many processes associated with critical interfaces on surfaces and even in regions that are deeply recessed.

[1] A. Lewis, M. Isaacson, A. Harootunian and A. Murray, Ultramicroscopy 13, 227 (1984).
[2] K. Lieberman, N. Ben-Ami and A. Lewis, Rev. Sci. Instr. 67, 3567 (1996).
[3] U. Ben-Ami, N. Ben-Ami, G. Fish, A. Lewis N. Tessler, R. Nagar, G. Eisenstein, J. M. Nielsen and A. Moller-Larson, Appl. Phys. Lett. 68, 2337 (1996).
[4] A. Lewis, I. Rousso, E. Khachatryan, I. Brodsky, K. Lieberman and M. Sheves, Biophys. J. 70, 2380 (1996).
[5] J. Y. Huang, Z. Chen and A. Lewis, J. Phys. Chem. 93, 3314 (1989).
[6] O. Bouevich, A. Lewis, I. Pinnevsky and L. Loew, Biophys. J. 65, 672 (1993).
[7] I. Ben-Oren, G. Peleg, A. Lewis, B. Minke and L. Loew, Biophys. J. 71, 616 (1996).
[8] G. Peleg, A. Lewis, O. Bouevitch, L. Loew, D. Parnas and M. Linial, BioImaging 4, 215 (1996).

Size and density effects on the magnetically induced Fano resonances in semiconductors

Shimshon Barad

School of Physics and Astronomy, Tel Aviv University

The quantum mechanical interference between a discrete state and a dense continuum is a fundamental problem in Physics. Known as the Fano interference in atomic physics, it is a prototype of irreversible decay, and one of a few exactly solvable models in many-body theory. Fano interference has recently been observed in the optical absorption of bulk semiconductors in high magnetic fields, where it is the result of Coulomb coupling between degenerate one-dimensional continuum states and magneto-excitons of different Landau indices. In this case one can use the quantum interference to study the hidden parameters of the "real" quasi-continuum, such as the energy spacing, linewidth, and collisional broadening of the lines. Here we demonstrate, experimentally and theoretically, size effects on magnetically induced Fano resonances in GaAs, due to discretization of the quasi-continuum. The transition from a dense quasi-continuum to a sparse quasi-continuum occurs as function of the thickness of the epitaxial layer of GaAs, at length scales which are unusually large for optical experiments. We also study, by amplitude and phase transmission measurements, the effects of excitation density on the Fano interference. A comparison of our experimental observations to an extension of the Fano model allows us to determine the relative contributions of two, usually undistinguished, effects of the photocarriers: the screening of the inter Landau level Coulomb coupling, and the induced collisional broadening of the states.

The Israeli Tandem FEL: Report on Recent Lasing Results and Options for Development of a Wide Spectral Range Radiation Source

A. Gover*, J. Shiloh** , A. Levin***, A. Abramovich*, A. Arensburg*, M. Canter*, M. Cohen***, A. Eichenbaum*, H. Kleinman*, I. Merhasin*, Y. Pinhasi****, A. Rosenberg**, I. Schnitzer**, O. Shahal***, J.S. Sokolowski*, Y. Yakover*

* *Faculty of Engineering - Physical Electronics, Tel - Aviv University, Ramat-Aviv 69978, Israel*
** *RAFAEL - Haifa 31021, Israel*
*** *NRCN - Beer Sheva 84190, Israel*
**** *Faculty of Engineering, Dept. of Electrical and Electronic Eng. The College of Judea and Samaria*

The Tandem - FEL is an Electrostatic Accelerator Free Electron Laser (FEL) operating presently at the mm wavelength regime. It was constructed by the Israeli FEL consortium (including Tel-Aviv University, Rafael, NRCN), who converted the old tandem van-der-Graaff ion accelerator of the Weizman Institute into a high current electron accelerator and modified it to include an internal wiggler and mm wave cavity. This Electrostatic-FEL configuration is the only one that can operate at high average power (potentially MWatts) and the Israeli group was the first to demonstrate pulsed lasing with it (at 1.2 kW power level) [1].
Recently the FEL was re-operated after improvements of its electron-optics, and it is now lasing at saturated pulsed power of 10kW with tuneability range of 40experiments of scientific applications are possible now: spectroscopy of H.T.S.C., intraband quantum well transitions and gas detection for remote atmospheric sensing. Other high average power applications, including sintering of ceramic layers and H.T.S.C. materials and surface treatment of metals, will be possible after an upgrading stage in which the intensity of the FEL will be raised to the 1kW average power level.
The FEL-Consortium examines options to expand the spectral range and pulse waveform of the radiation to make the radiation source useful for a wide scope of scientific and technological users of radiation. Incorporation of a photocathode injector pumped by a high peak power repetitively pulsed solid state laser will enable the FEL to operate in a super-radiant mode, producing ultra short radiation pulses in the mm wave to THz frequency range. The repetitively pulsed solid state laser can be used to produce bright radiation pulse trains also in the UV to X-ray regime, either by using Compton Scattering of the electron beam (Laser Synchrotron Source - LSS) or by use of laser plasma generation. The possibility to generate synchronized pulses of tunable radiation in two diverse ranges of the spectrum (e.g. U.V. and IR) opens the way for a class of pump-probe experimental techniques important in biological and material science research.
Recent experimental results of high power operation of the tandem - FEL will be presented.

[1] A. Abramovich et al, Appl. Phys. Lett. 71, 3776 (1997)

Lasing Without Inversion via Control of Coherence and Decay in Cavities

A. G. Kofman and G. Kurizki

Chemical Physics Department, Weizmann Institute of Science

Lasing without inversion (LWI) in multilevel atoms has been the subject of vigorous and highly successful investigations, in view of its potentially important applications. The simplest generic scheme of LWI, based on the Λ-configuration, consists in lasing of a weak probe that couples a coherent superposition of two lower states to an upper state, which is less populated than the two lower ones. This superposition, which is induced by coherent mixing of the lower states in the Λ-configuration, is the key to LWI: it gives rise to two interfering channels of resonant absorption. In the scheme proposed here atomic (or molecular) beams are injected into cavities or strong fields, where the lower state becomes split into a coherent superposition of two dressed states with the appropriate relative phase. We demonstrate the possibility of simply and effectively controlling the inversionless gain between two excited states in a ladder configuration. The control is effected by the decay and dephasing rates of the lower state and the resonant cavity mode (or, in the case of the strong field, the auxiliary state). This scheme is expected to be robust under conditions of non-selective pumping of adjacent excited states.

Pump-Probe Spectroscopy of H-bonds as the Level-Crossing Problem

A. I. Burshtein, B. M. Chernobrod, and A. Yu. Sivachenko

Dept. of Chemical Physics, Weizmann Institute of Science

Saturation of the H-bond absorption spectra by a strong laser field is described as a level-crossing problem with diffusional motion along the reaction coordinate.
The stationary populations of the ground and excited vibronic states were found assuming that the light induced transitions between them occur only at the point of exact resonance and the non-radiative decay of the upper state is uniform. The stationary distributions in both states are also obtained and shown to be Gaussian at slow vibrational relaxation but essentially distorted when relaxation is faster than diffusion.
The absorption spectra of the weak probe light in the framework of two-level and three-level models are calculated, which show either loss or gain in different spectral regions. The existence of bleaching and superabsorption branches in corresponding transmission spectra are confirmed. After the pumping is switched off the complex transformation of the absorption spectrum is traced during the evolution of the system to equilibrium.

Three dimensional focusing of cold atoms with on-resonance laser pulse

Lev Khaykovich, Nir Davidson
Dept. of Physics of Complex Systems, Weizmann Institute of Science, Rehovot 76100, Israel

Dense and cold atomic clouds free from of external perturbing fields are desirable in many applications in atomic physics. A common mechanism for collecting and cooling of thermal atoms, magneto-optical trap, provides highly perturbative environment and restricts the atomic densities due to repulsive light induced atom-atom interaction [1]. Suggestions to improve the atomic density were based on either reducing these interactions [2] or overcome them with much larger trapping forces [3]. They involve spatial or temporal changes of the trap parameters and do not remove the perturbative fields.

We analyze the light induced atom-atom interactions in optically thick atomic clouds and show that when the laser frequency is on resonance with the atomic transition the repulsive force caused by radiation trapping effect is reduced.

Based on this analysis, we propose and demonstrate a novel scheme to compress cold and dense atomic clouds by a short on-resonance laser pulse. The compression force arises from attenuation of the laser beams due to the large optical thickness of the atomic cloud. The following free propagation of the atoms shows a "lens-like" behavior, where at the focal time the atoms concentrate at the center of the cloud. The maximum density is thus achieved in free space without any perturbations of either laser or magnetic fields. Experimental results in three dimensional compression show an increase by factor of $\sim$4 over the maximal density of our trap, and a factor of $\sim$3.5 density increase in one dimension in good agreement with our calculations. Although density increase causes an increase of temperature, the phase space density can be improved by applying a cooling pulse as the atoms approach the focal point. We experimentally show the cooling down to initial temperatures by such off resonance laser pulse.

Applying our compression scheme to atomic clouds with higher initial densities may yield the highest atomic densities possible with optical methods.

[1] T. Walker, D. Sesko and C. Weimann, Phys. Rev. Lett. **64**, 408 (1990).
[2] W. Ketterly, et. al., Phys. Rev. Lett. **70**, 2253 (1993).
[3] W. Petrich, et. al., J. Opt. Soc. Am. B **11**, 1332 (1994).

Laser Frequency Stabilization Using an Optimal Control Loop

Oded Mor, Eran Inbar, and Ady Arie

Dept. of Electrical Engineering — Physical Electronics, Tel-Aviv University

The work presented includes a theoretical analysis of the performance of a frequency-stabilized laser, together with experimental measurements which agree with the theoretical predictions.
We analyze the frequency-stabilized laser using standard tools of control theory. The control loop contains the free-running laser, whose frequency needs to be stabilized, an optical frequency discriminator which generates an error signal, proportional to the laser frequency excursion from the set value, and a servo amplifier which amplifies this signal and feeds it back into the laser (negatively) using a frequency actuator.
If the servo amplifier has infinite gain and infinite bandwidth, the free-running laser frequency noise is completely suppressed. In this case the frequency noise of the stabilized laser is fundamentally limited by the shot-noise and the sensitivity of the discriminator. This current noise is imposed by the servo on the laser as frequency noise.
Under realistic conditions, however, the servo cannot have infinite gain or infinite bandwidth. Furthermore, the existence of loop time delays imposes additional constraints, namely loop stability, which limit the servo gain at all frequencies.
Theoretical analysis has been made [1] for the case of locking to a Fabry-Perot frequency discriminator by the Drever-Hall technique [2], using a proportional + integral (PI) servo amplifier. To experimentally test the analysis, a Nd:YAG laser was locked to a Fabry-Perot super-cavity (finnesse=86,000) with a 3.2 kHz linewidth. Spectral densities of frequency noise of $\approx 3\text{mHz}/\sqrt{\text{Hz}}$ have been achieved, which represent a suppression of 100,000:1 of the free-running laser noise.

[1] O. Mor and A. Arie, "Performance analysis of Drever-Hall laser frequency stabilization using a proportional + integral servo," *J. Quant. Elec.*, **33**, pp. 532-540, 1997.
[2] R. W. P. Drever, J. L. Hall, F. V. Kowalski, J. Hough, G. M. Ford, A. J. Munley, and H. Ward, "Laser phase and frequency stabilization using an optical resonator," *Appl. Phys. B.*, **31**, pp. 97-105, 1983.

Distance measurements using a noisy interferometer

Moshe Ben-Chorin, Silvia Chuartzman, Yehiam Prior
Dept. of Chemical Physics, Weizmann Institute of Science

The spectrum of white light passing through a Michelson interferometer develops sinusoidal modulation, the frequency of which is determined by the path difference between the interferometer arms. Dispersive white light interferometry is capable of measuring relatively large distances (hundreds of μm) with high precision, and without moving parts. However, as all interferometric methods it is very sensitive to phase noise, arising from such factors as vibrations or air turbulence. The random phase jumps reduce the visibility of the white light fringes. This limitation imposes stringent conditions on the stability of the interferometer, and its applicability to field measurements is thus restricted.

We suggest a method to overcome the problem of phase noise. A white light beam and a reference monochromatic light travel through the interferometer along the same path, and thus suffer the same phase fluctuations. The beating between the dispersed white light and the reference beam modulates the contrast of the fringes at half the difference frequency, which is not affected by the phase jumps. To recover the difference frequency, we implement Coherent Observation by Interference Noise (COIN), i.e. we measure the variance of the noisy signal, instead of its average. The phase noise averages the sum-frequency component to zero, and the variance is proportional to the envelope of the fringes. In interferometric measurements in which the contrast of the fringes is important rather than the fringe itself, the COIN signal can eliminate the influence of phase noise. These ideas are demonstrated experimentally, by constructing a surface profiler operating in the presence of air turbulence and mechanical vibrations.

The method can be extended to other synthetic wavelength distance measurement schemes. Furthermore, similar method applied to spatial instead of temporal noise, can be used to overcome incoherent scattering that smears the spatial features of an image.

[1] O. Kinrot, I. Sh. Averbukh and Y. Prior, Phys. Rev. Lett. **75**, 3822 (1995).

1D Toy Model for Trapping Neutral Particles

S. Gov, S. Shtrikman and H. Thomas*
Weizmann Institute of Science, Rehovot, Israel
**Basel University, Basel, Switzerland*

As a further step in our research program on trapping of neutral particles [1,2,3,4] we study the quantum mechanical 1D problem of a spin $S = 1/2$ neutral particle of mass m and magnetic moment $\mu = \gamma \mathbf{S}$ in an inhomogeneous magnetic field $\mathbf{H} = H\hat{\mathbf{z}} + H'x\hat{\mathbf{x}}$ given by the Hamiltonian

$$\mathcal{H} = -\frac{\hbar^2}{2}\frac{\partial^2}{\partial x^2} - \mu \cdot \mathbf{H} = -\frac{\hbar^2}{2}\frac{\partial^2}{\partial x^2} - \mu\left(H\hat{\sigma}_z + H'x\hat{\sigma}_x\right) \tag{1}$$

where $\hat{\sigma}_i$ are the Pauli matrices. This Hamiltonian serves for us as a toy model to study the trapping of neutral particles. Under the adiabatic approximation the precessional period T_{prec} of the spin is small compared to the vibrational period T_{vib} of the particle. We identify

$$K \equiv \frac{T_{\text{prec}}}{T_{\text{vib}}} = \frac{\hbar H'}{2\sqrt{\mu m H^3}} \tag{2}$$

as the small parameter for the perturbation from the adiabatic Hamiltonian of the problem and calculate the life time τ of the particle in its trapped state using Fermi's golden rule. We find that

$$\tau = T_{\text{vib}}\sqrt{\frac{2\pi}{K}}\exp\left[\frac{1}{2K}\right] \quad \text{where } T_{\text{vib}} = 2\pi\sqrt{\frac{mH}{\mu\left(H'\right)^2}} \tag{3}$$

For a neutron ($m \sim 10^{-25}$gr, $\mu \sim \mu_B/1000 \sim 10^{-23}$emu) and for $H'/H = 10$cm and $H = 100$ Oe we find that $K \sim 10^{-5} \ll 1$, $T_{\text{prec}} \sim 10^{-6}$sec, $T_{\text{vib}} \sim 10^{-1}$sec and $\tau \sim 10^{(10^4)}$sec. Our calculation is valid provided $\tau \gg T_{\text{vib}}$. Roughly speaking, the trap no longer works when $\tau \sim T_{\text{vib}}$ which, according to Eq.(3), occur for $K \simeq 0.67$. Interestingly enough we find by classical stability analysis that the trap becomes unstable at $K = 0.5$. We also calculated the effect of viscous friction and found that the system becomes unstable even for an infinitesimally small friction, be it translational or rotational. This is in contrast to the behavior of a particle in a potential well which friction does not destabilize.

Preliminary studies show that behavior similar to what we found in the toy model trap appear also in more realistic magnetic traps such as those used in Bose-Einstein condensation experiments.

[1] S. Gov, H. Matzner and S. Shtrikman, Bullet. of the IPS, **42**, 121 (1996).
[2] S. Gov, S. Shtrikman and S. Tozik, Bullet. of the IPS, **42**, 122 (1996).
[3] S. Gov and S. Shtrikman, Proc. of the 19^{th} IEEE conv. in Israel, 184 (1996).
[4] Flanders, Gov, Shtrikman & Thomas, Bullet. of the IPS, **42**, 44 (1997).

Mass and Tilt Tolerances for Magnetic Top Levitation

S. Gov, H. Matzner and S. Shtrikman
Weizmann Institute of Science, Rehovot, Israel

The dependence of the maximum tilt angle α_{max} on mass m for stable levitation of a spinning magnetic top above an axially magnetized disk and a ring is calculated in the adiabatic approximation. The results given in the figure below show a similar shape of the stability limit for both of these configurations, but the magnitude of the tolerance is much larger for the disk. We recall, though, that the flying height for the ring is about three times that for the disk. Note also that the tolerance is much larger for the standard launch in which the top is left with finite kinetic energy than when this energy is damped out, as we also find experimentally.
Preliminary results of this study were presented at the 1997 annual meeting of the Israel Physical Society at Beer-Sheva [1].

[1] S. Gov, H. Matzner and S. Shtrikman, *Bulletin of the Israel Physical Society,* **43**, 47 (1997).

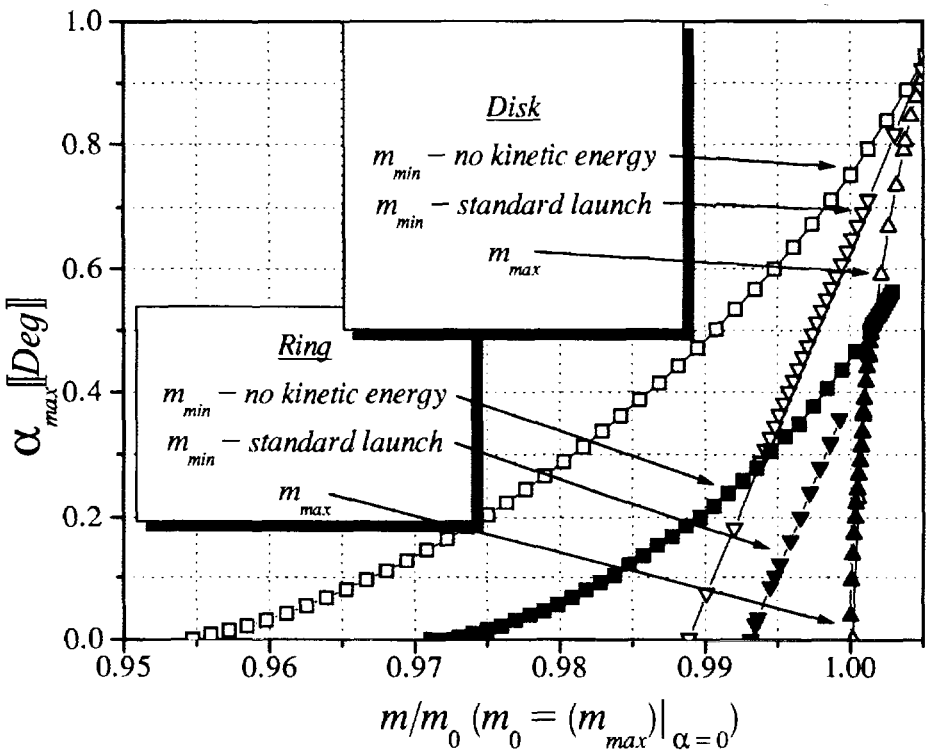

Mass m and tilt α tolerances for magnetic top levitation above a magnetized disk (white shapes) and a magnetized ring (black shapes)

Collective effects in collapses-revivals phenomenon and squeezing in the Dicke model

G. Ramon, C. Brif, and A. Mann

Department of Physics, Technion – Israel Institute of Technology, Haifa

Resonant interaction of a collection of two-level atoms with a single-mode coherent cavity field is considered in the framework of the Dicke model. We focus on the role of collective atomic effects in the phenomenon of collapses and revivals of the Rabi oscillations. It is shown that the behavior of the system strongly depends on the initial atomic state. In the case of the initial half-excited Dicke state interesting phenomena occur which have no single-atom analogs. The correlations between the atoms result in a suppression of the revival amplitude, and the revival time is halved, compared to the uncorrelated fully-excited and ground states. The phenomenon of squeezing of the radiation field in the atom-field interaction is also discussed. For the initial fully-excited and ground atomic states, the field is squeezed on the short-time scale, and squeezing can be enhanced by increasing the number of atoms. Some empirical formulas are found which describe the behavior of the system in excellent agreement with numerical results. For the half-excited Dicke state, the field can be strongly squeezed on the long-time scale in the case of two atoms. This kind of squeezing is enhanced by increasing the intensity of the initial coherent field and is of the same nature as revival-time squeezing in the Jaynes-Cummings model. The appearance of this long-time squeezing can be explained using the factorization approximation for semiclassical atomic states.

Exchange of squeezing and intelligent states for a system of cold trapped ions

C. Brif, G. Ramon, and A. Mann

Department of Physics, Technion - Israel Institute of Technology, Haifa

Exchange of squeezing between internal and motional degrees of freedom is studied for a system of laser-cooled ions in a linear harmonic trap. When the internal and motional subsystems are prepared in properly squeezed (intelligent) states, we find an interesting relation between the quantum noise reduction (squeezing) and the dynamical evolution. More specifically, the evolution of the system is fully governed by the relative strengths of spectroscopic and motional squeezing, including the phenomenon of the total destruction of the interaction when the initial squeezing parameters are equal.

A general theory of phase-space quasiprobability distributions

C. Brif and A. Mann

Department of Physics, Technion – Israel Institute of Technology, Haifa

We present a general theory of quasiprobability distributions on phase spaces of quantum systems whose dynamical symmetry groups are (finite-dimensional) Lie groups. The family of distributions on a phase space is postulated to satisfy the Stratonovich-Weyl correspondence with a generalized traciality condition. The corresponding family of the Stratonovich-Weyl kernels is constructed explicitly. In the presented theory we use the concept of the generalized coherent states, that brings physical insight into the mathematical formalism.

Resonant Scanning Near-Field Microscopy

Boris Chernobrod, Oleg Sedletsky, Ilya Averbukh, and Yehiam Prior

Dept. of Chemical Physics, Weizmann Institute of Science

Scanning Near-field Optical Microscopy (SNOM) is a powerful tool for optical testing on the nanometer-scale range. Combination of scanning probe microscopy (SPM) and high sensitivity fluorescence spectroscopy may provide an extreme detection efficiency combined with a high spatial resolution [1-5].
We report the results of a theoretical study of light scattering from a single resonant molecule near a nano-sized metallic tip of a scanning probe microscope. We investigate in detail the intensity of the scattered light as a function of the lateral and vertical displacements of the tip. The tip is modeled by a small elongated spheroid having a large aspect ratio. Surface enhanced resonant fluorescence of the "tip-molecule complex" is studied under conditions of plasmon resonance. The geometric effect of the tip sharpness has been investigated from the point of view of the spatial localization of the fluorescence signal.
The total dipole polarizability of the "tip-resonant molecule" system is analyzed under conditions of a configuration resonance which result from the coupling of the plasmon excitation in the tip to the molecular optical resonance.
We show that the spatial resolution of the resonantly re-emitted light may reach nanometer, and sub-nanometer scale when using visible, and even IR excitation. The dependence of the signal on the molecular and plasmon resonance detunings has been established, as well as the effect of the tip shape and material composition (i.e., gold compared to silver). Configuration resonances lead to complicated signal spatial dependencies, and may even result in sharp dips in the fluorescence emission at certain positions of the SPM tip. The prospects of using this phenomenon for an increased resolution of the hybrid optical SPM are discussed.
The work is supported by a grant from the Israel Ministry of Science.

[1] J.D. Pedaring, M. Specht, and T.W. Hansch, Proceedings of the NATO Advanced Research Workshop on Photons and Local Probes, Reichenau, Germany, (1994), ed. by O. Marti and R. Moller.
[2] A. Lewis and K. Lieberman, Nature **354**, 214 (1991)
[3] E. Betzig and R.J. Chichester, Science **262**, 1422 (1993)
[4] R. Kopelman and W. Tan, Science **262**, 1382 (1993)
[5] H.F. Hess, E. Betzig, T.D. Harris, L.N. Pfeiffer, K.W. West, Science **264**, 1740 (1994)

Phase considerations in intracavity second harmonic generation optimization

S. Pearl[1], H. Lotem[1], Y. Shimon[1] and S. Rosenwaks[2]

[1]*Laser Department, NRCN, P.O.B. 9001, 84190 Beer-Sheva, Israel*
[2]*Ben-Gurion University, P.O.B 653, 84105 Beer-Sheva, Israel*

In the process of intracavity second harmonic generation, the linear dispersion of the cavity medium is essential. This is due to interference effects between harmonic signals which are consecutively generated in the cavity. Such an interference may cause a strong power modulation of the harmonic waves. The important parameter that affects the efficiency of the harmonic generation is a phase term, Dj, which is the relative phase between the fundamental and harmonic wave. We have experimentally demonstrated power modulation of intracavity second harmonic generated wave by controlling the optical length of the cavity of a Nd:YAG laser. A simple steady-state plane wave numerical model was developed for a case of a double-pass intracavity second harmonic generation. The model takes into account second-order nonlinear interaction, laser gain and a dispersion contribution to the phase difference, Dj, between the fundamental and the harmonic field. The theoretical results are well agreement with our experimental observation of periodic power modulation. The model seems to be useful for a simple control of the harmonic outputs via the two cavity output-coupling mirrors, and in the optimization of the total harmonic power. The model basic considerations may be useful for different types of intracavity nonlinear interactions.

Atomic and Nuclear Physics

On the Relativistic Origin of Pseudospin Symmetry in Nuclei

Amiram Leviatan

Racah Institute of Physics, The Hebrew University, Jerusalem

We review the concept of pseudospin symmetry [1–2] and its role in nuclear spectroscopy [3]. We survey the attempts to arrive at a microscopic understanding of this symmetry [4–6]. In particular, we show that pseudospin symmetry in nuclei could arise from nucleons moving in a relativistic mean field which has an attractive scalar (V_S) and repulsive vector (V_V) potential nearly equal in magnitude but opposite in sign. We show that the generators of pseudospin symmetry are the non-relativistic limit of the generators of an SU(2) symmetry which leaves invariant the Dirac Hamiltonian with $V_S = -V_V$. Furthermore, within this framework, we demonstrate that this symmetry may be approximately conserved for realistic scalar and vector potentials [6]. This work was supported by a grant from the Israel Science Foundation.

[1] K.T. Hecht and A. Adler, Nucl. Phys. **A137** (1969) 129.
[2] A. Arima, M. Harvey and K. Shimizu, Phys. Lett. **B30** (1969) 517.
[3] A. Bohr, I. Hamamoto and B. R. Mottelson, Phys. Scr. **26** (1982) 267.
[4] A. L. Blokhin, C. Bahri and J. P. Draayer, Phys. Rev. Lett. **74** (1995) 4149.
[5] J. N. Ginocchio, Phys. Rev. Lett. **78** (1997) 436.
[6] J. N. Ginocchio and A. Leviatan, Phys. Lett. **B** (1998), in press.

IL9905646

Color Explosion and the Pion Wave Function

R. Weiss-Babai and D. Ashery *

School of Physics and Astronomy, Tel Aviv University

We report results of studies of diffractive dissociation of high energy pions that provide information on the internal wave function of the π meson. These are analogous to studies of Coulomb dissociation of accelerated molecules [1] which provided information about their structure. The $q\bar{q}$ pair fragment, after the dissociation into two jets which carry the momentum of the $q\bar{q}$ pair. By detecting the jets and measuring their momentum we can determine the momentum wave function of the $q\bar{q}$ pair in the pion. For Q^2 values near 10 $(GeV/c)^2$ the asymptotic wave function [2,3] describes well the measured one. The small dimensions of the pion at these Q^2 values allows tests of predicted color transparency effects [4].

* Representing Fermilab E791 collaboration.

[1] Z. Vager *et al.*, Science **244**, 426 (1989).

[2] G.P. Lepage, S.J. Brodsky, Phys. Lett. **B87**, 359 (1979).

[3] A.V. Efremov, A.V. Radyushkin, Theor. Math. Phys. **42**, 97 (1980).

[4] L. Frankfurt, G.A. Miller, M. Strikman, Phys. Lett. **B304** (1993), 1

IL9905647

CERES Results on Low-Mass Electron Pair Production in Pb–Au collisions

E. Socol for the CERES collaboration

Dept. of Particle Physics, Weizmann Institute of Science

CERES is an experiment dedicated to the measurement of low-mass electron-positron pairs and direct photons produced in ultra-relativistic heavy-ion collisions at the CERN SPS. These observables are important probes for studying the dynamics of the collision and in particular, the early stages where formation of the quark-gluon plasma (QGP) and restoration of chiral symmetry are expected to take place. For that, CERES has developed a dedicated spectrometer whose essential components are two Ring Imaging Cherenkov detectors, which are almost "blind" to the hadronic background, and two silicon radial drift chambers.
CERES has completed a systematic research programme including the measurements of electron pairs in p - Be and p - Au collisions at 450 GeV, and S - Au collisions at 200 CeV/nucleon. This systematic approach has revealed a very interesting result – the observation of a strong enhancement, over the known hadronic sources, of low-mass electron pairs in S - Au collisions[1].
Theoretical calculations suggest that a large fraction of the excess originates from the two-pion annihilation channel $\pi^+\pi^- \rightarrow \gamma^* \rightarrow e^+e^-$ providing first evidence of thermal radiation emitted by the high density hadronic matter formed in these collisions. However, in order to fully account for the excess, the models invoke also in-medium modifications of the vector mesons and in particular a decrease of the ρ-meson mass, as a precursor of chiral symmetry restoration.
The new CERES results[2] obtained in 160 GeV/nucleon Pb–Au collisions show also a strong enhancement of low-mass pairs very similar to that obtained in S–Au collisions. A comparison of the results for different multiplicity bins indicates that the excess increases faster than linearly with charged-particle multiplicity. We also present the transverse-momentum distributions of the observed pairs.

[1] G. Agakichiev *et al.* (CERES Collaboration), Phys. Rev. Lett. **75** (1995) 1272.
[2] G. Agakichiev *et al.* (CERES Collaboration), Phys. Lett. B. (in print).

IL9905648

Nuclear medium effects in K and $\bar{K}$ interactions

A. Gal

Racah Institute of Physics, The Hebrew University, Jerusalem 91904, Israel

Medium effects in the interaction of K and $\bar{K}$ mesons with nucleons are reviewed. Recent K^+ nuclear data confirm that conventional multiple scattering models fail to describe the interaction of K mesons for incoming momenta $p_L = 400 - 800$ MeV/c, suggesting a particular form of density dependence for the K nuclear optical potential.

K^- atom strong-interaction data, fitted using a density dependent nuclear optical potential which respects the low-density theorem, require an appreciably stronger attraction than that obtained using a $V_{opt} = t\rho$ form, of order 180 ± 20 MeV at nuclear-matter density. The relationship of this result to the physics of the $\Lambda(1405)$ $\bar{K}N$ unstable bound state is clarified, and the prospects of meeting the conditions for K^- condensation in high-density matter are discussed.

IL9905649

Atomic Collisions and Spectroscopy at the Heavy-Ion Storage Ring TSR

A. Wolf, G. Gwinner, A. A. Saghiri, M. Schmidt, D. Schwalm, J. Kenntner, T. Schüssler, U. Schramm, A. Müller*, T. Bartsch*, A. Hoffknecht*, S. Schippers*, D. W. Savin†, E. Traebert‡

Max-Planck-Institut für Kernphysik, Heidelberg, Germany
* *Strahlenzentrum der Universität, Giessen, Germany*
† *Dept. of Physics, Columbia Univ. New York, U.S.A.*
‡ *Ruhr-Universität, Bochum, Germany*

The storage ring TSR is used to cool and accumulate a wide range of heavy-ion beams produced at the Max-Planck Institute for Nuclear Physics in Heidelberg, Germany. With ionization stages reaching up to 50 (bare nuclei up to Cl^{17+}) and beam energies of typically 5–8 MeV/u, storage lifetimes amount to minutes up to hours; repeated cycles of injection and electron cooling (reducing the ion beam diameter from centimeters to millimeters in about 2 sec) make it possible to accumulate beam currents up to 1 mA in the ring.

With the circulating beam, in particular the interaction of multicharged atomic ions with electrons of variable, well defined energies (10 meV to 3 keV) is studied, detecting recombination and electron impact ionization. High-resolution spectra of the dielectronic recombination cross section have been obtained, which provide a sensitive test for atomic-stucture calculations describing the large number of doubly excited states contributing to the recombination rate. For lithiumlike ions (Si^{11+}, Cl^{14+}) all possible outer- and inner-shell excitations were investigated[1]. Low-energy dielectronic recombination measurements are presently being extended[2] also to more complex open-L-shell ions (Fe^{17+}–Fe^{23+}). Very recently the enhancement of dielectronic recombination by ambient electric fields was studied with Cl^{14+}; at well-controlled fields of order 100 V/cm the enhancement of the cross section by up to a factor of 3 in certain energy regions could be followed in detail[3].

In addition to the information on doubly excited levels from dielectronic recombination experiments, spectroscopic results on multicharged ions were also obtained by laser-stimulated recombination[4], allowing highly excited levels in multicharged ions to be reached by laser transitions from continuum states populated by surrounding free electrons. Moreover, for a number of metastable levels in multicharged ions the natural lifetimes in the millisecond to second range could be determined with high accuracies of about 0.2%, using dielectronic resonances to identify metastable ions and also direct optical observation of vacuum-ultraviolet emission[5].

[1] J. Kenntner et al., to be published
[2] D.W. Savin et al., Astrophys. J. Letters **489**, L115 (1997).
[3] T. Bartsch, A. Müller, S. Schippers, G. Gwinner, M. Grieser, A. Saghiri, G.H. Dunn, H. Danared, D. Schwalm, A. Wolf, M.S. Pindzola, D.C. Griffin, work in progress; see also T. Bartsch, et al., Phys. Rev. Lett. **79**, 2233 (1997).
[4] T. Schüssler et al., Phys. Rev. Lett. **75**, 802 (1995).
[5] H.T. Schmidt et al., Phys. Rev. Lett. **72**, 1616 (1994); J. Doerfert et al., Phys. Rev. Lett. **78**, 4355 (1997).

Dissociative Recombination of HD^+ - State-to-State Experimental Investigation Using Fragment Imaging and Storage Ring Techniques

Z. Amitay, A. Baer, M. Dahan, L. Knoll*, M. Lange*, J. Levin, D. Schwalm*, Z. Vager, R. Wester*, A. Wolf*, D. Zajfman

Department of Particle Physics, Weizmann Institute of Science, Rehovot, Israel.
** Max-Planck-Institut für Kernphysik, D-69029 Heidelberg, Germany.*

When a molecular ion collides with a free electron it can capture the electron and dissociate. The resulting process of *Dissociative Recombination* (DR) is a process of great significance in a wide variety of plasma environments. In this process, the capture of a free electron leads to the formation of an highly excited state of the neutral molecule, which then dissociates into neutral fragments with kinetic energy and, possibly, internal excitation depending on the energy balance of the reaction. Despite its importance, the DR process is still not yet completely understood theoretically. This is mainly due to the complexity of the nature and dynamics of highly excited molecular states, especially when several channels are involved, as is usually the situation in DR. ¿From experimental point of view, for direct comparison between experiment and theory, this complexity requires detailed experimental data, including the knowledge of both the initial state of the molecular ion, to which DR is very sensitive, and of the final quantum states of the DR products. Inherent uncertainties in the initial vibrational excitation of the laboratory molecular ions was the main drawback of the experiments conducted over the years to study DR.
A substantial progress in the understanding of the DR process was achieved with the introduction (about five years ago) of a new experimental approach, which uses heavy-ion storage ring technique. In a storage ring, one can store many molecular ions for a time which is long enough to allow complete radiative deexcitation of the initial electronic and vibrational excitation coming from the ion source. Those *vibrationally cold* ions are then merged with an intense electron beam to measure their DR cross section. Further experimental progress was the inclusion of two- and three-dimensional molecular imaging techniques [1] for the measurement of the *branching ratio* to different *final* quantum states of the neutral DR fragments.
This talk will present results of the next step forward of this method. Rate coefficients and branching ratios were obtained for DR of HD^+ in *selected initial vibrational quantum states* (ν=0–7), and not only in the ground vibrational state. The experiment was carried out at the Test Storage Ring (TSR) located at the Max-Planck-Institut für Kernphysik, Heidelberg with a 2-MeV HD^+ beam. The (initial)-state-to-(final)-state relative DR reaction rates were measured using two-dimensional imaging technique for the detection of the DR fragments. These rates were then converted to rate coefficients using the vibrational population distribution of the stored ion beam, as measured by Coulomb explosion imaging (CEI) of molecular ions which were extracted from the ring. Both measurements were done

as a function of storage time, during the radiative relaxation of the HD^+ molecular ions. Present theoretical predictions are in discrepancy with the data.

[1] Z. Amitay *et al.*, Phys. Rev. A **54**, 4032, (1996).

IL9905651

New results of nuclear transparency to wide angle quasi-elastic scattering

Israel Mardor*

School of Physics and Astronomy, Sackler Faculty of Exact Sciences, Tel Aviv University, Tel Aviv 69978, Israel.

We measured simultaneously pp elastic and quasi-elastic $(p, 2p)$ scattering in hydrogen, deuterium and carbon at incoming momenta of 5.9 and 7.5 GeV/c and center-of-mass scattering angles in the range 83.7^0 to 90^0. We extracted the cross section ratios of quasi-elastic $^{12}C(p, 2p)$ to elastic $^1H(p, 2p)$ (C/H) and quasi-elastic $D(p, 2p)$ to elastic $^1H(p, 2p)$ (D/H). The experiment was performed at the Brookhaven National Laboratory AGS accelerator using the EVA detector (experiment E850). For a detailed descripition of the experiment and the analysis, see Ref. [1].

We determined that at incoming momentum of 5.9 GeV/c, the C/H ratio increases by a factor of 2 from $\theta_{cm} = 89^0$ to $\theta_{cm} = 85^0$, while at 7.5 GeV/c it is consistent with being flat. Further, at $\theta_{cm} = 89^0$ the C/H ratio increases from 5.9 GeV/c to 7.5 GeV/c by more than 50%, while for lower θ_{cm} the incoming momentum dependence is consistent with being flat. The rise of the C/H ratio with incoming momentum is similar to that observed in the previous measurement of the C/H ratio at θ_{cm} near 90^0 [2]. The dependence of the C/H ratio on θ_{cm} was observed in our experiment for the first time. The D/H ratio does not depend on incoming momentum and θ_{cm}. Its absolute value is consistent with unity. The D/H ratio was measured in our experiment for the first time.

The ratios discussed above are directly related to the nuclear transparency of ^{12}C and D. Nuclear transparency is a measure of the initial and final state interactions that the incoming and outgoing protons undergo before and after the main $(p, 2p)$ reaction. The standard approach to nuclear transparency does not depend on the incoming momentum nor on θ_{cm}, in contradiction to the variation of the C/H ratio that we have observed.

The incoming momentum dependence of the C/H ratio that we measured is similar to those of the inverse scaled pp differential cross section $\left(s^{10}\frac{d\sigma}{dt}\right)^{-1}$, where s and t are the Mandelstam variables, and the inverse of the pp spin-spin correlation parameter $(A_{nn})^{-1}$. The θ_{cm} dependence of the C/H ratio is similar to that of $(A_{nn})^{-1}$. On the basis of some models, these similarities may suggest that our new experimental results indicate that the C nucleus filters away non-perturbative QCD components of the pp scattering amplitude.

[1] I. Mardor, Ph.D. Thesis, Tel Aviv University, 1997 (unpublished).
[2] A.S. Carroll *et al.*, Phys. Rev. Lett. **61**, 1698 (1988).

* Current address: Soreq NRC, Yavne 81800, Israel. Representing the E850 collaboration: J. Aclander[1], J. Alster[1], D. Barton[2], G. Bunce[2], A. Carroll[2], N. Christensen[3], H. Courant[4], S. Durrant[2], S. Gushue[2], S. Heppelmann[5], E. Kosonovsky[1], Y. Mardor[1], M. Marshak[4], Y. Makdisi[2], E. Minor[5], I. Navon[1], H. Nicholson[6], E. Piasetzky[1] T. Roser[2], J. Russell[7], S. Sutton[6], M. Tanaka[2] (deceased), J-Y Wu[5]. [1] *Tel Aviv University,* [2] *Brookhaven National Laboratory,* [3] *University of Auckland,* [4] *University of Minnesota,* [5] *Pennsylvania State University,* [6] *Mount Holyoke College,* [7] *University of Massachusetts Dartmouth.*

Nuclear Astrophysics with Beams of Radioactive Nuclei

M. Paul

Racah Institute of Physics, Hebrew University

Quantitative understanding of nucleosynthesis in stellar environment requires knowledge of thermonuclear cross sections on nuclei often outside the valley of stability. For instance, the break-out from the hot CNO cycle towards the rapid proton capture (rp) process, feeding nuclei up and somewhat beyond ^{56}Ni, involves a number of critical channels and gateways for which no laboratory data existed since they involve radioactive targets or projectiles. The development of methods to produce accelerated beams of these nuclei and the advances in highly selective and efficient detection techniques make now possible the direct investigation of such processes. At the ATLAS facility of Argonne National Laboratory, beams of ^{17}F(64.5 s), ^{18}F(110 min) and ^{56}Ni(6.1 d) are used to study important reactions in and out of the CNO cycle. A new resonance found in 19Ne is shown to dominate the reaction strength of the ^{18}F(p,alpha)^{15}O reaction and to drain the ^{18}F population, making the ^{18}F(p,gamma) reaction an unefficient way to break out of the CNO cycle.

Thermodynamic properties of a confining quark model

S. Schmidt[1,2], C.D. Roberts[3], D. Blaschke[2]

[1] *School of Physics and Astronomy, Tel Aviv University, 69978 Tel Aviv*
[2] *Fachbereich Physik, Universität Rostock, D-18051 Rostock, Germany*
[3] *Physics Division, Bldg. 203, Argonne National Laboratory, Argonne IL 60439-4843, USA*

We study the equilibrium thermodynamics of a simple, confining Dyson-Schwinger-equation-model of 2-flavour QCD at finite temperature and chemical potential [1]. The phase boundary between the confined and deconfined phases is defined by the zero of the vacuum-pressure difference. Chiral symmetry restoration and deconfinement are coincident with the transition being of first order, except for $\mu = 0$, where it is second order [1,2]. Nonperturbative modifications of the dressed-quark propagator persist into the deconfined domain. This entails that the Stefan-Boltzmann limit for the bulk thermodynamic quantities is attained only for large values of temperature and chemical potential.
We apply our model to the calculation of the quark condensate and hadronic properties, such as the m_π, f_π, $\pi^0 \to \gamma\gamma$ and m_ρ, and their dependence on temperature and density [3]. Where a comparison is possible, our results confirm those obtained in numerical simulations of lattice-QCD. We note a tendency for quantities that increase with T to decrease with μ.

[1] D. Blaschke, C.D. Roberts and S. Schmidt, Phys. Lett. B, in press, nucl-th/9706070.
[2] A. Bender, G.I. Poulis, C.D. Roberts, S. Schmidt and A.W. Thomas, Submitted to Phys. Lett. B, nucl-th/9710069.
[3] P. Maris, C.D. Roberts and S. Schmidt, Submitted to Phys. Rev. C, nucl-th/9801059,

Fermion Realization of the Symplectic Shell Model and Application to Electron Scattering

Jutta Escher

Racah Institute of Physics, Hebrew University, Jerusalem

Electron scattering experiments provide crucial tests for the applicability and limitations of modern nuclear models and further our understanding of the nucleon-nucleon interaction and its modifications in nuclear matter. A microscopic theory for deformed nuclei, which takes proper account of the exclusion principle as well as inter-shell couplings, is given by the symplectic shell model [1]. In the context of electron scattering it provides a multi-shell realization of the nuclear shell model and allows for a careful study of the relevance of multi-shell correlations. The relevant formalism for symplectic predictions of electron scattering form factors is developed and the effect of multi-shell correlations is investigated. Specifically, the expansion of the charge and current multipole operators in a second quantized fermion representation is reviewed [2]. A recursive process is presented in which symplectic matrix elements of arbitrary one-body operators of exciation $N\hbar\omega$ and $N'\hbar\omega$ in the same or in different symplectic bands are related back to valence shell matrix elements, which can be evaluated by standard shell model techniques [3]. The new formalism is employed to calculate electron scattering form factors for deformed light nuclei, such as ^{24}Mg, and to discuss the significance of multi-shell correlations.

[1] G. Rosensteel and D. J. Rowe, Phys. Rev. Lett. **38**, 10, (1977); D. J. Rowe, Rep. Prog. Phys. **48**, 1419, (1985).
[2] P. Rochford and J. P. Draayer, Ann. Phys. **214**, 341, (1992).
[3] J. Escher, Ph.D. Thesis, Louisiana State University (USA), (1997); J. Escher and J. P. Draayer, submitted.

IL9905654

π^0 Production in pp Collisions near Threshold in a Covariant OBE Model and χPT

E.Gedalin, A.Moalem and L.Razdolskaya

Department of Physics, Ben Gurion University, Beer Sheva

We have calculated S-wave pion production in $pp \to pp\pi^0$ using a fully covariant OBE model, where a boson B created on one of the incoming protons is converted into a neutral pion on the second. The amplitudes for the conversion process $BN \to \pi^0 N$ are taken to be the sum of s, u and t-channel pole terms. The model is consistent with the OBE picture of the NN force and accounts for relativistic effects, energy dependence and nonlocality of hadron interactions. The production rate is found to be dominated by a σ-meson pole in a t-channel.

The off-shell properties of the various partial production amplitudes are taken into account explicitly. For vector and scalar mesons, offshellness is contained in the nucleon form factor and has a marginal influence only. A pseudovector coupling for the pseudoscalar particles, as assumed in this work, introduces an extra factor of q to the amplitude. Consequently for the π and η, each of the s and u nucleon pole terms at $q^2 = -3.3fm^{-2}$ becomes a factor of ≈ 7 higher in comparison with its value on mass shell. To account for the off mass shell behavior of the σ-meson pole term, we have used Adler's consistency conditions and the isospin even π^0p scattering length to determine the $\sigma\pi\pi$ vertex in a rather general form. We have found that the $\pi^0 p \to \pi^0 p$ conversion amplitude off the mass shell is more than a factor ≈ 15 higher in comparison with its on mass shell value. Consequently, the π exchange contribution to the amplitude for the $pp \to pp\pi^0$ reaction dominates the production process and brings the calculated cross section to agree with data.

A meson production in NN collisions necessarily involves large momentum transfer and therefore, two-pion exchanges which describe short range interactions should play an important role. In the OBE model such contributions are represented by an effective scalar σ-meson pole term. In χPT, an approach which is generally believed to be an effective theory of QCD at low energies, such contributions result from one loop two-pion diagrams. We have extended the existing χPT calculations [1] taking into account all tree and loop diagrams up to chiral order D=2. With these one loop contributions added, it is found that the calculated cross section agrees very well with data and with predictions of the present OBE model calculations. In analogy with a dominant σ meson pole term in the OBE model, there are substantial contributions from isoscalar-scalar two-pion t-channel exchanges. We conclude that two-pion exchanges play an important role in the dynamics of π^0 in $pp \to \pi^0 pp$ and by taking these into account the OBE model and χPT approaches reproduce the cross section data.

[1] B.-Y. Park et al., Phys. Rev. **C53**, 1519 (1996). T. D. Cohen et al., Phys. Rev. **C53**, 2661 (1996). T. Sato et al., Phys. Rev. **C56**, 1246 (1997).

The $pn \rightarrow d\eta$ Reaction near Threshold in a Covariant OBE Model

E.Gedalin, A.Moalem and L.Razdolskaya

Department of Physics, Ben Gurion University, Beer Sheva

We use a relativistic covariant one boson exchange (OBE) model to study S-wave η-meson production in $pp \rightarrow d\eta$. The model is consistent with the OBE model picture of the nucleon-nucleon force, allowing for contributions from $\pi, \eta, \sigma, \rho, \omega$ and δ meson exchanges. The amplitudes for the conversion processes $BN \rightarrow B\eta$, where B designating the meson exchanged, are taken to be the sum over s and u-channels with nucleon and nucleon isobar N^* (1535 MeV) in the intermediate states. The model predicts the partial exchange amplitudes up to a relative phase. This model has been applied previously to evaluate the cross section for the $NN \rightarrow NN\eta$ reactions and with all relative phases taken to be $+1$, the model reproduces the cross sections for $NN \rightarrow X\eta$ reactions at energies close to threshold.
Production via N^* (1535 MeV) excitations in the intermediate states dominates the calculate cross sections. In the limit where all η's are produced via N^* excitations, interference terms between pseudoscalar and scalar meson exchanges with terms corresponding to vector meson exchanges cancel out. In practice and contrary to previous model calculations, the π and ρ exchanges add incoherently to the production rate and much of the ambiguities due to unknown relative phases are strongly eliminated. The calculated total cross section corrected to the ηd final state interactions reproduces both the scale and energy dependence of the data fairly well. In view of agreement between the model predictions with data for this process and the $pp \rightarrow pp\eta$ and the $np \rightarrow np\eta$ reactions reported in Ref.[1] we may conclude that the present model accounts fairly well for the dynamics of η production in NN collisions.

[1] E.Gedalin, A.Moalem and L.Razdolskaya, in press in Nucl. Phys. **A**

IL9905656

Near Threshold Production of η' and η in pp Collisions in a Covariant OBE Model

E.Gedalin, A.Moalem and L.Razdolskaya

Department of Physics, Ben Gurion University, Beer Sheva

The total cross section of the $pp \to pp\eta'$ at two energies close to threshold are found to be a factor ≈ 70 lower in comparison with those reported for the $pp \to pp\eta$ reaction[1]. We show that a fully covariant OBE model which explains consistently near threshold data for the $pp \to X\eta$ reactions, also accounts for the production rate of η' as quoted above.

The amplitudes for the conversion processes $BN \to MN$, where B designating the meson ($B = \pi, \eta, \sigma, \rho, \omega, \delta$) and M the one produced are taken to be the sum over s, u and t-channel pole terms (see contribution to this conference by E. Gedalin et al.). The later channel corresponds to meson formation on an internal meson line. In fact because of isospin and parity conservation only δ meson pole in a t-channel contributes to η and η'. To evaluate contribution from such a term we apply the Adler's consistency conditions and partial width of the δ decay into a $\pi\eta$ pair and write the $\delta\eta\pi$ vertex in a quite general form,

$$V_{\delta\eta\pi}(k,q) = m_\delta \left[0.05 - 5.95\,\frac{k^2}{m_\delta^2} - 3.46\frac{q^2}{m_\delta^2} + \; 3.3\frac{(k-q)^2}{m_\delta}\right] , \qquad (4)$$

where q and k are momenta of B and the meson produced M, respectively.

The couplings of the η' are not very well known. These are related through the pseudoscalar octet-singlet mixing to those of the η,

$$G_\eta = G_8 \cos\theta - G_1 \sin\theta, \qquad (5)$$

$$G_{\eta'} = G_1 \cos\theta + G_8 \sin\theta, \qquad (6)$$

where $G_1 \approx G_8$ and $\theta = -23^\circ$ as suggested by the linear mass splitting formula[2]. With the η' constants calculated from this last expression we find the following : (1) the amplitudes for the $\pi^- p \to n\eta'$ and $\pi^- p \to n\eta$ at their respective thresholds are $|f_{\eta'}|^2 = 9.7\ \mu b$ and $|f_\eta|^2 = 380\ \mu b$ in close agreement with experiment. The former amplitude is dominated by a contribution from a t-channel δ-meson pole term, strongly enhanced due to offshellness. (2) the total cross sections for the $pp \to pp\eta'$ at energies Q = 3.7 MeV and Q = 8.3 MeV above threshold are $\sigma = 12\ nb$ and $\sigma = 35\ nb$ in comparison with $\sigma = 19.2$ and $43.6\ nb$ as quoted by Hibou et al.[1]. The calculated cross section corrected for final state NN and η'N interactions is in good agreement with trend of the data.

[1] F.Hibou et al., Preprint IReS 98-05.

[2] Particle Data Group, Phys. Rev.**D50**1173, (1194).

IL9905657

Excitation cross sections of atoms in excited states

L.A.Vainshtein*, Yu.V.Ralchenko

Faculty of Physics, Weizmann Institute of Science
** The Michael Visiting Professor; on leave from Lebedev Physical Institute, Moscow, Russia*

The peculiarities in electron-impact excitation cross sections from excited levels are demostrated on the example of He atom. It is shown that at small energies the first Born approximatin strongly overestimates the cross sections because of the so-called "normalization" (unitarization) effect. For most of transitions this is related to the effect of some other strong transition (usually with $\delta n = 0$). Unlike excitation from the ground state, a very large number of channels is involved here so the interaction of channels is shown to be very important up to intermediate energies. We compare the results obtained in Born and K-matrix approximations with the accurate data calculated within the convergent close-coupling method.

New Methods in nanodosimetry, future tools for understanding radiation damage to DNA

S. Schemelinin, A. Breskin and R. Chechik

Department Particle Physics
Weizmann Institute of Science
Rehovot 76100, Israel.

We present novel methods for precise mapping of ionization patterns deposited by radiation in very small volumes of condensed matter, down to the nanometric scale. Our principal objective is to find new methods and tools for nanodosimetry, that would permit to understand better the causes for irreversible radiation damage to DNA.

The idea consists of individual collection, multiplication and counting of single electrons, or ions, deposited by ionizing radiation in a very dilute millimetric gas cell, used as an expanded model of the nanometric condensed matter. It will provide detailed direct microscopic information on the primary energy transfer process and its fluctuations.

We investigate three experimental approaches, which permit the measurement of ionization patterns on two complementary scales: tens of nanometers, relevant on the chromatin fibre scale, by an electron counting technique and by optical imaging of photon emission from electron avalanches; and tenths of nanometers, most relevant for the DNA, by a new technique of ion counting.

The research work encompasses model simulations of the ionization process and charge transport in very small gas volumes, the conception and realization of nanodosimeters based on electron and ion counting techniques, experimental investigations of ionization and transport parameters in selected tissue-equivalent gases and studies of ion beam interactions with gas samples and living cells.

The methods provide new tools for precise studies of highly fluctuating ionization effects in matter, on scales which are about two orders of magnitude smaller compared to that of presently employed techniques. It will permit, for the first time, to directly correlate gas model experimental data, with radiobiological cell survival data and with microscopic models describing the radiation interaction with DNA. It could have a strong impact on the field of radiobiology, radiotherapy and radioprotection, with possible spinoffs in radiation damage to polymers and to modern solid state devices.

Development of gas avalanche photomultipliers for visible light

E. Shefer, A. Breskin, R. Chechik, A. Buzulutskov[1], G. Garty and M. Prager[2].

Department of Particle Physics, The Weizmann Institute of Science, 76100 Rehovot, Israel.
[1]*presently at BINP, Novosibirsk, Russia*
[2]*ELAM Ltd., Jerusalem, Israel*

We present our work on the development of novel photon detectors, sensitive in the visible light range. They are based on efficient solid photocathodes coupled to modern, pixelized, gaseous avalanche electron multipliers. Gaseous imaging detectors, unlike vacuum photomultipliers, are less limited in their size and shape and can operate under strong magnetic fields. Such devices are very fast and provide high accuracy photon localization. Important applications exist in particle physics and in medical imaging.

The above detection principle has been successfully applied in the UV-light range, with air-stable CsI photocathodes. However, the extension of the sensitivity range towards longer wavelengths is non-trivial, involving vulnerable photocathodes, such as Cs_3Sb and K-Cs-Sb, which cannot withstand even 10^{-5} torr of oxygen. We are studying the detection of visible photons in the range of 250-500 nm, using these alkali-antimonide photocathodes, coated with thin alkali halide protective films. The coating, though attenuating the quantum efficiency, provides protection against chemical reaction with oxygen, humidity and other common detector gases impurities, and makes possible their long term operation in gas media.

We have systematically studied the photoemission from coated photocathodes and we report on our results with alkali-antimonides coated with a variety of thin films of alkali-halides, oxides and organic films. The best performance is of K-Cs-Sb coated with 300Å of CsBr or 250Å CsI. The first has a peak quantum efficiency of 5-8.5% at 312 nm and the latter has a quantum efficiency of $> 4\%$ at 250-325 nm. The alkali-halide coating extends the response of the composite photocathode towards the UV range.

We present the results of exposing coated photocathodes to controlled doses of oxygen and air and show that Cs_3Sb and K-Cs-Sb coated with NaI, CsI and CsBr have good stability in high pressures of oxygen. Some of these photocathodes can withstand the exposure to 150 torr of oxygen for over an hour. This may be considered as a breakthrough in the field, permitting handling of photocathodes in laboratory conditions (glove box for example) and opening the way for realization of the gaseous photomultiplier.

The long-term operation of coated photocathodes under intense photon flux was studied, and we present the results concerning upcharging and aging by photons.

We have studied several gas avalanche electron multiplying elements, based on modern micropattern techniques, e.g. microdot, microstrip and GEM, in view of their possible coupling to solid photocathodes. The main advantage of these amplifying elements in this application is the reduction in ion sputtering of the photocathode, due to the special geometry of the electric field lines. We shall present the results of these studies and discuss possible realistic designs of novel gaseous photomultipliers.

Particles and Fields

Brane Dynamics and Gauge Theory

Amit Giveon

Hebrew University, Jerusalem

We discuss some aspects of the interplay between the dynamics of branes in string theory and the classical and quantum physics of gauge theories with different numbers of supersymmetries in various dimensions.

Duality in String Cosmology

Ram Brustein

Department of Physics, Ben-Gurion University, Beer-Sheva 84105, Israel

Scale-factor duality, a truncated form of time-dependent T-duality, is a symmetry of string effective action in cosmological backgrounds [1,2]. The symmetry suggests a cosmological scenario ("pre-big-bang") in which two duality related branches, an inflationary branch and a decelerated branch are smoothly joined into one cosmology. In this scenario the Universe quickly becomes homogeneous, isotropic, and spatially flat, but quantum fluctuations superimpose on top of the smooth classical background inhomogeneity perturbations, which are then amplified by the accelerated expansion of the Universe and materialize as particles with specific energy spectra later on.

A new duality symmetry is obeyed by the lowest order equations for these perturbations [3]. In some cases it corresponds to a time-dependent version of T-duality, interchanging small and large scale factors [1,2], in some cases it corresponds to a time-dependent version of S-duality [4], interchanging weak and strong coupling and electric and magnetic degrees of freedom, and in most cases it corresponds to a time-dependent mixture of both. As in other applications, duality turns out to be a powerful tool for obtaining results that are inaccessible otherwise. In particular, lower bounds on the energy density of the produced particles.

Our analysis applies to all perturbations that can be described by a massless field Ψ with the following quadratic action $I = \frac{1}{2}\int d\eta\, d^3x\, S(\eta)\left[\Psi'^2 - (\nabla\Psi)^2\right]$. The function $S(\eta)$, sometimes called the "pump" field, is, for any given field Ψ, a known function of the scale factor, $a(\eta)$ and of additional scalar fields such as a dilaton, moduli, etc. The duality symmetry, involves interchanging the perturbation Ψ with its conjugate momentum Π as well as inverting the pump field $S \to S^{-1}$.

The amplification of perturbations is typically associated with a transition from an inflationary phase in which the pump field is accelerated (in cosmic time), to a post-inflationary phase in which the pump field is decelerated or constant. The energy spectrum obtained by truncating the solutions of the perturbation equations to the constant modes, $\frac{d\rho(\omega)}{d\ln\omega} = \omega^4\left[\frac{S_{ex}(\omega)}{S_{re}(\omega)} + \frac{S_{re}(\omega)}{S_{ex}(\omega)}\right] \simeq \omega^4\ \mathrm{Max}\left\{\frac{S_{ex}}{S_{re}}(\omega), \frac{S_{re}}{S_{ex}}(\omega)\right\}$, (where the subscripts ex and re refer to values at "horizon exit" and "horizon reentry") is characterized by a residual duality symmetry, reproduces known results of produced particle spectra, and can provide a useful lower bound on particle production when our knowledge of the detailed dynamical history of the background is approximate or incomplete.

[1] G. Veneziano, Phys. Lett. **B265** (1991) 287.
[3] A. Giveon, M. Porrati and E. Rabinovici, Phys.Rept. 244 (1994) 77.
[3] R. Brustein, M. Gasperini and G. Veneziano, hep-th/9803xxx.
[4] J. Polchinski, Rev. Mod. Phys. 68 (1996) 1245.

– Ram Brustein Department of Physics Phone: +972-7-6472-507 (inside BGU 2507) Ben-Gurion University FAX: +972-7-6472-904 Beer-Sheva 84105,ISRAEL e-mail ramyb@bgumail.bgu.ac.il

The Solar Neutrino Problem in the Presence of Flavor Changing Neutrino Interactions

Sven Bergmann

Dept. of Particle Physics, Weizmann Institute of Science

We study the effects of flavor changing neutrino interactions on the resonant conversion of solar neutrinos. In particular, we describe how the regions in the $\Delta m^2 - \sin^2 2\theta$ plane that are consistent with the four solar neutrino experiments are modified for different strengths of New Physics neutrino interactions.

Precise Estimates of High Orders in QCD

Marek Karliner

School of Physics and Astronomy
Raymond and Beverly Sackler Faculty of Exact Sciences
Tel-Aviv University
e-mail: marek@proton.tau.ac.il

The dramatic increase in the precision of experiments measuring QCD observables requires a fresh look at high orders in QCD perturbation theory. This is a difficult problem to deal with: perturbation theory is asymptotic and it is not Borel-summable. Moreover, no QCD observable has been computed beyond the three-loop order. Yet, it turns out that for many practical applications one can circumvent the problem by obtaining highly precise estimates of high orders in perturbation theory, using a recently developed technology based on Padé approximants. There are also some surprising bonuses, most notably a drastic reduction in the predicted dependence of observables on renormalization scale and scheme. The method will be reviewed, with examples from other fields and a brief description of some recent applications to concrete problems in analysis of experimental data.

[1] M.A. Samuel, J. Ellis and M. Karliner, hep-ph/9503411, Phys. Rev. Lett. **74**, 4380 (1995).
[2] J. Ellis, E. Gardi, M. Karliner and M.A. Samuel, hep-ph/9509312, Phys. Lett. **B366**, 268 (1996).
[3] J. Ellis, E. Gardi, M. Karliner and M.A. Samuel, hep-ph/9607404, Phys. Rev. **D54**, 6986 (1996).
[4] J. Ellis, M. Karliner, M.A. Samuel, hep-ph/9612202, Phys. Lett. **B400**, 176 (1997).
[5] S.J. Brodsky, J. Ellis, E. Gardi, M. Karliner and M. Samuel, hep-ph/9706467, Phys. Rev. D., **56**, 6980 (1997).
[6] J. Ellis, I. Jack, D.R.T. Jones, M. Karliner and M.A. Samuel, hep-ph/9710302, accepted for publication in Phys. Rev. D.

IL9905661

Higgs bosons at LHC

Ehud Duchovni

Dept. of Particle Physics, Weizmann Institute of Science

The Large Hadron Collider (LHC) will be commissioned in 2005 and will collide two counter circulating beams of 7 TeV protons with each other while providing high luminosity. Two general-purpose detectors - ATLAS and CMS - will detect and analyze the outcome. At the top of their priority list is the search for the Higgs boson(s). The search will end either with the discovery of the elusive Higgs bosons(s) or with the refutation of the Standard Model and probably also its minimal supersymmetric extension (MSSM). The various channels that will be used in the search for Higgs boson(s) will be reviewed together with the estimated sensitivity of the ATLAS detector to SM and MSSM Higgs bosons.

IL9905662

CP Violation in B decays

Yoram Rozen

Dept. of Physics, Technion Israel Institute of Technology

The phenomenon of CP violation and its explanation are of vital interest in our understanding of the structure of matter and perhaps of the excess of matter over anti-matter in the universe. The mixing between quark generations, represented by the CKM matrix, has been suggested as the mechanism responsible for CP violation and particle/anti-particle oscillation observed in neutral K mesons. The elements of the CKM matrix describe the phenomena of CP violation, particle/anti-particle oscillation and inter-generational transitions. All these phenomena were also predicted for hadrons containing the b quark. Since that prediction, particle/anti-particle oscillation has been observed in B_d mesons, however, no evidence has yet been seen for CP violation in the B sector.

All the phenomena related to the CKM mixing matrix in the b sector can be summarized in a 'unitarity triangle'. Once the sides and angles of this triangle have all been measured, whether or not they form a triangle will determine if the CKM prescription is the correct description of CP violation.

We will report about the status of particle oscillation in the B sector as well as on recent attempt to observe assymetry in the decay of neutral B mesons.

Orthogonality and Boundary Conditions in Quantum Mechanics

Alexander Gersten

Dept. of Physics, Ben-Gurion University of the Negev

One dimensional particle states are constructed according to orthogonality conditions, without requiring boundary conditions. Free particle states are constructed using Dirac's delta function orthogonality conditions. The states (doublets) depend on two quantum numbers: energy and parity ("+" or "-"). With the aid of projection operators the particles are confined to a constrained region -a¡x¡a, in a way similar to the action of an infinite well potential. From the resulting overcomplete basis only the mutually orthogonal states are selected. Four solutions are found, corresponding to different non-commuting Hamiltonians. Their energy eigenstates are labeled with the main quantum number n and parity "+" or "-". The energy eigenvalues are functions of n only. The four cases correspond to different boundary conditions: (I) the wave function vanishes on the boundary (energy levels: $1^+, 2^-, 3^+, 4^-,$) , (II) the derivative of the wavefunction vanishes on the boundary (energy levels $0^+, 1^-, 2^+, 3^-,$) , (III) periodic, symmetric boundary conditions (energy levels: $0^+, 2^+, 2^-, 4^+, 4^-6^+, 6^-,$) , (IV) periodic, antisymmetric boundary conditions (energy levels: $1^+, 1^-, 3^+, 3^-, 5^+, 5^-,$). Orthogonality seems to be a more basic requirement than boundary conditions. By using projection operators, confinement of the particle to a definite region can be achieved in a simple and unambiguous way, and physical operators can be written so that they act only in the confined region.

Effective equation of state for a spherically expanding pion plasma

Melissa A. Lampert and Carmen Molina-París*

School of Physics and Astronomy, Tel Aviv University
**Theoretical Division, Los Alamos National Laboratory*

Following a relativistic heavy ion collision, the quark-gluon plasma produced eventually undergoes a chiral phase transition. We assume that during this phase transition one can describe the dynamics of the system by the linear σ model and that the expansion can be thought of as mostly radial. Because the σ model is an effective field theory there is an actual momentum cutoff (Landau pole) in the theory at around 1 GeV. Thus it is necessary to find ways of obtaining a covariantly conserved, renormalized energy-momentum tensor when there is a cutoff present (which breaks covariance), in order to identify the effective equation of state of this time evolving system. We show how to solve this technical problem and then determine the energy density and pressure of the system as a function of the proper time. We consider different initial conditions and search for instabilities – regions where the effective mass squared of the scalar field is negative. This type of instability can lead to the formation of disoriented chiral condensates (low momentum domains of pions where the isospin can point in a particular direction). We find that the energy density and pressure both decrease quickly, as is appropriate for a rapidly cooling system, and that the energy is numerically conserved. An interesting feature of the expansion is that when the effective mass squared is negative, the pressure is also negative. A negative pressure implies cavitation, which could mean the formation of domains of disoriented chiral condensates.

Sampling Theorems in Quantum Mechanics

Alexander Gersten

Dept. of Physics, Ben-Gurion University of the Negev

The Dirac representation theory was applied to both signal [1,2] and quantum theories. The sampling theorem of signal theory was derived assuming that signals were orthogonal physical ket states. An orthogonal basis, which spanned the time space, ceased to be orthogonal and became overcomplete when the domain of frequencies was restricted to a bandwidth. For this case there existed an infinite number of subbases of discrete times which were orthogonal and complete. The relation between the overcomplete bases and a complete one came out to be the essence of the sampling theorem. We found that similar situations existed in quantum mechanics [3,4]. Sampling theorems for energy eigenstates were found. The physical consequences of such theorems have been analyzed.

[1] A. Gersten, Ann. Phys, **262**. 47-72 (1998).
[2] A. Gersten, Ann. Phys, **262**. 73-104 (1998).
[3] A. Gersten, Foundations of Phys. Lett. (1998), (in press).
[4] A. Gersten, Foundations of Phys. (1998), (in press).

Statistical Physics and Nonlinear Dynamics

Polymer induced coiling of membrane tubes

Daniel Kandel, Ilan Tzafrir, Yoel Stavans

Dept. of Physics of Complex Systems, Weizmann Institute of Science

An experimental study shows that membrane tubes, exposed to a solution of hydrophilic polymers with hydrophobic anchor groups along the backbone, tend to form strongly curved coils. We describe a theory which explains these experimental results. The basic assumption is that the hydrophobic anchors stick to the membrane. Moreover, they "prefer" to stick to locally curved portions of the membrane. The theory predicts that a small polymer concentration reduces the bending rigidity of a membrane tube. Above a critical value of the concentration the bending rigidity becomes negative, thus destabilizing the straight tube. The predicted new equilibrium state of such a tube is a maximally tight coil.

Interfaces of Modulated Phases: Diblock Copolymers and Magnetic Films

David Andelman[(1)], Roland Netz[(2)] and Michael Schick[(3)]

[(1)] *School of Physics and Astronomy*
Raymond and Beverly Sackler Faculty of Exact Sciences
Tel Aviv University
Ramat Aviv, 69978 Tel Aviv, Israel
[(2)] *Max-Planck-Institut für Kolloid- und Grenzflächenforschung*
Kantstrasse 55
D-14513 Teltow, Germany
[(3)] *Department of Physics, Box 351560*
University of Washington
Seattle, WA 98195-1560

The phenomenology of domain shapes and patterns as observed in a wide variety of two- and three-dimensional systems is briefly reviewed. Emphasis is given to a point of view attributing these phenomena to competing interactions which stabilize states characterized by periodic spatial variations of the pertinent order parameter field. Aspects of this simple picture have been rediscovered in many separate areas of chemistry and physics and it has been invoked to account for domain formation in a wide range of physical and chemical systems. Interfaces between lamellar, hexagonal and disordered phases have been studied experimentally, in particular, for diblock copolymers and in ferromagnetic garnet films. In order to model those interfaces we numerically minimize a continuous free-energy functional in two dimensions. Our numerical scheme has the advantage that it does not reply only on the most dominant q-mode. It rather gives an exact minimization in a multi-dimensional functional space. We obtain the exact shape of interfaces between modulated phases in several conditions: (i) Interfaces between lamellar and disordered phases; (ii) interfaces between hexagonal and disordered phases; and (iii) interfaces between hexagonal and lamellar phases. In addition, tilt boundaries, grain boundaries, Omega and T-junction morphologies are reproduced and analyzed in relation to their existence in diblock copolymers and magnetic garnet films.

Pattern formation in Evaporating Water Films

Nirit Samid-Merzel, S. G. Lipson and D. S. Tannhauser

Physics Dept., Technion - Israel Institute of Technology, 32000 Haifa, Israel

Simple dynamic systems, such as drying mud or wind-blown desert sands often spontaneously develop surprisingly complex patterns. The study of such pattern formation, both experimentally and theoretically, has become a major effort in recent years, largely because of the availability of fast computers for performing simulations and the observation that similar features are often seen in completely different systems. We recently discovered that thin layers of water evaporating from an atomically-flat mica substrate develop a variety of patterns that mimic widely different experiments and are also simple enough to be compared quantitatively with simulations. The water layers wet the mica completely when they are very thick, but during evaporation they separate into two phases consisting of thick and molecularly thin films. The phase-separation can be controlled by an external field, the sub-saturated vapour, and can be observed by optical interference. The type of pattern which develops depends on the rate of evaporation, and under various conditions can be compared to viscous fingering, spinodal decomposition or diffusion-limited growth. In particular, features called "doublons" appear prominently, and these have also been observed in simulations of solidification from the melt in two dimensions. They find a natural explanation in the theory of growth at high supercooling.

Dissipative Solitary States in Driven Surface Waves

J. Fineberg, O. Lioubashevski

The Racah Institute of Physics, The Hebrew University of Jerusalem

We present an experimental study of highly localized, soliton-like struc tures that propagate on the two dimensional surface of highly dissipative fluids. Like the well-known Faraday instability, these highly dissipativ e structures are driven by means of the spatially uniform, vertical accel eration of a thin fluid layer. These structures, harmonically coupled to the external driving frequency, are observed above a critical intrinsic " dissipation" in the system (i.e. the ratio of the viscous boundary layer height to the depth of the fluid layer) for a wide range of fluid viscosi ties and system parameters. These highly localized nonlinear states, unli ke classical solitons, propagate at a single constant velocity for given fluid parameters and their existence is dependent on the highly dissipati ve character of the system. The properties of these states are discussed and examples of bound states and two state interactions are presented.

[1] O. Lioubashevski, H. Arbel, and J. Fineberg, Phys. Rev. Lett. **76** , 3959 (1996).
[2] J. Fineberg and O. Lioubashevski, To appear in Physica A, (1998).

Precursors in Front Propagation

David A. Kessler

Dept. of Physics, Bar-Ilan University

We investigate the dynamical construction of the leading edge of propagating fronts. Whereas the steady-state front is typically an exponential, far ahead of the front, the front falls off much faster, in a fashion determined by the Green's function of the problem. We show that there is a universal transition from the steady-state exponential front to a Gaussian falloff. The transition region is of width $t^{1/2}$, and moves out ahead of the front at a constant velocity greater than the steady-state front speed. This Gaussian front then is in general modified even further ahead of the front to match onto the expected Green's function behavior. We demonstrate this in the case of the Ginzburg-Landau and Korteweg-De Vries equations. We also discuss the relevance of this mechanism for velocity selection in the Fisher equation.

Elastic similarity in a polymer solution flow.

Alexander Groisman and Victor Steinberg

Dept. of Physics of Complex Systems, Weizmann Institute of Science

Elastic effects in flows of polymeric liquids have been extensively studied during the last fifty years. Behavior of the elastic liquids in complex three dimensional flows remains, however, very much an open question. In order to approach this problem we have experimentally studied flow transitions in highly elastic polymer solutions in Couette-Taylor flow. These transitions occur solely due to elastic effects, so that the fluid inertia is of no importance there. As a result, the simple shear flow existing at low fluid velocity becomes a complex three dimensional flow when the velocity is increased. We have found close similarity between the elastic flow transitions and pattern formation in different polymeric liquids. So, stability of the basic shear flow is defined by the Deborah number, De, that is quite analogous to the Reynolds number, Re, for the usual inertial flow transitions. The characteristic time scale is defined by the polymer relaxation time that plays the same role as the viscous diffusion time for the inertial flow transitions. Based on these observations we introduce a concept of elastic similarity which is analogous to the hydrodynamic similarity for flows of the usual fluids. The experimental results agree fairly well with predictions of the Oldroyd-B model widely used for description of simple two dimensional flows of polymer solutions. Therefore, it is argued that this model can also be used for analysis of more complex flows including the turbulent drag reduction phenomenon.

The Classical Limit of Quantum Evolution in Chaotic Systems

Shmuel Fishman

Physics Faculty, Technion, Haifa

The singular behavior of quantum evolution in the classical limit is of particular interest for chaotic systems. The limit of long time behavior was studied for such systems. It is of special interest in the view of recent calculations of energy correlations, where deviations from Random Matrix Theory (RMT) related to the long time behavior of the classical systems were found. Specifically the semiclassical limit of the evolution operator of the Wigner function for bound systems was investigated. For this purpose coarse graining was introduced. It was argued in general, and tested numerically for the baker map, that in the limit of vanishing coarse graining the spectrum of the evolution operator consists of the Ruelle resonances, that are related to relaxation rates of disturbances of the classical invariant density.

[1] S. Fishman, Wave Functions, Wigner Functions and Green Functions of Chaotic Systems, to be published in the Proc. of the Nato ASI on "Supersymmetry and Trace Formulae", I. Lerner, editor, Cambridge, Sept. 1997

IL9905670

Magneto-Induced ac Electrical Permittivity of Metal-Dielectric Composites with a Two Characteristic Length Scales Periodic Microstructure

Yakov M. Strelniker and David J. Bergman

School of Physics and Astronomy, Raymond and Beverly Sackler Faculty of Exact Sciences, Tel Aviv University, Tel Aviv 69978, Israel

A new effect was recently predicted in conducting composites that have a periodic microstructure: an induced strongly anisotropic dc magneto-resistance [1]. This phenomenon is already verified on high mobility n-GaAs films [2]. Here we discuss the possibility of observing analogous behavior in the ac electric permittivity of a metal-dielectric composite with a periodic microstructure in the presence of a strong magnetic field. We developed new analytical and numerical methods to treat the low-frequency magneto-optical properties in composite media with both disordered and periodic conducting micro-structures. Those methods allow us to study composites with inclusions of arbitrary shape (and arbitrary volume fraction) at arbitrarily strong magnetic field. This is exploited in order to calculate an effective dielectric tensor for this system as a function of applied magnetic field and *ac* frequency. We show that in a non-dilute metal-dielectric composite medium the magneto-plasma resonance and the cyclotron resonance depend upon both the applied magnetic field as well as on the geometric shape of the inclusion. Near such a resonance, it is possible to achieve large values for the ratio of the off-diagonal-to-diagonal electric permittivity tensor components, $\epsilon_{xy}/\epsilon_{xx}$, (since $\epsilon_{xx} \to 0$, while $\epsilon_{xy} \neq 0$), which is analogous to similar ratio of the resistivity tensor components, ρ_{xy}/ρ_{xx}, in the case of dc magneto-transport problem. Motivated by this observation and by results of previous studies of dc magneto-transport in composite conductors, we then performed a numerical study of the ac magneto-electric properties of a particular metal-dielectric composite film with a periodic columnar microstructure which has a *two characteristic length scales.* The unit cell of such composite is prepared as follows: We placed the conducting square (in cross section) rods (first characteristic length scale) along the perimeter of the unit cell in order to create a dielectric host with large ρ_{xy}/ρ_{xx} ratio. Then the insulating island in the center of the unit cell serves as an effective obstacle (second characteristic length scale). When the frequency is in the vicinity of one of the sharp resonances, there appears a strong dependence of the real and imaginary parts of all the components of the bulk effective electric permittivity tensor, $\epsilon^{(e)}$, on both the magnitude and the direction of the applied static magnetic field, **B**, which is rotated in the film-plane [3]. The various magneto-optical properties (including Faraday rotation, etc.) of such composites are considered. The possibility of observing these new effects in a suitably synthesized composite film is considered in detail.

[1] D. J. Bergman and Y. M. Strelniker, Phys. Rev. B **49**, 16256 (1994).
[2] M. Tornow, D. Weiss, K. v. Klitzing, K. Eberl, D. J. Bergman, and Y. M. Strelniker, Phys. Rev. Lett. **77**, 147 (1996).
[3] D. J. Bergman and Y. M. Strelniker, Phys. Rev. Lett. **80**, 857 (1998).

Error Reduction in Perturbative Approximations to Nonlinearly Coupled Harmonic Oscillators

Peter B. Kahn, Yair Zarmi*

Physics Dept., SUNY, Stony Brook, NY 11794
** Inst. for Desert Research, Ben-Gurion University of the Negev, Sede Boqer Campus, 84990*

Error estimates for perturbative approximations to solutions of systems with small nonlinearities are limited in scope. For single oscillator systems, and for systems with more than one degree of freedom that depend on a single phase, the error between the approximation and the full solution is bounded by $O(\epsilon)$ for times of $O(1/\epsilon)$, where —ϵ—=AB1 is the strength of the perturbation. Otherwise, error estimates exist only on approximations to the *action* variables. Most of the error estimates have been derived for systems in which the unperturbed Hamiltonian is itself nonlinear. No information is available on errors in the *phases*. For the study of the topological structure of the solutions in phase space this may be sufficient. However, for good long-term approximations to the full solution of a dynamical system, this situation is not satisfactory.

Through a sequence of examples of growing complexity, of nonlinearly coupled harmonic oscillators, we have shown [1] that, by applying *minimal normal forms* (MNF) to the dynamical equations obeyed by the phases of all the degrees of fredom, the errors in the approximations to solutions are reduced siginficantly in comparison with the usual procedure for computing the perturbative approximations.

The normal form is given as a formal power series in the expansion parameter of the problem. Using the freedom inherent in any perturbation expansion, the normal form may be formally truncated into a finite sum, the MNF. In the present work this idea is applied to the phase part of the normal form equations.

[1] P. B. Kahn and Y. Zarmi, Physica D, in press (1998).

Self-Assembly in Mixtures of Amphiphilic Polymers and Surfactants

Haim Diamant, David Andelman

School of Physics and Astronomy, Tel Aviv University

We present a model for the self-assembly properties of an amphiphilic polymer consisting of a hydrophilic backbone and a large number of hydrophobic side groups. Both intra-chain association and polymer-surfactant binding are considered. Preference of the surfactant to bind to hydrophobic microdomains on the chain leads to an effective attraction between bound surfactants. Consequently, the surfactant-polymer binding exhibits two distinct regimes depending on a single physical parameter, ϵ, which represents the ratio between surfactant-polymer affinity and polymer hydrophobicity. For small ϵ the binding is non-cooperative and increases moderately with surfactant concentration. For large ϵ, due to the strong effective attraction between bound surfactants, the binding becomes cooperative and increases sharply at the so-called critical aggregation concentration, *cac*. These findings are in accord with recent experiments.

Spin glass dynamics above T_g: a μSR study of AgMn.

Amit Keren, Philippe Mendels*, Ian A. Campbell*, James Lord**
Physics Faculty, Technion, Haifa
* *Laboratoire de Physique des Solides, URA2 CNRS, Université Paris Sud, 91405 Orsay, France*
** *ISIS Facility, Rutherford Appleton Laboratory, Chilton Didcot, Oxfordshire OX11 0QX United Kingdom*

In this work [1] we use the zero and longitudinal field muon spin relaxation technique to map the Fourier transform of the spin-spin dynamical autocorrelation function $\tilde{q}(\omega)$ in the metallic spin glass AgMn(0.5 at %) at $T > T_g$. We find that at high longitudinal field the muon polarization obeys a time-field scaling relation (see Fig. 1) which could be explained by a power law decay of $\tilde{q}(\omega)$ while in zero field the muon relaxation is finite implying that $\tilde{q}(\omega = 0)$ is bound. We therefore conclude that $\tilde{q}(\omega)$, at $T > T_g$, is best described by a cut off power law correlation function. We contrast our findings with spin glass models.

[1] A. Keren et al. Phys. Rev. Lett. **77**, (1996) 1386.

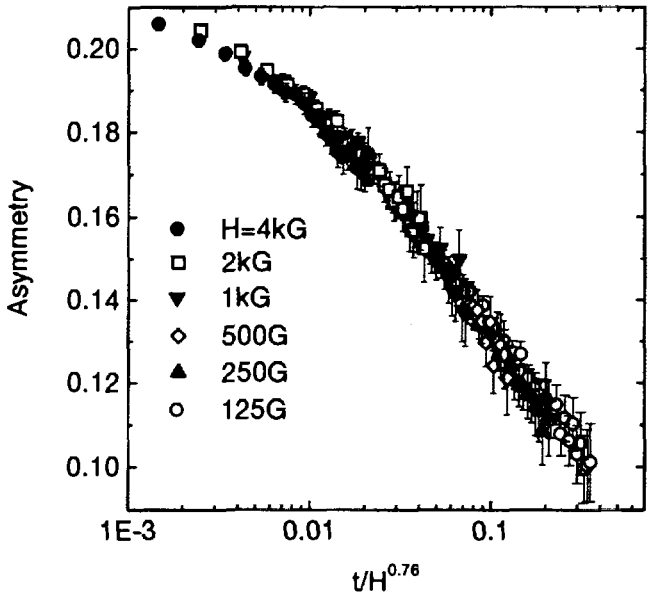

Structure of self-avoiding walks on percolation clusters at criticality

Anke Ordemann[1,2], Markus Porto[1,2], H. Eduardo Roman[1,3], Armin Bunde[1,2], and Shlomo Havlin[1,2]

[1] *Institut für Theoretische Physik III, Justus-Liebig-Universität Giessen, Heinrich-Buff-Ring 16, 35392 Giessen, Germany*
[2] *Minerva Center and Department of Physics, Bar-Ilan University, 52900 Ramat-Gan, Israel*
[3] *Dipartimento di Fisica, Universita di Milano, Via Celoria 16, 20133 Milano, Italy*

We study the structure of linear polymers in disordered media modelled by self-avoiding random walks (SAWs) on two- and three-dimensional percolation clusters at criticality. To this end, extensive computer simulations are performed using different algorithms. Since the aim is describing 'infinitely' long chains, we work directly on the backbone of the clusters, where dangling ends are absent on all length scales. The best results are obtained by exactly enumerating all possible SAW configurations of N steps (up to $N = 40$) on a single backbone configuration, averaging over many backbone configurations to extract the mean quantities of interest. We determine the distribution functions and critical exponents for the mean end-to-end distance after N steps, characterizing the structure of SAWs in both Euclidean and topological space. The distribution functions $\langle P_{\rm B}(r,N)\rangle$ and $\langle P_{\rm B}(\ell,N)\rangle$ can be described by a scaling function of the variables $x = r/N^{\nu_r}$ and $y = \ell/N^{\nu_\ell}$ respectively. The critical exponents of these functions can be more accurately obtained in topological ℓ-space and then translated into r-space. For the fractal dimension of the SAWs for $N \to \infty$ we obtain $d_{\rm f} = 1/\nu_r = 1.272 \pm 0.010$ for $d = 2$ and $d_{\rm f} = 1.515 \pm 0.005$ for $d = 3$. Due to the excluded volume constraint, the polymers are more stretched in disordered media than in ordered media, leading to a smaller fractal dimension. The numbers of possible N-step SAW configurations on the backbone $C_{N,{\rm B}}$ fluctuate strongly for different configurations, we find that $\ln C_{N,{\rm B}}$ is approximately normally distributed. To characterize the fluctuations of $C_{N,{\rm B}}$ more generally, we study the moments $\langle C_{N,{\rm B}}^q\rangle^{1/q}$. We find that they scale like $\mu(q)^N N^{\gamma(q)-1}$, where the effective coordination number of the backbone $\mu(q)$ and the enhancement exponent $\gamma(q)$ depend explicitely on q. We suggest a relation between the exponents characterizing the asymptotic shape of the end-to-end distance distribution and $\gamma(q)$, which is supported by numerical results.

Chaos of the Relativistic Forced van der Pol Oscillator

Y. Ashkenazy[a], C. Goren[a], and L. P. Horwitz[a,b]

[a] *Department of Physics, Bar-Ilan University, Ramat-Gan 52900, Israel*
[b] *School of Physics, Raymond and Beverly Sackler Faculty of Exact Sciences Tel-Aviv University, Ramat-Aviv, Israel*

A manifestly relativistically covariant form of the van der Pol oscillator in $1+1$ dimensions is studied. We show that the driven relativistic equations, for which x and t are coupled, relax very quickly to a pair of identical decoupled equations, due to a rapid vanishing of the "angular momentum" (the boost in $1+1$ dimensions). A similar effect occurs in the damped driven covariant Duffing oscillator previously treated. This effect is an example of entrainment, or synchronization (phase locking), of coupled chaotic systems. The Lyapunov exponents are calculated using the very efficient method of Habib and Ryne. We show a Poincaré map that demonstrates this effect and maintains remarkable stability in spite of the inevitable accumulation of computer error in the chaotic region. For our choice of parameters, the positive Lyapunov exponent is about 0.242 almost independently of the integration method.

On how a joint interaction of two innocent partners (smooth advection & linear damping) produces a strong intermittency

Michael Chertkov

Department of Physics, Princeton University

Forced advection of passive scalar by a smooth d-dimensional incompressible velocity in the presence of a linear damping is studied. Acting separately advection & dumping do not lead to an essential intermittency of the steady scalar statistics, while being mixed together produce a very strong non-Gaussianity in the convective range: q-th (positive) moment of the absolute value of scalar difference, $\langle|\theta(t;\mathbf{r})-\theta(t;0)|^q\rangle$ is proportional to r^{ξ_q}, $\xi_q=\sqrt{d^2/4+\alpha dq/\left[(d-1)D\right]}-d/2$, where α/D measures the rate of the damping in the units of the stretching rate. Probability density function (PDF) of the scalar difference is also found.

Higher Order Parametric Level Statistics in Quantum Chaotic Systems

E. Kanzieper[1] and V. Freilikher[2]

[1] *The Abdus Salam International Centre for Theoretical Physics*
P.O.B. 586, 34100 Trieste, Italy
[2] *The Jack and Pearl Resnick Institute of Advanced Technology*
Department of Physics, Bar-Ilan University, 52900 Ramat-Gan, Israel

We show that the problem of parametric level statistics [1] in disordered/chaotic systems with broken time–reversal symmetry is equivalent to the model of large coupled Hermitian matrices. The equivalence is established on the level of supersymmetric generating functionals [2] which are proven to be identical in both problems, provided $N\alpha_c^2 = \pi^3\varphi^2 g$. Here $\alpha_c^2 \ll 1$ is the effective coupling of $N \times N$ matrices in the two–matrix model, φ and g are the magnetic flux and the dimensionless conductance in the microscopic problem, and Δ is the mean level spacing. The close connection between the two models, being interpreted in the language of multiple Hermitian matrix integrals, allows us to compute the $(p+q)$–point dimensionless parametric correlator $k_{p,q}(\{\omega\};\{\Omega\};X^2) = \Delta^{p+q}\left\langle \prod_{i=1}^{p}\nu(E+\omega_i,0)\prod_{j=1}^{q}\nu(E+\Omega_j,\varphi)\right\rangle$ of the densities of states in quantum chaotic systems. It is expressed through the determinant $k_{p,q}(\{\omega\};\{\Omega\};X^2) = \mathrm{Det}M_{ij}^{\alpha\beta}$ of the block matrix $M_{ij}^{\alpha\beta}$. The block–diagonal $p \times p$ and $q \times q$ matrices M^{11} and M^{22} are the sine kernels,

$$M_{ij}^{11} = \frac{\sin[\pi\Delta^{-1}(\omega_i-\omega_j)]}{[\pi\Delta^{-1}(\omega_i-\omega_j)]}, \qquad M_{ij}^{22} = \frac{\sin[\pi\Delta^{-1}(\Omega_i-\Omega_j)]}{[\pi\Delta^{-1}(\Omega_i-\Omega_j)]},$$

while the off–block–diagonal $p \times q$ and $q \times p$ matrices

$$M_{ij}^{12} = -\int_1^\infty d\lambda_1 \cos[\pi\lambda_1(\omega_i-\Omega_j)\Delta^{-1}]\exp\left\{-(\pi^2X^2/2)\lambda_1^2\right\},$$

$$M_{ij}^{21} = \int_0^1 d\lambda \cos[\pi\lambda(\Omega_i-\omega_j)\Delta^{-1}]\exp\left\{(\pi^2X^2/2)\lambda^2\right\}$$

reflect the response of chaotic system to an external perturbation encoded through the parameter $X^2 = 4\pi g\varphi^2$ governing the level motion. Extension to the multi-parameter perturbations is addressed. The results obtained are also applicable to description of the higher order space–time correlation functions in the Calogero–Sutherland–Moser model at coupling strength $\lambda = 1$.

[1] B. D. Simons, P. A. Lee, and B. L. Altshuler, Phys. Rev. Lett. **70**, 4122 (1993); Phys. Rev. Lett. **72**, 64 (1994).
[2] K. B. Efetov, Adv. Phys. **32**, 53 (1983); J. J. M. Verbaarschot, H. A. Weidenmüller, and M. R. Zirnbauer, Phys. Rep. **129**, 367 (1985).

Anomalous Diffusion in Polymers, Membranes, and Fractal Gels

A. G. Zilman and R. Granek

Dept. of Materials and Interfaces, Weizmann Institute of Science

The dynamics of flexible and semi-flexible fractal manifolds in solutions is described in terms of the spectral dimension d_s and the fractal dimension d_f. Particular attention is given to linear polymers ($d_s = 1$), membranes ($d_s = 2$) and gel clusters ($1 < d_s < 2$).

Semi-flexible manifolds, having size much smaller than the persistence length, can be described by an Helfrich-type bending Hamiltonian. Here we study both the transverse and longitudinal mean square displacement (MSD) of a tagged "monomer" [1,2]. The two types of MSD, transverse and longitudinal, show anomalous subdiffusion on the short time scale, MSD$\sim t^p$, where $p = (4 - d_s)/(5 - d_s)$ in a 3-dimensions. We demonstrate how the latter behavior leads to a stretched exponential decay of the dynamic structure factor[1] $S(q,t) \sim e^{-(\Gamma_q t)^p}$. For membranes where $p = 2/3$ and $\Gamma_q \sim \kappa^{-1/2} q^3$ (with κ the bending modulus) this relaxation has been recently observed by light scattering [3]. For linear polymers where $p = 3/4$ the MSD has been recently measured in real space [4]. For both linear polymers and membranes, the longitudinal motion also leads to a new type of reptation motion [2]. This concept is used to model polymer motion in semi-dilute solutions in which the persistence length is longer than the entanglement length, e.g., actin filament networks which form the cytoskeleton of plasma membranes.

Flexible, self-avoiding, fractal manifolds, i.e., those having size much larger than the persistence length of the building blocks, appear in sol-gel systems and can be described by the Edwards Hamiltonian. The dynamics is treated within a linearization self-consistent approach [5]. When hydrodynamic interaction is not screened (Zimm model) we find again MSD$\sim t^p$ now with a universal exponent $p = 2/3$ (in 3-dimensions) *independent* of the fractal and spectral dimensions. This behavior has been recently measured in colloidal gels by light scattering [6] and is attributed to the long range hydrodynamic interaction which makes the fractal characteristics irrelevant. The frequency dependent viscoelastic modulus behaves as $G(\omega) \sim (i\omega)^\alpha$ with $\alpha = d_f/3$ (in agreement with previous theoretical studies). When hydrodynamics is screened (Rouse model) we find $p = 2/(2 + d_f)$ and $\alpha = d_f/(2 + d_f)$. We conclude that measurements of $p = 2/3$ indicate unambiguously that Zimm model is applicable and thus should be correlated with $\alpha = d_f/3$ in rheological measurements.

[1] A. G. Zilman and R. Granek, Phys. Rev. Lett. **77**, 4788 (1996).
[2] R. Granek, J. Phys. II France **7**, 1761 (1997).
[3] E. Freyssingeas, D. Roux, and F. Nallet, J. Phys. II France **7**, 913 (1997).
[4] A. Caspi, M. Elbaum, R. Granek, A. Lachish, and D. Zbaida, Phys. Rev. Lett. **80**, 1106 (1998).
[5] A. G. Zilman and R. Granek, to be published.
[6] A. H. Krall and D. A. Weitz, Phys. Rev. Lett. **80**, 778 (1998).

Transport in Stochastic Media

O. Haran[1,2], D. Shvarts[1], R. Thieberger[2]

[1] *Department of Physics, Nuclear Research Center - Negev*
[2] *Department of Physics, Ben-Gurion University, Beer-Sheva*

Classical transport of neutral particles in a binary, scattering, stochastic media is discussed. It is assumed that the cross-sections of the constituent materials and their volume fractions are known. The inner structure of the media is stochastic, but there exist a statistical knowledge about the lump sizes, shapes and arrangement.

The transmission through the composite media depends on the specific heterogeneous realization of the media. The current research focuses on the averaged transmission through an ensemble of realizations, from which an effective cross-section for the media can be derived.

The problem of one dimensional transport in stochastic media has been studied extensively [1]. In the one dimensional description of the problem, particles are transported along a line populated with alternating material segments of random lengths.

The current work discusses transport in two-dimensional stochastic media. The phenomenon that is unique to the multi-dimensional description of the problem is obstacle bypassing. Obstacle bypassing tends to reduce the opacity of the media, thereby reducing its effective cross-section. The importance of this phenomenon depends on the manner in which the obstacles are arranged in the media.

Results of transport simulations in multi-dimensional stochastic media are presented. Effective cross-sections derived from the simulations are compared against those obtained for the one-dimensional problem, and against those obtained from effective multi-dimensional models, which are partially based on a Markovian assumption.

[1] F. Malvagi, G. C. Pomraning, "A Comparison of Models for Particle Transport Through Stochastic Mixtures", Nucl. Sci. Eng. 111,215 (1992)

Semi-flexible Network Dynamics - A View From Inside

A. Caspi, M. Elbaum, R. Granek, A. Lachish, and D. Zbaida

Department of Materials and Interfaces, Weizmann Institute of Science

The thermally driven dynamics of a polymer network are studied by direct view observation of the motion of a single point within a single polymer [1]. Taking advantage of rather rigid biological microtubules as a case study, we expand the space and time scales of the system to those accessible by optical microscopy and standard video tools. Tracking is achieved by chemically attaching an optically resolved micro-sphere to a single point on the filament. We measure a sequence of instantaneous positions, from which we compute the mean squared displacement vs time. Typical behavior in a network shows two distinct regimes. At short times, we observe anomalous diffusion with power law 3/4. At long times (seconds) the undulation amplitude saturates as a consequence of the finite length of the polymer. In the network, entanglements effectively divide the filament into segments shorter than the physical length. In a pre-stressed network we find a short time sub-diffusive regime with power law $0.4 - 0.5$, interpreted as a signature of tension along the individual filament.

[1] A. Caspi, M. Elbaum, R. Granek, A. Lachish, and D. Zbaida, Phys. Rev. Lett, **80**, 1106, (1998).

The Return Probability of N Strongly Repelling Classical Diffusing Particles in Quasi-1D, an Exact Solution.

U. Gavish, Y. Imry

Dept. of Condensed Matter Physics, Weizmann Institute of Science

N classical particles diffuse inside the one dimensional interval [0,L]. There are reflecting walls at the edges of this interval. The diffusion constant of each particle is assumed independent of its energy and position. The particles interact through short range repulsive interaction that prevents them from exchanging positions - they stay ordered in there initial ordering on the line. The probability that at time t, all the particles are back at the points there were at t=0 (up to a distance less than a mean free path), and the configuration space average of this probability, are calculated. The interaction is dominating these quantities, even for times in which it is not expected to affect most of the dynamics of the system. Both results are exact, analytic, and have the form of the sum over terms that represents different kinds of many body processes - describing different ways of clustering of particles in the system. Connections to the Bethe ansatz method, to quantum chaos and mesoscopic systems, and to random walks in nonequilibrium statistical mechanics, are pointed out.

Relativistic Arnol'd Diffusion and Stochastic Web of an Electrically Kicked Oscillator

Y. Ashkenazy[a] and L.P. Horwitz[a,b]

[a] *Department of Physics, Bar-Ilan University, Ramat-Gan 52900, Israel*
[b] *School of Physics, Raymond and Beverly Sackler Faculty of Exact Sciences Tel-Aviv University, Ramat-Aviv, Israel*

Zaslavski *et al* showed some time ago that an electrically kicked oscillator undergoes a chaotic motion under which energy flows through a stochastic web in phase space in an Arnol'd type diffusion. Since the energies reached in this process are unbounded, several authors have studied the analogous relativistic problem. They have used dynamical formalisms in which the accelerated motion is described in terms of a sequence of comoving inertial frames, or in accelerated frames. We argue that these methods are not accurate or consistent. We provide a consistent dynamical scheme based on Stueckelberg's manifestly covariant dynamics, resulting in a new relativistically corrected form of the Lorentz force, and show that the kicked oscillator generates a covariant stochastic web with (light speed) bounded velocities.

Shear-Induced Buckling Instability in The Lamellar Phase:a Mechanism for Onions Formation?

A.Zilman, R.Granek

Dept. of Materials and Interfaces, Weizmann Institute of Science

We present a model of coupling of shear flow to microscopic degrees of freedom in the lyotropic Smectic A (lamellar phase).This coupling is then shown to produce macroscopic buckling instability unalogous to well known undulation instability appearing in thermotropic smectics under dilatation in the direction perpendicular to the layers.[2]
The lyotropic lamellar phase is experimentally known to become unstable under shear flow.The instability occurs at shear rate $\gamma \sim 1sec^{-1}$ and the so called 'onions' (multilamellar vesicles) are formed[1].
We propose that the instability occurs in two stages.At the first stage,the layers are buckled by shear -induced *microscopic* tension $\sigma \cong \eta_e \dot{\gamma} d$ where η_e is an effective viscosity of the system (which can be very large :$\eta_e \cong 1000\eta_{solvent}$) and d is an interlayer spacing.As the membrane projected area cannot increase (for example,being sandwiched between defects) it has to *buckle* in the direction perpendicular to itself.There is a critical tension however due to energy cost of compression of layers in the buckled state and of bending and expansion of individual layers.Then one is able to calculate the buckling amplitude U_0 and the wavevector k as a function of $\dot{\gamma}$.Denoting K usual smectic bending modulus and B the compressional one ,the result is that the transition occurs at $\sigma_c \cong \frac{T}{Dd}$,where D is the width of a film.For $\sigma - \sigma_c \gg \sigma_c$ we have $k \cong \sigma^{\frac{1}{6}}$, $U_0 k \cong \sqrt{\frac{8\sigma}{3dB}}$.
At the second stage the buckled structure is deformed by shear (by coupling to *nacroscopic* degrees of freedom) nad eventually broken ,resulting in the formation of onions. We speculate that the buckled state will become unstable when the relaxation time of the buckling structure $\tau_c \cong \frac{\eta_e}{Kk^2}$ is shorter than the one needed for shear to deform the structure to a degree that maxima are shifted to the position of neigbouring minima.The estimate is $\dot{\gamma} \cong Kk^2(U_0 k)^{-1}$ which gives $\dot{\gamma}_c \sim d^{-a}$ with $7/3 < a < 17/7$ which is consistent with experimental data $a = 2.4 \pm 0.4$[3,1]

[1] D.Roux,F.Nallet and O.Diat,Europhys .Lett.,**24** (1),53 (1993)
[2] N.A.Clark and R.B.Meyer,Appl.Phys.Lett.,**22**,493 (1973)
[3] A.Zilman and R.Granek (to be published)

Unusual(pre-)critical exponents in cubic (anti-)ferromagnets

S.I. Ben-Abraham[a] and A. Nudelman[b]

[a]*Department of Physics, Ben Gurion University, POB 653, IL-84105Beer-Sheva, Israel*
[b]*Department of Physics, University of California, Santa Barbara CA 93106-9530, USA*

Consider a cubic crystal structure with dipoles sitting on sites with cubic symmetry and locked into the directions of the cube axes $\langle 100 \rangle$. We shall refer to magnetic dipoles, even though they could be electric or elastic as well. We are interested in the critical exponents for ferromagnetic or antiferromagnetic ordering that follow from mean field theory applied to this system. They turn out to be non-classical. The dipoles as well as the internal field which is proportional to the magnetization are all assumed to be parallel to one of the cube axes.
A standard and straightforward, though somewhat tedious calculation utilizing the canonical (isothermal) ensemble and expansion to lowest nonvanishing order in the neighborhood of the critical point yields the set of exponents

$$\alpha = \alpha' = 1/2;\ \beta = 1/4;\ \gamma = \gamma' = 1;\ \delta = 5\ .$$

These values normally occur at tricritical points (cf.[1,2]). They should = be compared to the "classical" set of mean field exponents

$$\alpha = \alpha' = 0;\ \beta = 1/2;\ \gamma = \gamma' = 1;\ \delta = 3\ .$$

The justification of this exercise is that there are some interesting physical realizations thereof. Some perovskite-like compounds, such as $KFeF_4$, $RbFeF_4$, $CsFeF_4$, $(CH_3NH_3)_2CuCl_4$, $(C_2H_5NH_3)_2CuCl_4$ display antiferromagnetic transitions with a wide range of validity for (5) [3]. Eventually, very close to the critical point a crossover to the genuine critical exponents does occur. Yet, it is certainly remarkable that our extremely simple model accounts for an important range of what might be called *precritical* behavior. Finally, we wish to point out that the calculation goes through also for tetragonal or even only orthorhombic symmetry as long as all six $< 100 >$ axes can be considered equivalent. Practically speaking, this refers to a slight breaking of the cubic symmetry which, in these cases, is usually present anyway.

[1] H E Stanley, *Introduction to phase tramsitions and critical phenomena*, Oxford University Press 1971.
[2] A. Aharony, *Multicritical points* in *Critical phenomena*, F J W Hahne, ed., Springer, Berlin 1983.
[3] H Keller and I Savić, Phys.Rev. B28 (1983) 2638-2652 and references therein.

Fractons with scalar and vector interactions and two scaling ralations between the static and dynamic critica exponents

Asya S Skal

The Research Institute
The College of Judea and Samaria

Using new equilibrium equation [Physica A 242 (1997) 13] and Einstein's relation, new critical exponents for Young modulus $Y(p) \propto (p-p_c)^{2t-g}$ and regular diffusion $D^e_\infty(p) \propto (p-p_c)^{t-g}$ are introduced, where t is the conductivity critical exponent and g=0.6 is the Hall coefficient critical exponent above the threshold. These results allows us to introduce two superuniversal fractons dimensions: with the scalar displacements $d_s=4/3$ (the Alexander and Orbach conjecture) and with the vector displacements $d_v=21/20$) which leads to new scaling relations between the static and dynamic critical exponents: $t=1/2[(3d-4)\nu-g]$; $t=[2\nu(20d-21)+21g+2\beta)/42$ in all $(3 \preceq d \preceq 6)$ space dimensions.

Equivalence in mapping of diffusion and conductivity equations appears or disappears

Asya S Skal

The Research Institute
The College of Judea and Samaria

For asymptotic long-time behavior one exponent of regular diffusion coefficient above the threshold $D^e_\infty(p) \propto (p-p_c)^{t-g}$ and two below the threshold $D^e_\infty(p) \propto (p-p_c)^{-s-g}$ and $D^e_\infty(p) \propto (p-p_c)^s$ are introduced using the conductivity critical exponents (t and s) and the Hall coefficient critical exponent $R^e \propto (p-p_c)^{-g}$ if $R_2/R_1 > 1$ and $R^e(p) \propto (p-p_c)^{2s}$ if $R_2/R_1 > \infty$ and $p<p_c$. In the latter diffusion and conductivity reduce to the same mathematical problem but in the former the equivalence in mapping is disappears. These results allows us to introduce the new formulae for low-frequency ac conductivity.

THE STRENGTH OF LOCALIZATION FOR FRACTONS IN THE SUPERCONDUCTIVE PERCOLATION

Asya S Skal

The Research Institute
The College of Judea and Samaria

Using new equilibrium equation [1] and Einstein's relation, the new critical exponents for elastic moduli and for regular diffusion are introduced though the conductivity and the Hall coefficient critical exponents. Conductivity and the Hall coefficient belong to different universality classes, while diffusion and elastic moduli belong to both of them. This result allows us to introduce new formulae for vibrational density of state and the strength of localization.

[1] Asya Skal, "The starry sky model Part 3: A new equilibrium equation and two kinds of 'special' elastic nodes." Physica A 242 (1997) 13-26

THE STARRY SKY MODEL OF SUPERCONDUCTIVE PERCOLATION PART 4: TRANSMISSION OF ORDER BY TWO KINDS OF NUCLEATION NODES AND CRITICAL FLUCTUATIONS

Asya S Skal

The Research Institute
The College of Judea and Samaria

Why do we need a new model and what is the problem with all previous models? All previous models have described the behavior of classical electron with resistivity along path, however we have unexpected paradoxical situation in the percolation phase transition: superconductive behavior below and above the threshold. If in the complex plane one has the Julia set and the Fisher's zeros or poles, in percolation the 'special' nodes are the singularities of kinetic coefficients in real space.
We have introduced a new picture of 'propagation of order' for kinetic coefficients and a new dynamic scaling region consisting of component 1 and component 2 parts, which are interchanged (the special nodes (poles) convert in the nucleation nodes (zeros), which become again the poles in other side of the critical point). The critical fluctuations appear as a result of singularities disappearing.

Physics in Medicine

The Generation and Modulation of the Heart Beat: A Phase Response Curve Based Model of Interacting Pacemaker Cells

Sarit Abramovich-Sivan, and Solange Akselrod

The Abramson Institute of Medical Physics, Sackler Faculty of Exact Sciences,

Tel-Aviv University

The goal of this work is to introduce a series of simple physical- mathematical models for the generation and modulation of the heart beat. The dynamic communication of the cardiac pacemaker cells can be explained based on the physical theory of a one-dimensional limit cycle oscillator. Therefore, in our models, the pacemaker cell is fully characterized by its intrinsic cycle length, reflects its active properties. The pacemaker interaction with the outside world (its neighboring cells or an external stimulus) is fully characterized by its phase response curve (PRC), reflects its passive properties. First, we developed a single pacemaker cell model to investigate the basic properties of our PRC based model and to analyze its entrainment phenomena in response to a periodic train of depolarization stimulations. Next, we applied our approach to a pacemaker cell pair model, to investigate the nature of the dynamic interaction between pacemaker cells. Thereafter, we investigated the dynamic behavior of a single pacemaker cell in response to the application of simulated vagal and sympathetic stimulations. We qualitatively investigated the phenomenon of "accentuated antagonism" between parasympathetic and sympathetic autonomic branches, in regulating the pacemaker periodicity. In addition, we demonstrated that the dynamics of the respiratory sinus arrhythmia (RSA) can be interpreted in terms of the entrainment of the pacemaker cell by the respiratory modulation of vagal activity. As a next step, we expanded our model to a two-dimensional matrix of pacemaker cells, which reflects the mutual interaction among many pacemaker cells in the SA node. In addition, this model successfully reproduces a wide range of activity patterns,analogous to familiar cardiac rhythm disturbances (e.g. tachycardia, spiral wave, conduction barrier). Finally, we developed a new model of the atria. This model is based on our hypothesis that atrial cells have features of pacemaker cells. They are,however, characterized by a normally longer intrinsic cycle length and a different type of "electrical" connection than between the SA node pacemaker cells. We gain insight into the conditions which predispose the genesis of a wide variety of normal and abnormal atrial rhythms, analogous to familiar atrial rhythm disturbances, that have been observed clinically and experimentally (e.g. tachycardia, pacemaker shift, reentry, fibrillation). Especially, this approach yields insight into the mechanism of transition from the normal pattern of atrial activity to the disordered state of atrial fibrillation.

Scientific Methods in Criminal Investigations

Joseph Almog

Investigations Department, Division of Forensic Science
Israel Police National Headquarters

A number of cases will be presented where the use of scientific methods, mostly from the persuasion of physics, played a major role in deciphering crimes.
The investigations involved the use of lasers (for latent fingerprint recovery), electrostatic development apparatus (for indented handwriting), scanning electron microscopy (for particle characterisation and more.

Twin Gradient Technology - A New Concept in MRI System Design.

Paul R. Harvey Ph.D.

Elscint MRI Centre,
P.O. Box 550, Haifa 31004, Israel.

Magnetic Resonance Imaging (MRI) relies on the use of extremely accurate static, spatially and time varying magnetic fields. One of the key components of a modern MRI system, besides the magnet, is the gradient coil subsystem. The gradient coil subsystem comprises three electromagnetic coils which can generate orthogonal magnetic fields that vary linearly along the X, Y and Z axes of the magnet bore. During imaging these gradient fields are modulated according to a pre defined pattern as required to generate an MR image. It is desirable in modern MRI procedures to utilize gradient fields that are both high in amplitude and short on risetime.
The varied selection of MR imaging techniques currently in use place different demands on gradient coil performance. When designing a high performance gradient subsystem for whole-body MR imaging it is necessary to consider many opposing factors which include: peak gradient amplitude, slew rate performance, gradient field linearity/volume, efficiency, safety with respect to peripheral nerve stimulation and free bore diameter.
Many of these parameters are conflicting in the sense that, for example, a very spatially linear coil tends to be high in inductance and requires a high voltage power supply to provide a high slew rate. In addition, a coil which has a large linear imaging volume is advantageous for spine imaging but is disadvantageous in terms of dB/dt when switched with a high slew rate. Efficiency of a gradient coil can generally be improved by a reduction in the size of the linear volume of the coil. This has been achieved by reducing the diameter of the coil with the disadvantage that only head imaging can be performed. A less severe approach is simply to shorten the linear volume of the coil. This provides a more efficient coil with a diameter large enough for whole-body imaging and the added benefit that the peak dB/dt can be kept within reasonable limits whilst providing a high slew rate performance. The disadvantage of this approach, on a clinical system, is that large field of view imaging, as required in the spine, is no longer possible.
During this presentation the important aspects of gradient coil design and its relevance to MRI will be outlined. Methods of overcoming the various limitations described above will be discussed. Finally, a new concept of gradient subsystem design will be presented. The new gradient subsystem has three modes of operation. In each mode the physical properties of the gradient coil can be modified, depending upon the application and performance requirements, in order to make the best use of the gradient power supply unit and reduce the possibility of physiological side effects to patient.

[1] Turner R., Mag. Res. Imaging, Vol. 11, pp. 903-920, (1993).
[2] Mansfield P. and Harvey P.R., Mag. Res. Med., 29: 746-758, (1993).
[3] Ehrhardt J.C., et al., JMRI 7:405-409 (1997).

Neural, Mechanical and Geometric Factors in The Control of Posture and Movement

Tamar Flash

Dept. of Applied Mathematics and Computer Science, Weizmann Institute of Science, Rehovot

The generation of human goal-directed multi-joint arm movements requires of the central nervous system to deal with complicated computational and control problems. These problems include the selection and planning of specific motions among the large number of possible ones and the solution of the inverse kinematics and dynamics problems. In my talk I will review several experimental and mathematical modeling studies aimed at investigating the nature of the underlying control processes and of the internal neural representations subserving movement generation. The focus of our studies has been on trajectory planning, on-line modification and motor adaptation during reaching, curved and handwriting movements. The mathematical techniques that we have used are based on optimization theory, Lie group theory and differential geometry. A basic approach used in these studies involves the identification of different invariants of motor behavior. Based on the experimental observations we then seek to identify and characterize the rules that govern the resolution of the redundancies existing at the task and joint levels, the coordinate systems and variables subserving internal motor representations and the solutions that have evolved to deal with the mechanical problems associated with motor execution. Evidence will be presented for the hierarchical structure of the movement generation processes and for the separability between motion planning and execution levels. Possible neural constraints and optimization principles underlying motion planning and evidence for the modularity of the system will also be discussed.

Diagnosis of Tissue Abnormalities Using Optical Fiber Based Methods.

A. Salman, S. Mordechai, A. Gersten H. Reubeni*, H. Mnitentag*

Dept. of Physics, Ben-Gurion University, Beer-Sheva
** Soroka Medical Center, Beer-Sheva*

Recently, significant progress has been made towards the development of a new optical, noninvasive technology for early detection of malignant tissue [1].
The Optical Biopsy System **OBS** and the Laser Induced Fluorescence **LIF** systems invoke a unique approach to optical diagnosis of tissue pathology based on the elastic scattering and autofluorescence properties of the microscopic structure of the tissue. The architectural changes in the cellular and sub-cellular levels developing in abnormal tissue, including a majority of cancer forms, manifest themselves in different optical signatures which can be detected in elastic scattering, Raman and fluorescence scattering spectroscopy.
There was a real increase of malignant melanoma over the last twenty years, therefore it is clinicaly important whether pigmented nevi may develop into malignant melanoma. We use the OBS for the detection of skin (nevi) tumors and other abnormalities.
Recent results, obtained in Soroka Medical Center in collaborations with researchers from Ben-Gurion university [2], will be presented and discussed.

[1] K. Svanberg et. al., Progress in Biomedical Optics Vol 2135, P.2 (1994).
[2] H. Reuveni, A. Salman, H. Mnitentag, A. Gersten and S. Mordechai"Optical Spectroscopy methods for tissue characterization" to be published.

Evaluation of the Extension of the Cerebral Blood Flow and its Main Parameters

Alexander Gersten

Dept. of Physics, Ben-Gurion University of the Negev

Among the major factors controlling the cerebral blood flow (CBF) - cerebral perfusion pressure , arterial partial pressure of oxygen (PaO2), cerebral metabolism, arterial partial pressure of carbon dioxide (PaCO2), and cardiac output , the effect of PaCO2 is peculiar in being independent of autoregulatory CBF mechanisms and it allows to explore the full range of the CBF. We have developed a simple physical model, and have derived a simple four parameter formula, relating the CBF to PaCO2. The parameters are: B_{max} , the maximal CBF, B_{min} the minimal CBF, p_0 the value of PaCO2 at the average CBF and the parameter A, the slope at this point. The parameters can be extracted in an easy way, directly from the experimental data. With this model experimental data sets of human, rats, baboons and dogs were well fitted. The same type of parametrization was also used successfully for fitting experimental data of PaO2 of dogs. We have also looked on the dependence of the PaCO2 parameters on other factors and were able to evaluate their dependence on the mean arterial blood pressure.

Radiological Imaging Quality with MV X-rays in Radiation Therapy

Yanai Krutman, Sergio Faermann, and Alex Tsechanski

Soroka Medical Center
Institute of Oncology, Be'er Sheva

"Portal image" is defined as the patient image produced throughout the radiation treatment by means of electronic or non-electronic devices. In the MeV energy range (1–15 MeV), photon beams will interact mainly by Compton scattering, producing the very low contrast observed in portal images. Image degradation could also be caused by bad positioning of the detector or bad exposure. In our study to improve portal imaging (PI), a special portal mode was added to a Clinac 18 (Varian Associates, Palo Alto, USA). This mode includes a low-energy unflattened x-ray beam and a separate target port. The physical parameters of this port (electron beam energy, target port thickness and material) are determined exclusively by diagnostic PI quality requirements. The electron beam energy of the new port was lowered to 4 MeV to increase the low-energy contribution to the photon spectrum. The beam energy was changed by decreasing the DC current feeding the accelerator bending magnet. The amount of RF power applied to the accelerator guide in the new low-energy mode was set by optimizing the position of a metal plunge within the waveguide by means of the shunt-drive assembly. To determine the optimum parameters of the separate target port we performed EGS4 Monte Carlo (MC) calculations. The bulk of the calculations involved simulations of monoenergetic electrons (2–10 MeV) incident normally on slabs of Cu, Ti, Al, graphite, Be. Downstream of the target was positioned a column of air 10 cm in diameter and 100 cm in length. As a result of the simulations, it was concluded that the maximum total fluence for 4 MeV electron beam is obtained with a 1.5 mm thick Cu target. The integrated photon fluence ratio Ψ(0–150 keV)/Ψ(0–4 MeV) obtained for this target was high ($\simeq$ 0.27). Two sets of experiments were performed: the first with a 1.5 mm thick Cu target and the second with a 5 mm Al target (Cu mass equivalent) installed in the accelerator. Portal films were taken with a Rando anthropomorphic phantom. To emphasize the low-energy response of the new port we used a Kodak Min-R mammographic film and cassette combination. Because of its high sensitivity only 1 cGy are required. The new portals show a drastic improvement in sharpness and contrast in anatomical detail compared to existing ones.

Plasma and Space Physics

Spatial and Temporal Diagnostics of Plasma Channel Waveguides for High Intensity Laser Pulses

Y. Ehrlich, D. Kaganovich, C. Cohen, P.V. Sasorov*, and A. Zigler
Racah Institute of Physics, Hebrew University
* *Institute for Theoretical and Experimental Physics, Moscow*

Optical guiding of high intensity laser pulses has a grate importance in accelerating schemes and X-ray lasing medium generation[1]. Capillary electrical discharge is a very convenient technique for plasma waveguide generation[2]. Recently a new double capillary scheme have been proposed by authors[3]. Time and space resolved electron density measurements of plasma waveguides, formed by this capillary discharge, are presented. A hollow electron distribution is obtained during a certain period of the discharge. Channel depth is up to a few 10^{18} cm^{-3} and channel duration is a few hundreds of nsec. Numerical simulations of plasma dynamics proved to be in a good agreement with the experimental data. Optical guiding experiments were conducted using these waveguides. High intensity ultrashort laser pulses have been guided over distances of up to 6.6 cm. Guiding results matched the described channel depth.

[1] P. Sprangle *et al*, Phys. Fluids B **4**, 2241, (1992).
[2] Y. Ehrlich *et al*, Phys. Rev. Lett. **77**, 4186, (1996).
[3] D. Kaganovitch *et al*, Appl. Phys. Lett. **71**, 2925 (1997).

Cyclotron-Resonance and Free-Electron Masers at Low-Voltages: Concepts, Experiments, and Applications

E. Jerby, A. Shahadi, R. Drori, Li Lei, M. Korol, M. Einat, A. Kesar, V. Dikhtyar, Y. Leibovitch, and R. Caspi

Faculty of Engineering, Tel Aviv University Ramat Aviv 69978, Israel

Cyclotron-resonance masers (CRMs) and free-electron masers (FEMs) are well known as high-power microwave (HPM) sources. These are operating, typically, as fast-wave devices with high-energy electron beams (i.e., with high accelerating voltages). In this talk, we present low-voltage CRM and FEM variants studied experimentally and theoretically in our laboratory. These include: Periodic- and dielectric-loaded CRMs and FEM experiments. FEMs operating at VHF and UHF ranges with extremely low voltages (500 V). Fluid-loaded FEM and CRM devices. Multi-beam CRM-arrays, and the active phased-array antenna concept. Microwave-pumped CO2 lasers and hybrid devices. Reflex-gyrotron. Operating principles of these schemes and their experimental results are presented. The feasibility of low-voltage HPM sources, and their possible applications, are discussed.

Low-Frequency Waves in Relativistic Pair Plasma of Pulsar Magnetospheres

Michael Gedalin and Ella Gruman

Dept. of Physics, Ben-Gurion University

High brightness temperature pulsed radioemission is believed to e generated in the pulsar magnetosphere which is filled with an ultra-relativistic electron-positron plasma. This plasma is embedded in the strong magnetic field of the pulsar which achieves the magnitude of 10^{12}G on the surface. Most models assume that the radiowaves are generated in the region between 10 and 100 pulsar radii from the pulsar surface. Although the mechanism of generation and spectrum formation is not quite clear it is understood that it should be intimately related to the features of low-frequency (frequencies much below the electron gyrofrequency) waves in the relativistic pair plasma of pulsar magnetosphere. We analyze the properties of these waves. It is shown that in the pulsar magnetosphere conditions the number of possible modes is limited by three only. We perform a position-frequency mapping for the observed radio-range and show that typically two modes fall in this range in the above mentioned region. We also critically reconsider the model of the radio-spectrum formation based on the nonlinear wave interactions in the relativistic plasma. In this model electromagnetic waves are excited by some mechanism (presumably some instability) in the high frequency range and afterwards are converted into the low frequency range due to nonlinear interaction. It is assumed that the spectrum is formed in the inertial range where the memory about the source and sink is essentially lost. Three-wave interaction requires pre-excitation of the other (non-electromagnetic) mode too, is quasi-one-dimensional, and is expected to be inefficient in the spectrum formation. Induced (nonlinear) scattering of electromagnetic waves on plasma particles results in the transformation of the wave energy into the low-frequency range and diffusion in the **k**-**B** angle space. The resulting spectra should be anisotropic. Rough estimates show that a quasi-power spectrum is formed in the stationary regime.

[1] M. Gedalin, D.B. Melrose, and E. Gruman, Phys. Rev. E, **57**(3), 1998 (in press).
[2] M. Gedalin, E. Gruman, and D.B. Melrose, Nonlinear interactions in the relativistic pair plasma in pulsar magnetospheres, Preprint BGU PH-98/03.

Plasma-Propellant Interaction in Electrothermal-Chemical Guns

Chay Goldenberg, Roger Alimi, Lior Perelmutter, Morris Sudai, David Zoler*, David Melnik

Propulsion Physics Division, Soreq NRC, Yavne 81800
**School of Physics and Astronomy, Tel Aviv University*

A conventional gun[1] consists of a chamber, which is initially filled with grains of solid propellant, and a barrel in which the projectile is accelerated. The ballistic process is initiated by igniting the solid propellant, using the combustion products of a primer containing a fast-burning energetic material. Consequently, the propellant starts burning, generating hot gases which expand, almost adiabatically, in the barrel and deliver kinetic energy to the projectile.
In a Solid Propellant Electrothermal-Chemical (SPETC) gun[2], plasma is generated by a pulsed high-power electric discharge in an ablative capillary. This plasma is injected into the gun chamber, igniting the propellant. Typical parameters of the plasma at the injector exit[3] are: temperature>20000°K, velocity~10000 m/s, density~1 kg/m^3. The ignition of solid propellant by plasma has been shown to have several advantages over conventional ignition. It is faster, more homogeneous and more reproducible. It also provides additional degrees of freedom which allow a better control of the ballistic process. In addition, this technology enables the ignition of advanced propellants which are hard to ignite using a conventional primer.
A SPETC gun is being developed at Soreq[2]. In order to gain a better understanding of the physical processes involved, the interaction of a plasma jet with solid propellant has been studied at Soreq both experimentally and theoretically. The process is rather complicated, involving the mixing of the plasma with the air present in the chamber, its propagation through the granular bed of propellant, and various mechanisms of heat transfer to the propellant.
Several studies are presented, including a theoretical model for the ignition of solid propellant by plasma[4], an experimental study of the spatial properties of the ignition process and the plasma propagation velocities in the chamber[5], the radiative properties of the plasma-air mixture, and an experimental study of the heat transfer mechanism.

[1] J. Corner, *Theory of Interior Ballistics of Guns*, John Wiley & Sons (1950).
[2] D. Melnik et al., *The Solid Propellant Electrothermal-Chemical Technology Development at Soreq*, Proc. 1st Int. Conf. on All Electric Combat Vehicle, Haifa, Israel (1995).
[3] A. Loeb and Z. Kaplan, IEEE Trans. on Mag. **25**, 342 (1989).
[4] R. Alimi, C. Goldenberg, L. Perelmutter, D. Melnik and D. Zoler, Proc. 4th Int. Symposium on Chemical Propulsion, Stockholm, Sweden (1996).
[5] L. Perelmutter, C. Goldenberg, M. Sudai, R. Alimi, Moran Furman, David Kimhe, Gabriel Appelbaum, Shlomo Arie, Zvi Zeevi, David Melnik, Proc. 9th Electromagnetic Launch Symposium, Edinburgh, Scotland, UK (1998), to be published in IEEE Trans. on Mag. (Jan. 1999).

Observation of downstream energetic electron/ion flow and accompanied high-power microwave radiation during the opening of submicrosecond plasma opening switch

Ya. E. Krasik, A. Dunaevsky, and J. Felstreiner
Physics Faculty, Technion, Haifa

In this report, results of experimental investigations of high-energy electron beam generation and transportation in the downstream region with respect to the load of a submicrosecond plasma opening switch ($I_{pos} \leq 35kA, \tau_{1/4} \cong 300ns$) are presented. This electron beam with non-complete charge and current neutralization is accompanied by collectively accelerated ions having energy of several times higher than the energy of electrons. Experiments were carried out with different loads: short-circuit inductance, open-circuit load, and planar diode. It was shown that the electron beam appearance in the downstream region with respect to the load occurs almost simultaneously with the beginning of the inductive voltage, independently of the type of the load. In addition, a generation of high-power microwave radiation was observed for all types of loads. We believe that the generation of the microwave radiation is related to a non-complete charge neutralized electron beam injection into the drift region and a formation of a virtual cathode in this region. Received experimental data and qualitative explanation of the generation of the inductive voltage and microwave radiation are discussed.

NUMERICAL SIMULATIONS OF FAST AND SLOW MICROWAVE SOURCES

M. Botton[1] , T. M. Antonsen Jr.[2], B. Levush[3], K. Nguyen[4], and S. Cooke[2].

[1]*Rafael, P.O. Box 2250, Haifa 31021, ISRAEL*
[2]*Institute for Plasma Research, University of Maryland, College Park, MD 20740, U.S.A.*
[3] *Naval Research Laboratory, Washington D.C. 20375, U.S.A.*
[4]*KN Research, Silver Spring, MD 20906, U.S.A.*

In this work we present the development of a new MAGY code which is designed to be an effective tool for modeling slow and fast microwave sources, using a reduced description of the system. The key step in the derivation of the reduced description is the description of the fields as a superposition of (relatively few) eigen-modes of the waveguide where the interaction takes place. Accordingly, Maxwell's equations are reduced to a set of coupled partial differential equation(axial coordinate and slow time variation). As the wall radius of the waveguide is, in many cases, a function of the axial coordinate (tapering or discontinuities), the modal representation makes use of "local eigen modes" which are axially dependent, and coupling terms among the various modes are introduced. This coupling is added to the one introduced by the finite conductivity of the walls, and the coupling due to the electronic current source. Besides speeding up the electromagnetic calculations, the reduced description also facilitates the computation of the electronic trajectories. A significant savings of computation time is obtained by periodically launching ensembles of beam particles each time step, calculate the trajectories and deduce the currents sources for the electromagnetic fields. The reduced description was successfully applied in a series of MAGY codes. The current version of MAGY is intended to generalize the analysis and include additional features such as mode coupling (TE and TM) for an arbitrary wall geometry (including jump discontinuity), rigorous self-consistent calculations, relativistic electron dynamics, arbitrary guiding magnetic fields [1]. As an example, we compare the numerical simulations with the experimental results for two types of microwave sources, namely the 35GHz Gyroklystron amplifier [2] and a relativistic Backward Wave Oscillator [3]. The agreement between the simulation and the experimental data is very good for both systems. We conclude that MAGY is a relatively simple and compact code which can be used for modeling of wide verity of electron beam systems utilizing modest computing resources.

1. M. Botton, T. M. Antonsen Jr., B. Levush, K. Nguyen, and A. Vlasov, "MAGY: A Time Dependent Code for Simulation of Slow and Fast Microwave Sources" IEEE Trans. Plasma Science, Special Issue on High Power Microwaves, 1998.

2. J. Choi, A. McCurdy, F. Wood, R. Kyser, J. Calame, K. Nguyen, B. Danly, T. Antonsen, B. Levush and R. Parker "Experimental Investigation of a High Power, Two-cavity, 35 GHz Gyro-klystron Amplifier", ibid.

3. Y. Carmel, W.R. Lou, J. Rodgers, H. Guo, W.W. Destler, V.L. Granatstein, B. Levush, T. Antosnen, Jr. and A. Bromborsky, Phys. Rev. Lett., 69, 11, 1992

Determination of the time-dependent radial distributions of the electron density, electron temperature, and ion charge states in a cylindrically imploding plasma

Yu.V.Ralchenko, L.Gregorian, G.Davara, E.Kroupp, and Y.Maron

Faculty of Physics, Weizmann Institute of Science

We have recently reported the time-dependent measurements of the particle velocity [1] and magnetic field [2] distributions during the implosion phase of a moderate-density gas-puff Z-pinch plasma. Here we will discuss the results on spectroscopic determination of electron density N_e, electron temperature T_e, and charge state distribution under the same conditions. The gas-puff system is used to produce a hollow cylinder of CO_2 gas in the 1.35-cm wide anode-cathode gap. A high-voltage discharge circuit produces a plasma pinch in about 600 ns with a peak current of 220 kA. The spectroscopic measurements with a temporal resolution of 10 ns, were carried out by observing the plasma along the z axis at various radial locations throughout the implosion process, thereby providing a complete mapping in (r, t) of the line emission from plasma.

The time-dependent electron density radial distribution was determined from the measured Stark line widths of the different ions of oxygen at different radial positions. The time-dependent intensities of the visible lines from the same or successive charge states were used to obtain the electron temperature. Both the electron density and temperature were determined self-consistently by measuring the ionization times of the various charge-state ions. These results are used together with the collisional-radiative (CR) calculations to determine the time-dependent plasma composition. The CR simulations with the NOMAD code were carried out with account of temporal variations of the electron density and opacity effects.

[1] M. E. Foord, Y. Maron, G. Davara, L. Gregorian, and A. Fisher, Phys. Rev. Lett., **72**, 3827, (1994).

[2] G. Davara, L. Gregorian, E. Kroupp, and Y. Maron, Phys. Plasm., to be published (1998).

IL9905688

Inertial Confinement Fusion Ignition Criteria using Self-Similar Solutions

Roy Kishony[1,2], Dov Shwarts[1], Eli Waxman[1] and Itzhak Kelson[2]

[1] *Physics department, Nuclear Research Center - Negev, Beer-Sheva*
[2] *School of Physics and Astronomy, Tel-Aviv University, Tel-Aviv*

The ignition conditions, under which a thermonuclear burn wave propagates from an initial hot spot, and the characteristics of the propagating burn wave are investigated using a set of self similar solutions.[1] Although the self similar solutions exist only for external density profile that decreases as $\rho_{out}\ r^{-1}$, they are shown to provide natural ignition criteria and critical profiles for more general density profiles. The self similar solutions are also used to investigate the effect of 2-D perturbations on the ignition conditions. The concept of Working Lines (WL's), attractors of trajectories in the $\rho * R - T$ plane of propagating burn waves, is introduced for density profiles $\rho_{out}\ r^{-\omega}$. The WL's are found to be close and almost parallel to the ignition line (IL). The spatial profiles of a burn wave propagating along the WL's are shown to be closely related to the self similar critical profiles.

[1] Roy Kishony, Eli Waxman and Dov Shwarts, Phys. Plasmas, **4**, 1385, (1997).

High-frequency electron beam modulation in a diode with a plasma cathode

A.Dunaevsky, Ya.E.Krasik, and J.Felstreiner
Physics Faculty, Technion, Haifa

A novel phenomenon of high frequency modulated electron beam generation is presented. Experiment was carried out with an electron diode having active source of the cathode plasma. Modulated electron beam with duration of $\geq 1\mu s$ was generated during more than one hour with a frequency of $2Hz$. The frequency of the modulation was found to be $\geq 325MHz$. The modulation of the beam current amplitude reaches $\geq 30\%$. The generation of the modulated electron beam is accompanied by electromagnetic radiation with the same frequency and power of several tens of kW. Based on the experimental data a qualitative model of the observed phenomenon is described.

Plasma light beacons for astronomical adaptive optics

Erez N. Ribak

Department of Physics, Technion, Haifa

It is proposed to create reference airglow spots for measuring atmospheric turbulence for adaptive optics. Laser guide stars are now starting to replace natural guide stars as references for the wave-front sensing systems. However, even a single such laser is a complex undertaking for an observatory, and it yields a very narrow correction; three or more lasers are required for tomography of the turbulence and a wide field of view.

By using radio transmitters, artificial airglow can be created. Below 100 km the power requirements are high, but the spots are well defined. A phased array or a big dish will create an array of plasma spots which will yield visible signals for the measurement. Such experiments (for radio reflection off the ionized region) were carried in a laboratory simulation of the atmosphere [1].

Above 100 km, less power is needed, but the shape of the ionized regions is less controlled. Striations can be formed which are of the right size, but their location and spacing varies with time, complicating the data processing. Airglow patterns were observed after radio heating of the ionosphere, but their global extent was much too large; better concentration will be required for astronomy.

Since the radio transmitters can be far removed from the observatory, power dissipation problems are alleviated there, compared to laser transmitters. However, safety of aircraft is still a problem. The question of infra-red airglow, which might hamper some of the astronomical measurements, has to be solved, or perhaps used also for wave-front sensing.

[1] A. V. Gurevich, N. D. Borisov, and G. M. Milikh, *Physics of microwave discharges: artificially ionized regions in the atmosphere*, Gordon and Breach (1997).

Restoration of the Ionospheric Convection Patterns in the Polar Cap

P. L. Israelevich, and A. I. Ershkovich

Department of Geophysics and Planetary Sciences, Tel Aviv University

A new method for restoration of instantaneous convection pattern in the Earth's polar ionosphere is suggested. Plasma convection in the polar cap ionosphere is described as a hydrodynamis incompressible flow. This description is valid in the region where the electric currents are field aligned (and hence, the Loretz body force vanishes). In addition, the problem becomes two-dimensional, and may be described by means of stream function. A solution of hydrodynamic equation for stream function is solved numerically. It is shown that the convection pattern may be restored with a reasonable accuracy by means this method, by using only the minimum number of satellite crossings of the polar cap.

On the Prediction of Great Flare Energetic Particle Events to Save Electronics on Spacecrafts

Lev Dorman
Physics Faculty, Technion, Haifa and ICRC, affiliated to TAU, Tel Aviv

The problem of influence of galactic cosmic rays and solar flare energetic particles (FEP) on micro-electronics code on spacecrafts is very important and was developed deeply by many authors (see [1]-[3] and references within). Especially dangerous are single event phenomena (SEP)[4] which can destroy computer memories on earth and with much bigger probability in spacecraft systems; according to [4] in the periods of great energetic particle fluxes is necessary to swich off some part of electronics to protect computer memories from SEP. How to predict this period of time? In principle it can be made by using high energy particles which came from the Sun much more early than main part of middle energy particles caused dangerous situation for electronics. The flux of these high energy particles is very small and can not be measured with enough accuracy on spacecrafts, but are measured continuesly by ground based neutron monitors and muon telescopes with very small statistical errors (because they have very big effective surfaces).

Here we will show that this prediction can be made exactly by the International Cosmic Ray Service (ICRS) [5], which will be organized in near future on the basis of the Israel Cosmic Ray Center (ICRC), affiliated to Tel Aviv University and on the basis of some part of world-wide network of cosmic ray observatories (the Project was present to UNESCO). The idea of this method is as following. In Internet will be organized a special page for ICRC and then for ICRS. In this page in real time scale will go 5-minute or/and 1-minute data from our Cosmic Ray Observatory on Mt. Hermon, from observatories Rome, Moscow, Kiev, Apatity, Irkutsk, Novosibirsk, Almata, Aragaz, Mexico, Haleakala, Chacaltaya and others. These data will be continuesly processing in real time scale by our Central computer in Qazrin. If at any observatory will be observed cosmic ray intensity increase more than 3σ, will be start the program "Alert 1", which will compare this increase with data of other observatories and with situation in the next time period. If it will be show that it is real beginning of the FEP event, will be start the program "Alert 2", which will take into account the position and properties of solar flare (if this information will be available) and determine the preliminary model of FEP event: to calculate the energetic spectrum of FEP, parameters of FEP source on the Sun, and propagation parametrs in corona and in interplanetary space. On the basis of this model will be preliminary estimate expected radiation situation after 20-60 minutes. In the case if the expected level of radiation will be dangerous for electronics in spacecraft systems, will be send the prliminary alert, and will be start the program "Alert 3". This program will continue to work with data including next period and made correction of preliminary model to obtain the final model of FEP event and more exactly calculate the expected time profile of FEP flux in dependence of particle energy. Will be calculate also the expected radiation hazard for different types of spacecraft orbits and for spacecrafts in the Heliosphere in dependence from the distance to the Sun. This information will be send by the final alert. If the expected radiation will be very high, the same will be made for aircrafts in dependence of

altitude and cut-off rigidity as well as for people and technology on the earth and mountains. The programs Alert 1, 2 and 3 as well as procedure of automatically formating preliminary and final models of FEP events and preliminary and final alerts will be training on the basis of historical great FEP events data, discribed in details in [6]-[12].

[1] J. Levinson et al., Appl. Phys. Lett, **63**, 2952, (1993).
[2] J. Barak et al., IEEE Trans. Nucl. Sci., **43**, 907, 979, (1996).
[3] A.J. Tylka et al., IEEE Trans. Nucl. Sci., **44**, 2150, (1997).
[4] J. Barak et al., Annual Report, Israel Atomic Energy Comission, (1995).
[5] L.I. Dorman et al., Astrophys. and Space Sci., **208**, 55, (1993).
[6] L.I. Dorman, Cosmic Ray Variations, Moscow, Gostehteorizdat, (1957); Washington DC, (1958).
[7] L.I. Dorman, Cosmic Ray Variations and Space Research, Moscow, Nauka, (1963).
[8] L.I. Dorman, Astrophysical and Geophysical Aspects of Cosmic Rays, in serie "Progress in Elementary Particle and Cosmic Ray Physics", Vol. 7, Amsterdam, North-Holland, (1963).
[9] L.I. Dorman, L.I. Miroshnichenko, Solar Cosmic Rays, Moscow, Fizmatgiz, (1968); NASA, (1976).
[10] L.I. Dorman, Cosmic Rays: Variations and Space Investigations, Amsterdam, North-Holland, (1974).
[11] L.I. Dorman, Cosmic Rays of Solar Origin, Moscow, VINITI, (1978).
[12] L.I. Dorman, D. Venkatesan, Space Sci. Rev., **64**, 183-362, (1993).

Cosmic Ray Propagation in Space Plasma With Two Types of Scatterers

Lev Dorman[1], Vjacheslav Shogenov[2]
[1] *Technion and ICRC, affiliated to TAU, Israel*
[2] *Kabardino-Balkar State University, Russia*

We determine the transport parameters for cosmic ray particles in space plasma with two types of charged particle scatterers according to our model [1]. In this model first type of scatterers are magnetic inhomogeneities frozen in a background plasma moved with some velocity $\vec{U}_1$. These scatterers are characterized by transport path $L_1(R)$, where R is the rigidity of charged particles. The second type of scatterers are magnetic clouds, high speed streams, shock waves (considered only as scatterers) moved with some average velocity $\vec{U}_2$ and characterized by transport path $L_2(R)$. We suppose that the magnetic field of the background plasma $\vec{B}_1 = \vec{B}_{10} + \delta\vec{B}_1$, where regular part $\vec{B}_{10} = \left\langle \vec{B}_1 \right\rangle$ and for fluctuating part $\left\langle \delta\vec{B}_1 \right\rangle = 0$. For cosmic ray distribution function we suppose $f = f_0 + \delta f$, where $f_0 = \langle f \rangle$ and $\langle \delta f \rangle = 0$. We suppose also that $\vec{U}_1$ and $\vec{U}_2$ contain regular parts $\vec{U}_{10} = \left\langle \vec{U}_1 \right\rangle$, $\vec{U}_{20} = \left\langle \vec{U}_2 \right\rangle$ and fluctuated parts $\delta\vec{U}_1 = \vec{U}_1 - \vec{U}_{10}$, $\delta\vec{U}_2 = \vec{U}_2 - \vec{U}_{20}$. From the collisional Boltzmann equation we derive the diffusion approximation described the propagation and acceleration of cosmic ray particles which coincide with usually used at $\vec{U}_{10} = \vec{U}_{20}$. The acceleration and its application to different astrophysical objects we consider in [2]. Here we consider cosmic ray propagation and modulation in this system. We found that it will be determined by diffusion tensor $\kappa_{kl} = \frac{v^2\nu}{3(\nu^2+\omega^2)}(\delta_{kl} - \omega_k\omega_l/\nu^2 - e_{kil}\omega_i/\nu)$ and by the effective convection speed $\vec{U} = \vec{U}_{10}\nu_1/\nu + \vec{U}_{20}\nu_2/\nu$, where collision frequency of cosmic ray particles $\nu = \nu_1 + \nu_2$ (here $\nu_1 = v/L_1(R)$ and $\nu_2 = v/L_2(R)$) and $\vec{\omega} = Zec\vec{B}_{10}/E$, e_{kil} is unity antisymmetric tensor, E is the total energy of cosmic ray particle. It is shown that this mode of cosmic ray propagation and modulation is important in the Heliosphere and can be important in the Galaxy.

[1] L.I. Dorman, V.Kh. Shogenov, Zh. Eksp. Teor. Fiz., **89**, 1624, (1985).
[2] L. Dorman, V. Shogenov, Report on IPS98 (Astrophysics and Cosmology), (1998).

Toroidal Dielectric Tensor-Operator for Arbitrary Aspect-Ratio and Wave Frequency: an Anisotropic-Resistivity MHD Formulation

K Komoshvili, S Cuperman, C Bruma

School of Physics and Astronomy, Tel Aviv University
69978 Tel Aviv, Israel

Motivated by the recently increased interest in small aspect ratio tokamaks, we have derived a $2\frac{1}{2}$D dielectric tensor-operator which can properly describe the plasma response to r.f. waves, under conditions prevailing in the pre-heated stages of *arbitrary aspect ratio*, axisymmetric toroidal fusion devices.
The derived dielectric tensor elements are based on a two-fluid, weakly collisional plasma description, with the Hall term included. They are characterized by the following features:

(i) They are cast in a form evidencing the dielectric (non-operator) and operator contributions - the latter being due to the toroidal structure of the ∇-operators present in Maxwell's equations, on the background of equilibrium currents and pressure gradients;

(ii) They are *not subject to any limitation* on the (relative) magnitude of the toroidal effects — no expansion in the inverse aspect ratio parameter is used for their derivation;

(iii) They include *anisotropic* — parallel and perpendicular to the magnetic field — contributions to the plasma resistivity;

(iv) They are *not limited by any restriction* on the (relative) value of the wave frequency.

The explicit, physically transparent formulation of the dielectric tensor is intended for the numerical solution of the full ($E_{\|} \neq 0$) wave equation and subsequently, evaluation of the Alfvèn wave current drive in small aspect ratio tokamaks.

Solution of Full Wave Equation for Global Modes in Small Aspect Ratio Tokamaks with Non-Circular Cross-Section

S Cuperman, C Bruma, K Komoshvili

School of Physics and Astronomy, Tel Aviv University
69978 Tel Aviv, Israel

The wave equation for *strongly toroidal* small aspect ratio (spherical) tokamaks with non-circular cross-section is properly formulated and solved for global waves, in the Alfvèn frequency range. The current-carrying toroidal plasma is surrounded by a helical sheet-current antenna, which is enclosed within a perfectly conducting wall. The problem is formulated in terms of the vector and scalar potentials ($\mathbf{A}$,Φ), thus avoiding the numerical pollution occuring in the case of ($\mathbf{E}$,$\mathbf{B}$) formulation. Adequate boundary conditions are applied at the vacuum – metallic wall interface and the magnetic axis.

A recently derived *dielectric tensor-operator* [1], able to describe the anisotropic plasma response in spherical tokamaks, is used for this purpose; except for its linear character, no physical or geometrical limitations are imposed on it. The *equilibrium profiles* (magnetic field, pressure and current) are obtained from a numerical solution of the Grad-Shafranov equation.

Specifically, the wave equation is solved by the aid of a numerical code we developed for the present problem, based on the well documented $2\frac{1}{2}$D finite element solver proposed by E.G.Sewell [2]. With the definitions $V_i(\theta,\rho) = U_i(-\theta,\rho)$ ($V_i, U_i = A_j, \Phi; j = \rho,\theta,\phi$), *our code solves simultaneously 16 second order partial differential equations* (eight equations for each of real and imaginary set of functions V_i, U_i).

A systematic analysis of the solutions obtained for various values and combinations of wavenumbers and frequencies in the Alfvèn range is presented.

[1] K Komoshvili, S Cuperman and C Bruma, *Toroidal Dielectric Tensor-Operator for Arbitrary Aspect Ratio and Wave Frequency: an Anisotropic-Resistivity MHD Formulation* (this conference).

[2] G Sewell, *PDE2D*, Advances in Engineering Software, **17**, 1993, 105

Basic Toroidal Effects on Alfvèn Wave Current in Small Aspect Ratio Tokamaks

C Bruma, S Cuperman, K Komoshvili

Dept. of Particle Physics, Weizmann Institute of Science
** Physics Faculty, Technion, Haifa*

The Alfvèn wave current drive (AWCD) in small aspect ratio tokamaks is properly calculated, with consideration of the basic toroidicity effects present in (i) *the dielectric tensor-operator* (involving the strongly toroidal equilibrium profiles), (ii) *the structure of the r.f. fields* obtained as a solution of the wave equation (through Maxwell's equations' toroidal operators as well as the conversion rate and conversion layer location, depending also on the equilibrium profiles) and (iii) the *formulation of the AWCD* (which, besides its dependence on the r.f. fields — affected by toroidicity as mentioned at points (i) and (ii) — also requires the equilibrium-magnetic-surface averaging of non-resonant forces involved).
Thus, (1) we consider *consistent equilibrium profiles* with neo-classical conductivity corresponding to an ohmic START-like discharge [1]; (2) use a *resistive (anisotropic) MHD dielectric tensor-operator with practically no limitations*, adequate to describe the plasma response in the pre-heated stage [2]; (3) solve numerically the $2\frac{1}{2}$D *full-wave equation* by the aid of an advanced finite element code developed in [3]; and (4) evaluate the AWCD by the aid of the recently proposed, quite general formulation holding in the case of *strongly toroidal fusion devices* [4] and including contributions due to helicity injection, momentum transfer and plasma flow.
A general discussion of the results obtained in this work is presented.

[1] H R Wilson, *SCENE-Simulation of Self-Consistent Equilibria with Neoclassical Effects*, Report of UKAEA Government Division - Fusion, UKAEA FUS 271.
[2] K Komoshvili, S Cuperman and C Bruma, *Toroidal Dielectric Tensor-Operator for Arbitrary Aspect Ratio and Wave Frequency: an Anisotropic-Resistivity MHD Formulation* (this conference).
[3] S Cuperman, C Bruma and K Komoshvili, *Solution of Full Wave Equation for Global Modes in Small Aspect Ratio Tokamaks with Non-Circular Cross-Section* (this conference).
[4] V S Tsypin *et al.* Phys. of Plasmas **2** (1995) 2784.

SPECTROSCOPIC INVESTIGATIONS OF A MICROSECOND PLASMA OPENING SWITCH

R. Arad, K. Tsigutkin, Yu. Ralchenko, A. Fruchtman*, and Y. Maron
Dept. of Particle Physics, Weizmann Institute of Science
* *Center for Technological Education Holon*

We study the interaction between plasmas and magnetic fields in a configuration called a plasma opening switch (POS). A current of 160 kA is conducted by a previously prepared plasma during 400-600 ns before the plasma resistance increases sharply and the current is diverted to a parallel inductive load within ≈100 ns. Our POS is planar and the plasma is produced by two flashboards and enters the 2.6 cm inter-electrode region through slots in the anode. Spectroscopic measurements local in 3D are made by doping the plasma with various species using a molecular-beam injection and observing the characteristic emission of the doped particles. Measurements of the magnetic field evolution from Zeeman splitting, ion velocities from Doppler shifts, and electron density and temperature from line intensities and collisional-radiative calculations are made. A 3-D map of the magnetic field evolution was obtained and the magnetic field is seen to penetrate into the POS region in the form of a broad current channel at an average velocity of $\approx 3 \times 10^7$ cm/s. The light intensities of all species were seen to rise and drop during the current conduction. The duration of the rise is ≈50 ns and it propagates axially at the same velocity as the magnetic field. It is shown that this rise is due to a rise in the mean electron energy and a rise by a factor of two in the electron density. The drop of the electron density which follows results from a drop in the electron density from its initial value of $\approx 5 \times 10^{14}$ cm^{-3} to $< 5 \times 10^{13}$ cm^{-3}. We determined the local velocities of doped helium and argon ions, and line-integrated velocities of carbon ions. The velocity of protons was measured spectroscopically by observing the spectral profile of Ha emitted from atoms produced by proton charge-exchange. The axial velocities of the protons, HeII, and CIII were found to be nearly the same ($1.2 \pm 0.3 \times 10^7$ cm/s), while the velocity of ArIII was found to be much lower ($< 1 \times 10^6$ cm/s). We attempt to understand these results by modeling the magnetization and drifts under the effects of the electric and magnetic fields assuming a collisionless plasma. Possible mechanisms to explain the broad current channel in the plasma and the fast magnetic field penetration will be discussed.

Physics in Biology

Biophysics of the Nuclear Shell

Michael Elbaum, Hanna Salman

Dept. of Materials and Interfaces, Weizmann Institute of Science

Living cells of yeast, plants, and animals are subdivided into internal membrane-bound compartments called organelles. Each of these performs a specific set of biochemical functions, allowing the cell to organize its biochemistry spatially. Among the organelles, the most prominent is the nucleus. It contains the cell's genetics in the stable form of DNA, and the apparatus to create from it RNA whose code specifies the sequence of amino acids in proteins. The actual production of proteins, however, takes place entirely outside the nucleus. Messenger RNA is exported from the nucleus bearing the appropriate code, while proteins used inside the nucleus must be reimported, including the "molecular machines" responsible for the DNA to RNA transciption itself. All of this points to an important bidirectional transport taking place across the boundary which separates the nucleus from the remainder of the cell interior.

The nucleus is enveloped by a double bilayer lipid membrane, the overall thickness of which is approximately 40 nm. Large channels are studded throughout this envelope, each known as a "nuclear pore complex" (NPC). The NPCs pass though both bilayer membranes, opening a passive diffusion channel for water, ions, and small molecules of effective diameter less than $\sim$ 8 nm. For proteins this corresponds to a molecular weight cutoff of 30 $\sim$ 40,000. Larger proteins enter the NPC only if they contain a short peptide sequence known as a "nuclear localization signal" (NLS), or if they bind to another protein which has one. This transport is active, in that it stops if the supply of chemical energy, as ATP, is depleted. Export of RNA and RNA-protein complexes is also dissipative, and takes place through the same NPCs as protein import.

The past decade has seen tremendous progress in identifying various types of NLS and their biochemical partners involved in the transport. In spite of much effort, however, no protein whose structure suggests a muscle or motor-like activity has been found to take part. From the mechanistic point of view, the questions as to how this molecular pump works are entirely open.

I will describe a set of physical experiments whose aim is to address the simple engineering parameters of nuclear transport. How fast does the pore pump? What kind of force can it apply? How does this force depend on the size of the molecular cargo or on the type of NLS? What role does passive diffusion play in the transport process? Our experiments are based on an in vitro reconstitution system using extract from frog eggs, which is capable of producing nuclear membranes with functioning nuclear pores. The idea, in brief, is to tether an NLS-bearing protein at a distance from a micron-sized bead which can be manipulated on a microscope by optical tweezers. The string used for tethering is a single molecule of DNA. We can exploit the tools of molecular biology to vary the placement and density of NLS-bearing proteins along the DNA, and as well as to try to understand the nuclear import of DNA itself. The optical tools are ready to make quantitative force and velocity

measurements. Building on the biochemical studies, we hope to add to the physical understanding of this selective molecular transport.

From Neurons to Brain

E. Ben-Jacob

Tel-Aviv University

During embryonic morphogenesis, a collection of individual neurons turns into a functioning network with unique capabilities. Only recently has this most staggering example of emergent process in the natural world begun to be studied. Here we propose navigational strategy for neurites growth cones, based on sophisticated chemical signaling. We further propose that the embrionic envirnment (the neurons and the glia cells) acts as an excitable medium in which concentric and spherical chemical waves are formed. Together with the navigation strategy, the chemical waves provide a mechanism for communication, regulation and control required for the adaptive self-wiring of neurons.

The emergence of spatial synchronization and periodic temporal rhythm in self-assembled heart-cell networks

Yoav Soen, Netta Cohen, and Erez Braun

Dept. of Biophysics, Physics Faculty, Technion, Haifa

It is generally accepted that collective periodicity in heart cell networks emerges through mutual entrainment among a-priory periodic centers. By using a new recording technique which enables continuous non-invasive monitoring of contraction dynamics throughout the life time of self-assembled, spontaneously beating heart cell networks, we show that spatial synchronization always precede the onset of collective regular (mono-periodic) beating. This finding excludes the mutual entrainment mechanism as responsible for the emergence of collective periodicity in such a self-assembly process. Our non-invasive extremely long recordings reveal rich and highly non-trivial temporal dynamics in spatially synchronized extended networks, whose manifestation in their activity includes: intermittency, period multiplicity, sudden collective rate changes and other rhythm disorders, some of which similar to those observed in real hearts. The spontaneous emergence of such non-trivial dynamical patterns calls for a study of the underlying mechanisms, and raises new questions regarding their role in network development, their scaling properties (from the single cell level to networks), and their potential effects on long-term pacemaker function and stability.

Physics in Industry

Are Physicists needed in Industry ?

Michael Brunstein,

Applied Materials Israel

The cycle time between scientific inventions and their maturity into industrial products will be presented with few examples. A study [1] on the citation of scientific papers in US patents indicates the contribution of scientific academic research to industry patents . The role physicists play in Industry and some specific data on the Physicists in the Electronics Industry in Israel will be discussed.

[1] F. Narin, K. Hamilton, D. Olivastro. Research Evaluation, 183-187, Dec 1995

Multi-Spectral Imaging

N. Ben-Yosef

Applied Physics Division
The Hebrew University of Jerusalem

Multispectral imaging stands for a large number of experimental techniques utilized in physics, biology, medicine, remote sensing and more. The present discussion will focus on a number of specific applications related to medical diagnostics, laser physics, ecology and military tasks.
The common topic to all being the need to merge physics, data processing and an instrument in order to manufacture (and sell) a problem oriented working device.
An example in ecology will show the use of satellite multispectral imaging on the measurement of the degree of pollution in waste water reservoirs. The success is based on the understanding of the radiation transfer in such turbid medium.
Similar techniques are applied on the light propagation properties inside the retina, enabling a number of diagnostics instruments for opthalmology.
The understanding of the exact processes in a quantum well lasers is supported by merging near field microscopy with multispectral imaging.
The data processing and mathematical techniques needed in order to design a working device will be briefly mentioned.

Visualization of 3D Medical Images

Roni Yagel

BMed, Jerusalem

Once medical imagery has been acquired, by a contemporary scanner such as CT, MRI and US, one would like to explore and utilize the wealth of information it encompases. We explain the technological barriers confornting us when we approach the task of displaying this information on a computer screen. We survey methods for rapid rendering of large 3D medical models. We present some algorithmic innovations, parallel implementation, tricks of the trade and other types of wizardry. It is hoped, that by the end of this presentation, one would become superficially familiar with the main trends in this field and intimately aware of the great difficulties and pitfalls lying ahead.

Quantum Well Infrared Photodetectors (QWIP)

E. Finkman, G. Bahir, S.E. Schacham, S. Maimon, and A. Fraenkel

Dept. of Electrical Engineering and Solid State Institute, The Technion, Haifa

Quantum Well Infrared Photodetectors (QWIP) form a new generation of infrared detectors based on carrier confinement in ultra-thin semiconductor heterostructures. The energy levels in these wells are designed to tailor any optical transition in the 3-20 micrometer photon wavelength range by adjusting the quantum well width and the barrier composition. The major advantages of this technology over Hg(x)Cd(1-x)Te which is the most frequently used material system for high quality infrared staring arrays are: 1) III-V (GaAs) technology is much more mature, assuring uniformity over large areas, low cost, thermal stability, radiation hardness, high yield, etc. New functions, such as multispectrality (detecting several wavelengths using the same wafer), tunability, band switching (using different voltages), and all optical devices are all feasible using this concept, and are much more difficult to realize using conventional detectors. The talk will concentrate on the study of some of the physical mechanisms governing this type of devices, which are quite different from those found in bulk structures. The possible advantages in implementing quantum dot infrared photodetectors will be pointed out, with some new experimental evidence.

Surface Currents in Shallow n^+p Silicon Junctions Made by Ultra Clean Technology

Herzl Aharoni[1], Tadahiro Ohmi[2], Akira Nakada[2,3], Yukio Tamai[2] and Mauricio Massazumi Oka[2,3]

[1]*Department of Electrical and Computer Engineering, Ben Gurion University of the Negev, Beer-Sheva 84105, Israel*
[2]*Department of Electronic Engineering, Faculty of Engineering, Tohoku University, Aza-Aoba, Aramaki, Aoba-ku, Sendai 980-77, Japan*
[3]*Laboratory for Electronic Intelligent Systems, Research Institute of Electrical Communications, Tohoku University, Aza-Aoba, Aoba-ku, Sendai 980-77, Japan*

The transition from Very Large Scale Integration (VLSI) towards Ultra Large Scale Integration (ULSI), in the present silicon microelectronics technology, involves a variety of problems. Among these is an increase of the surface current component I_s which is considered to be a loss in comparison to the bulk current I_A, which comprises the useful component for transistor actions, such as amplification and switching. I_s flows between the device terminals via the device's surface, bypassing its bulk, and hence does not contribute to the device's operation, while degrading its performance. In the current silicon device technology, I_s is considered to be much smaller than I_A, and therefore is often neglected in calculations. However, since I_s is proportional to the junction perimeter L, a problem arises as the junction area A in which the bulk current I_A flows, is decreased, in order to increase the device packaging density for example. This is due to the fact that in device geometries routinely used, the ratio L/A increases as A becomes smaller, resulting in an increase in the fraction of the loss due to surface current at the expense of the useful bulk current.
In this work, some experimental results are presented regarding surface currents in shallow n^+p single crystal silicon junctions made under ultra clean fabrication technology, as required in future ULSI technology. The results show that the ratio of the surface/bulk current is further increased, specifically due to the above processing environment. This environment results in an improvement of both bulk and surface properties, due to the reduction of the introduction of undesirable heavy metal atoms and other contaminants into the device during its fabrication As a a result the net influence of the related bulk and surface trapping centers energy levels causes a reduction of the bulk and surface generation current components. However, the improvements in the bulk properties exceed those of the surface properties, which are largely determined by the oxide-silicon interface properties, resulting in the above increase in I_s/I_A ratios. Unless special steps are taken to overcome the above,then, paradoxically, the expected advantages of future ULSI circuits may be curtailed as the device's dimensions are scaled down.

Computational Physics

Simulating Granular Flow

D. C. Rapaport

Department of Physics, Bar-Ilan University

We describe some of the results obtained during a series of molecular dynamics simulations of granular materials. The problems discussed are the following: (a) The flow through a horizontal aperture of disk-like particles that are subject to normal and transverse damping forces, with a continuous feed mechanism used to eliminate transient effects. (b) The aperture flow of particles with a sufficiently complex shape to allow partial interlocking that mimics the asperities of real grains. (c) The size-dependent segregation (inverse grading) that occurs during sheared flow down an inclined chute. (d) The formation of subharmonic surface waves in a vertically vibrated layer. (e) The appearance of horizontal transport in a vertically vibrated system whose base has a sawtooth-shaped profile. Both qualitative and quantitative aspects of the phenomena, as reproduced by these two-dimensional simulations, will be examined.

Cosmic Lacunarity

R. Thieberger, E.A. Spiegel*, A. Provenzale†

Dept. of Physics, Ben Gurion University
* *Dept. of Astronomy, Columbia University, N.Y., U.S.A.*
† *Ist. di Cosmogeofisica, Turin, Italy*

The present distribution of galaxies in space is a remnant of their formation and interaction. On a large enough scale, we may represent the galaxies as a set of points. We concern ourselves here with the analysis of the observed distribution of galaxies treated as an abstract point set. We quantify the structures in this set by its generalized dimensions[1], and attempt to study the lacunarity. The term lacunarity was introduced by B. Mandelbrot[2] it measures the voids (lacunae) in a fractal structure,and later this term was generelized from a constant to a lacunarity function[3].
For the study of the dimensions, we introduce the moments[1]

$$C_q(r) = \left(\frac{1}{N}\Sigma_i \left[\frac{1}{N}\Sigma_j \theta(r|\mathbf{X}_i - \mathbf{X}_j|)\right]^{q-1}\right)^{\frac{1}{q-1}}$$

where q is to be specified, the coordinates in the embedding space are denoted by $\mathbf{X}_i$ and θ is the Heaviside function. Since the set occupies a certain volume, some points are near the edge.To avoid the resulting distortion in the results, we sum j over the points of the set and i over a subset of points away from the edge. In our calculations we take the $C_q(r)$ at 256 points at equal spacing then we apply a least square fit.
After obtaining the D_q by least square fit the lacunarity function can be calculated from the relation:

$$log\Lambda = logC_q - D_q logr$$

The presently available data of the Center for Astrophysics redshift catalogue[4] permit reasonable estimates of a few of the Renyi dimensions (the D_q's) and, remarkably, allow the detection of the corresponding lacunarities[5,6].

[1] G. Paladin and A. Vulpiani, Phys. Rep. **156**, 147, (1987).
[2] B.B. Mandelbrot, The Fractal Geometry of Nature, (W.H. Freeman and Co. ,N.Y.), (1982).
[3] L.A. Smith, J.D. Fournier and E.A. Spiegel, Phys. Lett. **114A**, 465, (1986)
[4] J.P. Huchra, M.J. Geller, C.M. Clemens, S.P. Tokarz and A. Michel. The 1993 version available at ftp://cdsarc.u-strasbg.fr/pub/cats/VIII/164
[5] A. Provenzale, E.A. Spiegel and R.Thieberger, Chaos **7**, 82, (1997).
[6]G. Murante, A. Provenzale, E.A. Spiegel and R. Thieberger, *MNRAS* **291**, 585, (1997).

Roughening transitions and surface tension in an HCP lattice with higher neighbor interactions

Adham Hashibon, Joan Adler, and S. G. Lipson

Department of Physics, Technion-IIT, 32000 Haifa, Israel

We report on Ising lattice-gas simulations of surfaces of a hexagonal-close-packed (HCP) crystal as a function of temperature and higher neighbor interactions using sample sizes up to $160 \times 160 \times 40$ sites. The HCP lattice represents He^4 on which three roughening transitions have been observed experimentally. Most previous simulation studies on roughening transitions were performed for other lattices where less experimental data is available. We measured roughening temperatures for these three surfaces as a function of higher neighbor interactions of both signs. We also measured the surface tension of the three facets. In most cases good qualitative and reasonable quantitative agreement with experiment was found with appropriate values of interactions, confirming the basic validity of the model as applied to surface roughening.

Physics Teaching

Using an annotated catalog of websites in high school physics

Bernd Saering

The Israel Arts and Science Academy, Jerusalem
Dept. for Science Teaching, Weizmann Institute, Rehovot

The Internet offers a wealth of materials, both textual and visual, to the science teacher. The variety of these materials, their availability at low cost, their actuality and their visual quality should make the Internet an important resource for science teaching. Locating and evaluating relevant documents is, however, a time-consuming task, and because of long access times, on-line use of Internet resources is often a frustrating exercise. In addition, the integration of new materials in existing curricula requires rewriting of lesson-plans and redesign of long-term teaching schedules.

The Department for Science Teaching at the Weizmann Institute of Science has initiated a project, by means of which we try to bridge the gap between the Internet's potential as a teaching resource and the community of science teachers, who find it difficult to actually exploit this resource. We are presently creating a website, which offers an annotated catalog of relevant websites for physics teachers. Every item in this catalog is evaluated according to a set of technical and pedagogical criteria, and a short review, written by a physics teacher, is attached. Every item carries a link to a document, which presents a lesson plan based on the materials from the respective website. Items are catalogued according to a wide range of intersecting criteria, such as to facilitate the search for relevant materials. A group of interested physics teachers participate in a special class, which teaches advanced techniques in using the Internet, and develop exemplary lesson plans. We hope, that the work carried out by this group, together with our annotated catalog, will enhance the Internet's attractiveness as a teaching resource, and facilitate the design of attractive physics courses in Israeli high schools.

An instructional framework to support learning inquiry skills in high school physics

Dorothy Langley

Department of Science Teaching , Weizmann Institute of Science

The traditional emphasis in high school physics education on the acquisition of content knowledge and problem solving skills tends to obscure the generative nature of physics knowledge, which allows basic formal knowledge to be extended using theoretical and experimental inquiry methods. We shall describe an inquiry-oriented instructional intervention which is currently being field tested with view to providing insight and materials towards a future, inquiry-enhanced physics curriculum. The main components of the proposed intervention are a supportive instructional approach and the use of an information technology rich environment. The small but growing number of motivated physics teachers who do integrate knowledge extension through inquiry into their classroom practice provide an important resource for the proposed intervention. The instructional approach employs purpose-designed instructional materials and a regime of gradually diminishing teacher support. The use of information technology (spreadsheets, mbl and simulations) is intended to provide time efficient inquiry environments which can allow students to go beyond the limits of their mathematical deductive skills. The instructional goals of the proposed intervention include improved question posing skills, greater awareness of the inquiry process, improved technical inquiry skills and an improved inquiry vocabulary. We shall describe some examples of implementing our inquiry oriented approach and discuss the related research results.

The motion of charged particles in electric and magnetic fields - learning by simulation

Zeev Krakover

Center for Preacademic Studies, Hebrew University
** Science Teaching Department, Weizmann Institute of Science*

The motion of charged particles in electric and magnetic fields is an important and nontrivial manifestation of Newton's second law. By exploring the details of the motion, students analyze various aspects of the second law, and get an insight into classical experiments in particle physics. The use of the strength of computer graphical presentations is very effective here, and enables us to explore the subject.

Learning from mistakes - a workshop for physics teachers on feedback and control in problem solving

I. Yerushalmi

Dept. of Science Teaching, Weizmann Institute of Science

Searching for a solution to an unfamiliar problem is a characteristic activity of scientists and engineers, involving such capabilities as learning from one's own mistakes and invoking analogies. These capabilities seldom receive deliberate attention in traditional test-directed physics teaching. While some students possess these capabilities naturally, most of the students survive, if at all, by memorizing studied problem solutions. Changing teachers' and students' roles with respect to feedback, diagnosis, and evaluation are valuable ingredients towards an improvement of the current situation. Teachers need to undergo profound changes in their views about goals and methods of physics teaching as a pre-requisite to changing their classroom practice. We claim that such changes can only be achieved by inducing teachers to become concerned with the situation, and by cooperating with them in searching for ways to improve it.

We shall report on a yearlong course aimed at promoting such change. The course guides the participants in learning from their experience through a repeated learning cycle. This cycle includes documenting classroom experiences, peer feedback, formulating and discussing improvements.

Using an intranet communication method proved to have a critical impact on the clarity and conciseness of the documentation, and on the teachers' ability to formulate questions about their instructional concerns.

The Blossoms of Science Internet Astronomy School

David Pundak and Shaul Yannai

Alperin Academic College of the Jordan Valley

This is an on-line school for students from fourth through twelfth grade which has been open to the public since March 1996. It is available in both Hebrew and English. Currently IAS receives 1000 per month.

Individual enrollments are encouraged so that students may study directly from their homes, but it is intended that science teachers enroll their classes and use the IAS within the framework of their science courses. In the latter case class students are expected to supplement class work with home-based work, just as are the individual enrollment students.

A class using the Internet as part of its learning environment should be radically different from a traditional class with respect to many of the learning dimensions. Standard classroom situations do not commonly provide for contact with out-of-class experts, nor for the use of remote libraries or data-bases. They rarely make it possible for students to address questions directly to subject matter experts and researchers and to receive responses within a time frame suited to the class learning program. The ability to retrieve information such as sun spot data, moon landscapes, solar and lunar eclipses and up to the minute pictures and descriptions of countless other topics, drastically changes the learning environment and extends the range of possible learning activities.

Blossoms of Science offers a number of tools to students and teachers. One is "Conceptual Frameworks in Astronomy" which enables both teachers and students to check the way they perceive the universe. Another is the "Space Crown" quiz-game which provides for student self-assessment of learning, covering the different lessons within IAS. Each of the learning topics carries within an evaluation form which students complete and forward to the IAS team. This makes it possible to give students credit for their opinions on how learning topics are structured, on whether the learning topics answer their expectations, and on changes they would like to implement.

"Search the Net", a tutorial file designed to introduce users to the net and to the identification of information which is relevant to their needs. The other is a glossary of astrophysical terms and definitions taken, with the author's permission, from Hamilton's "Views of the solar system". Two complementary tools to be found on Internet are the Internet Compass for Schools (1996) which is a guide to educational sites on Internet and Carvin's EdWeb dictionary of Internet terminology (1996).

In addition a bulletin board for IAS students and users has been set up for discussion and the exchange of ideas. The Sea of Galilee Astrophysical Observatory, operated by the Blossoms of Science astrophysicists, has been made available to students taking part in the Blossoms of Science projects, and links are being set up with a number of overseas learning sites.

At our talk we will report on some projects that we have made with IAS with formal and non-formal education.

Calculation of Density-of-State Tails Due to Disorder Using One-Particle Ward Identtity

Mark Auslender

Dept. of Electrical and Computer Engineering, Ben-Gurion Universty of the Negev
P.O.B. 653 Beer-Sheva

There exist many topics where a lecturer, while teaching, is faced with a necessity to exploit a heuristic method in order to demonstrate desired result. On the one hand, this sort of methods is valuable for training highly intelligent individuals. On the other hand, the educational 'factory' needs routine methods which can be used by an average student in his own research and development work.
I consider the example of studying band tails in solids with disorder, e.g. heavily doped semiconductors. This subject is of scientific and technological importance. To teach it the heuristic method of optimal fluctuation is used [1]. In the book [1] rather more systematic method due to L. Keldysh based on the Green-function technique is outlined. However, this method is, incidentally, applied to less interesting case of far gaussian tails. In this presentation I bring this technique in a focus of attention as an adequate tool for teaching the subject as a whole.
In the first part I prove one-particle Ward identtity for Gaussian impurity potential without using diagram technique. In the second part Ward identity is combined with a leading approximation in small momentum transfer to obtain closed differential equation for the self-energy part $\Sigma(k, E)$ of Green function. The asymptotic of solution to this equation at $E \to -\infty$, that determines the tail of density of states, $\rho(E)$, is considered for different models of impurity potential. In the third part I discuss some cases where the above equation can be exactly solved, and a closed formula for $\rho(E)$, e.g. Langer formula for in 1D white-noise potential case [2], can be obtained.

[1] B.I. Shklovskii and A.L. Efros, *Electronic Properties of Doped Semiconductors*, Springer Series in Solid-State Sciences (Springer-Verlag Berlin, 1984).
[2] J. Langer, Phys. Rev. **120**, 714 (1960).

Author Index

Index

מכון ויצמן למדע
הפקולטה לפיסיקה

הכנס השנתי ה-44
של האגודה הישראלית לפיסיקה

תשנ"ח